ASPECTS OF THE WATER BALANCE OF AN OATS CROP GROWN ON A LAYERED SOIL

A thesis presented in partial fulfilment
of the requirements for the Degree of
Doctor of Philosophy
in Soil Science at
Massey University

BRENT EUAN CLOTHIER

1977

ABSTRACT

The increasing pressure on our water resources, for irrigation in particular, has resulted in a growing awareness of the importance of water balance studies. In this thesis three aspects of the field water balance are investigated; evapotranspiration (ET) from well-watered crops, the upper limit of soil water storage in the field, and drainage.

Daily ET values, measured by the Bowen ratio-energy balance method, are presented for an oats crop grown in winter and also for a number of summer crops, all of which were well-watered. ET measurements were also made over longer periods using a drainage lysimeter. It was found that the Penman, and Priestley and Taylor ET estimation procedures predicted ET with an accuracy of 15-20% and 8% for daily and weekly periods, respectively. The Priestley and Taylor method is simpler to use but requires an empirical constant to relate the 'equilibrium ET' to ET. This constant was found to be 1.21 for winter, spring and summer over a range of crops in the Manawatu. Net radiation data on a daylight basis were used to evaluate this constant, as seasonal variations in the constant were introduced when 24-hour data were used. Also it is easier to empirically estimate daylight than 24-hour net radiation. Long term ET estimates using the Priestley and Taylor method with net radiation calculated from incoming solar radiation, were in reasonable agreement with the drainage lysimeter measurements of ET for the oats crop.

A theoretical development is presented that describes water retention in soils underlain by a coarse-textured stratum. This development accounts for the physical character of the overlying soil, the depth to the coarse layer, and the coarseness of the underlay. Field data are presented for the Manawatu fine sandy loam, a soil with a coarse-textured layer at 90 cm. For this soil the layering resulted in an additional 55 mm of water

storage at the cessation of drainage, an increase of 31% over a similar hypothetical soil with the coarse stratum absent.

Drainage from a permeable soil underlain by a coarse-textured layer is investigated. Simplified theory is used to develop a model relating the drainage flux at the base of the soil to the water stored in the overlying soil. Despite significant hysteresis in both the water retentivity curve of the overlying soil and the hydraulic conductivity-pressure potential relationship of the coarse layer, hysteresis had little effect on the storage-flux relation. The model simulated both the field drainage in the Manawatu fine sandy loam measured by a lysimeter, and field profile water storage found by neutron probe moisture measurements. The model indicates that only simple field measurements are needed to find the storage-flux relationship.

The components of the water balance of an autumn-sown oats crop grown in the Manawatu are resolved. Drainage loss was found to constitute 60% of the rainfall, with the remaining amount being lost as ET.

ACKNOWLEDGEMENTS

I express my sincere thanks to my supervisors, Drs. Dave Scotter, Jim Kerr and Max Turner for their direction, encouragement and friendship during all the stages of my work. I would also like to thank Prof. Keith Syers and Dr Ken Mitchell for making it all possible. This work was carried out whilst I held a U.G.C. Postgraduate Scholarship and the 1974 B.P. (N.Z.) Postgraduate Scholarship, for which I am grateful. To the D.S.I.R. I am grateful for the help that enabled me to do this work.

Thanks also to John Talbot, Peter Menalda, Peter Rollinson and Jim Gordon for assistance both in the field and laboratory.

To Penny Clothier, thanks for the continual encouragement and warm understanding.

For much typing I wish to thank Erin Temperton.

TABLE OF CONTENTS

Page

CHAPTER 4

CHAPTER 5

APPENDIX I

APPENDIX II

Page

APPENDIX III

APPENDIX IV

LIST OF FIGURES

Page

Page

Page

Page

Page

LIST OF TABLES

	LIST OF SYMBOLS	UNITS
a	empirical constant in Eq. 1.3	
b	exponent in Eq. 1.3	dimensionless
C	convective term in the combination evaporation equation	mm day^{-1}
C.R.	counts per second in soil/counts per second in neutron probe radiation shield	dimensionless
C_p	specific heat capacity of air	J g^{-1} C^{-1}
d	soil depth	cm
D	soil water diffusivity	cm^2 day^{-1}
Dm	plant dry matter %	dimensionless
ΔD	change in surface water detention	mm
e	vapour pressure	mb
Δe	difference in vapour pressure between two levels above crop	mb
e_s	saturated vapour pressure	mb
ET	evapotranspiration	mm day^{-1} or Wm^{-2}
ET_p	Penman's evapotranspiration estimate	mm day^{-1}
ET_{eq}	equilibrium evapotranspiration rate	mm day^{-1}
ET'_{eq}	daylight equilibrium evapotranspiration rate	mm day^{-1}
ET''_{eq}	nocturnal equilibrium evapotranspiration rate	mm day^{-1}
f(u)	wind function in Penman's equation	mm day^{-1} mb^{-1}
f(w)	drainage flux-profile storage relationship	mm day^{-1}
G	soil heat flux	mm day^{-1} or Wm^{-2}
H	sensible heat flux	mm day^{-1} or Wm^{-2}
J	drainage flux	mm day^{-1}
J_i	drainage flux in coarse underlay	mm day^{-1}

		UNITS
K	hydraulic conductivity	cm day^{-1}
K_i	hydraulic conductivity of the coarse underlay	cm day^{-1}
K_f	hydraulic conductivity of the overlying soil	cm day^{-1}
K_s	saturated hydraulic conductivity	cm day^{-1}
$K\downarrow$	incoming solar radiation	mm day^{-1} or Wm^{-2}
L	latent heat of vapourization	Wm^{-3}
LAI	leaf area index	dimensionless
L_1, L_2	characteristic length of soil particles	mm
m	slope of the K-$\log_e(\theta)$ curve	
P	atmospheric pressure	mb
Ph	energy used in CO_2 fixation by photosynthesis	mm day^{-1} or Wm^{-2}
r_s	crop resistance to water vapour	sec cm^{-1}
R_n	net radiation	mm day^{-1} or Wm^{-2}
RO	run off	mm
RF	rainfall	mm
R	simple correlation coefficient	dimensionless
S.D.	standard deviation	
ΔS	crop heat storage change	mm day^{-1} or Wm^{-2}
s	slope of the saturated vapour pressure-temperature curve	mb C^{-1}
S_{yx}	standard error of the regression estimate	
$\bar{T}$	mean daily temperature	C
T_{max}	maximum daily temperature	C
T_{min}	minimum daily temperature	C
T_d, T_W	dry bulb, wet bulb temperature	C
ΔT_d, ΔT_W	dry bulb, wet bulb temperature difference between two levels above crop	C

		UNITS
t	time	day
u	windspeed	m sec^{-1} or km day^{-1}
VPD	saturation vapour pressure deficit	mb
W	profile soil water storage	cm
W_t	profile soil water storage at time t	cm
W_u	uniform soil profile water storage	cm
W_L	layered soil profile water storage	cm
ΔW	$W_L - W_u$	cm
W_{max}	maximum profile soil water storage	cm
W_{min}	minimum profile soil water storage	cm
z	soil depth measured from soil surface	cm
z_i	soil depth to coarse layer interface	cm
z_L	soil depth to secondary layering	cm
z_o	aerodynamic surface roughness	cm
z^*	depth defined by Eq. 3.8	cm

α	empirical constant, ET/ET_{eq}	dimensionless
β	Bowen ratio	dimensionless
γ	psychrometric constant	mb C^{-1}
γ^*	psychrometer constant	mb C^{-1}
δ	error operator	
η	slope of the log K- logθ curve	
θ	volumetric soil water content	$cm^3\ cm^{-3}$
θ_t	volumetric soil water content at time t	$cm^3\ cm^{-3}$
θ_s	saturated volumetric water content	$cm^3 cm^{-3}$
Λ	difference between γ^* and γ (Eq.A1.12)	mb C^{-1}
λ	pore size distribution index	dimensionless
λ_{max}	pore size distribution index when $d(\Delta W)/d\lambda = 0$	dimensionless

		UNITS
ξ	ratio of the molecular weight of water to air	dimensionless
ρ_b	soil bulk density	g cm^{-3}
τ	time	day
ψ	tensiometer pressure potential	cm
ψ_e	air entry pressure potential	cm
ψ_c	pressure potential when J = 1 mm day^{-1}	cm
ψ_i	pressure potential when J_i = 1 mm day^{-1}	cm

CHAPTER 1

WATER BALANCE STUDIES

1.1 INTRODUCTION

Late last century the soil physicist F.H. King stated that "It is doubtful if there are agricultural soils to be found anywhere under existing climatic conditions where, in the majority of seasons, deficiency of available moisture must not become a marked limiting factor in yield" (King, 1896). Since existing climatic conditions have not changed significantly over the last 80 years, this statement is probably just as applicable to present day dryland farming. However, as 14% of the world's farmland is now irrigated (Rawlins and Raats, 1976), the deficiency of available moisture can be reduced, if not overcome, in such soils.

Improvement of both dryland and irrigated agricultural production systems must be based on an understanding of both the size and seasonal changes in the components of the soil water balance. Under irrigation, water balance information can be used to develop schedules by which water can be applied. Efficient use of water is important particularly where supplies are limited, and where application costs are significant. Also fertilizer leaching losses that may result from over-watering can in the case of nitrogen, transform an expensive agricultural input into a potentially dangerous pollutant. Water balance information can be used in dryland farming management strategies so that maximum use can be made of the soil water reserves.

1.2 THE FIELD WATER BALANCE EQUATION

The water balance of a soil growing a crop can be expressed simply in terms of the conservation of water mass, and written per unit surface area for a soil profile of depth d below the root zone and over the time interval t = 0 to τ, as

$$RF = \int_0^{\tau} ET\,dt + \int_0^{\tau} J\,dt + W_{\tau} - W_0 + \Delta D + RO \qquad \text{(1.1)}$$

In Eq.(1.1) RF is the rainfall or irrigation (mm), ET the evapotranspiration rate (mm/day), J the drainage rate (mm/day), and W_τ and W_0 the water storage in the soil profile to depth d (mm) at times τ and 0 respectively, with $W_t = \int_o^d \theta_t \, dz$ where θ_t is the volumetric water content at time t, ΔD is the change in surface detention (mm), RO the surface runoff (mm), and z the depth from the soil surface. In most relatively flat agricultural areas with permeable soils RO and ΔD may be assumed zero with little error.

Eq.(1.1) may be solved to find the soil water storage (W_t) and infer when crop growth is likely to be affected by root zone water shortage. Therefore, the quantity of irrigation water that should be applied to replenish this deficit without causing drainage, can be estimated.

Rainfall data for a particular site are generally available, or may be easily measured. However evapotranspiration and drainage data are more difficult to measure or estimate. This thesis examines the measurement and estimation of the evapotranspiration and drainage components of the water balance, plus the related problem of the retention of water in the soil profile.

1.2.1 EVAPOTRANSPIRATION (ET)

None of the various direct or indirect methods for measuring ET have complete preference as they differ in both short- and long-term accuracy, and in convenience and cost. The selection of the method of measurement depends on the way in which the results are to be applied. As ET is an important component in the water balance there is a need for means of predicting it. In this section it is proposed to review the methods presently available for both ET measurement and estimation.

For direct measurement of ET a weighing lysimeter may be used to provide ET information, or to check indirect methods of ET measurement or estimation. However the expense involved, and the need to ensure that a representative soil volume and crop is used, can limit the applicability of this approach.

In principle the eddy-flux technique (Swinbank, 1951) could be used to provide accurate measurements of ET, however until a reliable fast-response humidity sensor is developed, application of this approach will be limited to specific micrometeorological research problems. Even given such a technological development, it is unlikely that routine measurement of ET over long periods of time, such as during crop growing seasons, will eventuate. Current micrometeorological methods of measuring or estimating ET are often less direct and involve an assessment of the surface energy budget, as a large amount of latent heat is involved in the change of state that takes place during evaporation of water. In fact unless the crop is under severe water stress, ET is likely to be energy-limited rather than limited by the supply of water.

The energy balance for a crop may be written (Tanner, 1960)

$$R_n = H + L.ET + G + Ph + \Delta S \qquad \text{---(1.2)}$$

where R_n is the net radiation at the crop surface, H the sensible heat flux, L the latent heat of vapourization in Wm^{-3}, G the soil heat flux, Ph the energy used in the fixation of CO_2 in photosynthesis, and ΔS the heat storage change in the crop canopy. Generally Ph and ΔS are less than about 2% R_n, and so can be ignored. The units of the terms in Eq.1.2 are Wm^{-2}, or alternatively if the equation is divided through by L, in units of equivalent depth of water (m, or mm as is usual).

The Bowen ratio-energy balance method (Tanner, 1960) used in this study involves measuring (R_n-G) and determination of the Bowen ratio (β = H/ET) from measurements of the temperature and vapour pressure gradient above the crop. This procedure is discussed in more detail in Appendix I. The use of on-line mini-computers has made this method more tractable for research studies conducted over many days, however it is still unsuitable for routine use.

Because of the present intractability of direct or indirect ET measurement over long time periods, means of empirical ET estimation are often used in water balance studies. The starting point for any such procedure is to consider the ET from a well-watered surface. Since in this case ET is dominantly controlled by the available energy at the surface and the state of the immediately overlying air, estimates of ET may be based on meteorological information. The character of the evaporating surface limits the accuracy of all ET estimation procedures based solely on meteorological data because of variations in the resistance offered by the crop to the transport of water vapour. However the methods of ET estimation based on the work of Penman (1948, 1956) and Priestley and Taylor (1972) have been shown to provide reasonable estimates of well-watered crop ET (Tanner and Pelton, 1960; Tanner and Jury, 1976). Thornthwaite's (1948) method of ET estimation is not based on sound physical principles and employs empirical constants found in the continental climate of the U.S.A.

Rickard and Fitzgerald in 1970 stated that 'there have been no published references to the measurement of evapotranspiration in New Zealand, and the majority of workers have relied on the Thornthwaite estimates'. Since 1970 there appears to have been only one New Zealand publication presenting measured daily water use by crops (Kerr et al. 1973).

Clothier et al. (1975) showed that for Palmerston North, ET estimates based on Penman's (1956) method and that of Priestley and Taylor (1972) were in reasonable agreement (Fig.1.1). This is to be expected because of the dominance of the radiation term in both equations. However the estimates based on Thornthwaite's (1948) formulation did not correlate well and were lower than those based on the other two methods.

Numerous overseas studies have shown Thornthwaite estimates to often be seriously in error (van Wijk and de Vries, 1954; Chang, 1968), and in New Zealand Coulter (1973a) found Thornthwaite values to be significantly lower than Penman values or pan evaporation estimates, particularly in summer. For mid-Canterbury, Fitzgerald and Rickard (1960) found Thornthwaite values to compare well with ET estimated from soil profile water storage changes. They worked on a shallow Lismore stony silt loam, where some plant water uptake may have occurred below the 30 cm profile depth, leading to an underestimate of the water balance value of ET. This possibility of water uptake is supported by the unusually low values for the "crop factor" f in the 1948 Penman equation, inferred from their water balance ET data. The main reason for its widespread application is probably that Thornthwaite's method requires only temperature data. Because of its weak physical basis Thornthwaite's method will not be considered further.

In Chapter 2 ET from well-watered full-cover crops is considered. Since this constraint is generally fulfilled in irrigation studies, such information is pertinent. The divergence of ET away from the well-watered rate forms the basis of many crop yield-water use models (Hanks, 1974). The accuracy of the Penman and Priestley-Taylor estimates of ET is examined by comparison with ET measured using the Bowen ratio-energy balance method over a range of climatic conditions and for a variety of well-watered crops.

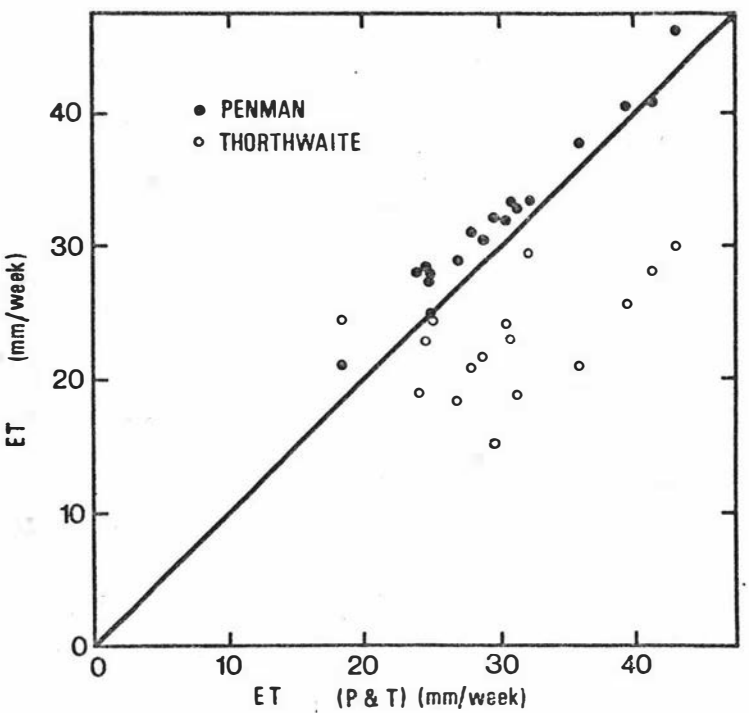

Fig.1.1 Penman and Thornthwaite estimates of weekly ET for Palmerston North over the summer of 1974/75 compared to estimates using Priestley and Taylor's method (ET (P & T)). (After Clothier et al. 1975).

1.2.2 MAXIMUM PROFILE WATER STORAGE (W_{max})

The decline in W due to evapotranspiration is a continuous process, its replenishment by rainfall or irrigation is intermittent, thus the ability of the soil to store plant available water is important. The upper limit of available water storage capacity in the root zone is conventionally considered as some maximum profile water storage, W_{max} (traditionally termed the 'field capacity') which may occur after heavy rain or irrigation. The lower limit of this storage capacity, W_{min}, is the profile water storage when the crop is unable to extract further soil water by root uptake (termed the 'permanent wilting point'). The available water storage is found as the difference between W_{max} and W_{min}. In this section it is proposed to review the concept of field capacity and outline its subsequent misuse. The inapplicability of laboratory estimates of W_{max} is also discussed.

Viehmeyer and Hendrickson (1949) defined field capacity as "the amount of water held in the soil after excess water has drained away and the rate of downward movement of water has materially decreased ..... as compared to the rate of extraction of water by plants". They realised however that soil texture, uniformity, soil depth and other factors affected the value of the field capacity. In 1931 they conducted field flooded-plot experiments and found the measured field capacity moisture content to be effectively the same as the moisture equivalent, in fine textured uniform soils. The moisture equivalent is the water content after centrifuging a soil sample for 30 minutes at 1000 times the acceleration due to gravity. Viehmeyer and Hendrickson (1931) concluded "that the moisture equivalent can be used to indicate the field capacities of deep, well-drained soils with no decided changes in texture or structure ..... at least for the fine textured soils".

They found that an impermeable plough sole impeded water movement in one of their soils and mentioned the work of Alway and McDole (1917), which showed that coarse layering results in an increase in field capacity. They also cited the problems found by Harding (1919) using laboratory estimates to infer field capacity in a study involving 10,000 soil samples. Subsequently the use of the moisture equivalent was replaced by use of the water content at -1/3 bar pressure potential, which is usually similar to the former (Richards and Weaver, 1944; Colman, 1947).

However because of the desire to obtain easily an estimate of maximum profile water storage, many workers have estimated W_{max} solely on the basis of a laboratory measurement of the water content at an arbitrary pressure potential. This useage frequently ignores Viehmeyer and Hendrickson's carefully worded definition of field capacity, and their qualifications as to the applicability of laboratory estimates.

Because of this flagrant misapplication, Richards (1960) suggested a moratorium on the use of the term 'field capacity' and considered that, "although it is the author's prejudice the concept of field capacity has done more harm than good". Richards (1960) however recognised that retentivity values over a certain range of potentials are usefully correlated with the upper limit of soil water storage in the field (i.e. W_{max}). It is the dynamics of the soil-water system that are responsible for determining the retentivity values at which water redistribution has for all practical purposes ceased. The reduction in the drainage flux and hence the reduced decline in W when $ET \approx 0$, is a continuous process, generally occurring as a result of the marked reduction in the hydraulic conductivity (K) with decreasing pressure potential (ψ). Hence the selection of W_{max} is somewhat arbitrary, and is often considered to occur when the drainage flux is less than about 1 mm/day (Miller, 1969).

Thus such commonly used equilibrium values as the moisture equivalent, the -1/10, -1/5 or the -1/3 bar pressure potential are related to W_{max} only to the extent that they are related to the unsaturated hydraulic conductivity of the soil. The K (ψ) relationship varies markedly within the soil profile and from soil to soil. Also, the rate at which the drainage flux becomes negligible at any given depth in the soil depends also on the character of the soil above and below it, a fact that cannot be easily taken into account in laboratory measurements.

For soils underlain by coarse layers Miller (1969) found that the available water storage found from a conventional field capacity estimate of the -1/3 bar water content, can in some cases be 55% lower than the value measured in a field plot several days after irrigation (Table 1.1). In view of such possible errors, Richards' (1960) suggestion that the determination of maximum water storage in soil profiles should be based on theory involving both the retentivity and unsaturated conductivity functions along with appropriate initial and boundary conditions, warrants consideration.

In Chapter 3 a theory is derived that incorporates the factors involved in determining the water storage in soils with a coarse-textured layer underneath. Such soils are important as most of the irrigation schemes presently under consideration in New Zealand are on soils underlain by a coarse layer. Similar soils are common overseas. Soils underlain by a coarse layer display quite a clear cut W_{max} value, (Miller, 1969) because after wetting the pressure potential profile fairly rapidly approaches a quasi-static equilibrium. The value of W_{max} can be influenced markedly by the coarse-textured layer.

Table 1.1 Estimates of the available water storage based on W_{max} at a pressure potential of -340 cm, in relation to that observed in the field, for 4 soils underlain by a coarse layer (Miller, 1969).

Soil	Soil depth (cm)	Estimated available water based on:- observed field value minus the -15,000 cm water content (cm)	Estimated available water based on:- the -340cm water content minus the -15,000 cm water content (cm)	Ratio
Ephrata	0-60	14.6	6.4	2.28
Timmerman	0-75	15.3	6.6	2.32
Rupert	0-75	9.2	4.5	2.04
Scooteney	0-90	26.6	21.0	1.27

1.2.3 PROFILE DRAINAGE (J)

In most field water balance studies when W exceeds W_{max}, drainage is often assumed to be (RF-ET) and occur instantaneously so that always $W \leq W_{max}$. However field drainage is never instantaneous, often occurring over a number of days. As the downward movement of water through the soil has important implications in both water and fertilizer balance studies, it is often necessary to account for it more realistically than as outlined above. Profile drainage is difficult to measure and presently there is no direct method for reliable and representative measurement of J. Consequently in water balance studies J is often solved for as the unknown in Eq.1.1. In this section methods of describing the decline in J with time since wetting are discussed. Also the numerical techniques and simplified analytical methods used to predict drainage are discussed.

Much of the early drainage work was carried out in covered plots, and the results analysed qualitatively as the experiments were designed solely to find the "field capacity". Some workers however have sought to express J as a function of time. Richards *et al.* (1956) used an expression of the form

$$W = at^{-b} \qquad \text{——(1.3)}$$

or $$J = dW/dt = -abt^{-(b+1)} \qquad \text{——(1.4)}$$

with a and b being found by regression. Later Gardner *et al.* (1970) showed that an equation of the form of 1.3 could be derived analytically by specific solution of the one-dimensional unsaturated flow equation.

Miller and Aarstad (1974) rearranged Eq.1.4 to give

$$J = ab\,(W/a)^{(b-1)/b} \qquad \text{——(1.5)}$$

and found that the value of W in 100 cm long soil columns, which were initially saturated and subjected to known evaporation rates, could be predicted.

Wilcox (1959) presented values for a and b for a range of soils and found statistical correlations between the texture of the soil (as typified by the bulk density and the value of a) and J at various times. However such an approach is applicable only to deep uniform soils, because Miller's (1969) data (Fig.1.2) show that layering in the profile has a marked effect on the W (t) relationship for the overlying soil. In addition empirical drainage estimation using this approach requires that every drainage event begin at W = a. Consequently this procedure has limited application .

A general analytical solution describing the redistribution of water within the soil following infiltration does not exist. Therefore it is impossible to analytically predict drainage from soil water properties given the boundary and initial conditions. Usually the problem is further confounded by hysteresis (Philip, 1957; Dane and Wierenga, 1975). Because of the importance of the process approximate ways of predicting drainage have been proposed.

Numerical techniques of solving the unsaturated flow equation have been developed (Hanks and Bowers, 1962) and applied (de Wit and van Keulen, 1972). These solutions require accurate retentivity and unsaturated conductivity data, and a large computer.

Some success in the estimation of field drainage has been achieved using simplified analytical solutions. Black et al. (1969) assumed that $\partial\psi/\partial z=0$, which holds approximately for a deep uniform soil, and showed that the one-dimensional flow equation could be simplified so that the flux at depth z could be expressed as some function of the water stored above that depth. They found this procedure to be successful in predicting drainage from the uniform Plainfield sand. Extending this, by assuming an exponential relationship between

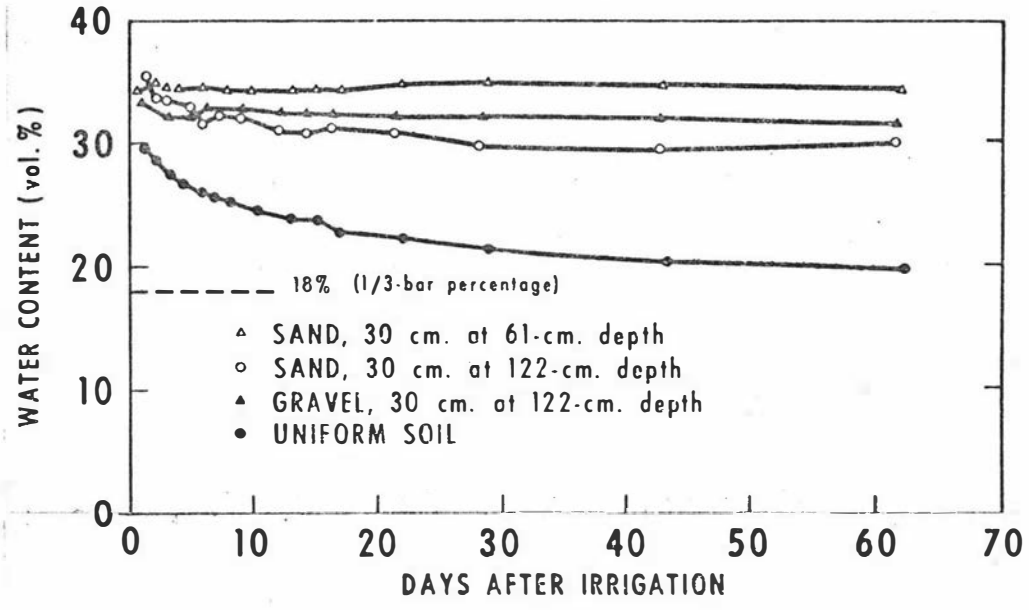

Fig.1.2 Water content at 30 cm depth in uniform sandy loam soil, and the same soil underlain by sand at 61 cm and 122 cm depths and by gravel at 122 cm, as affected by the time after irrigation. Surface evaporation prevented.(After Miller, 1969).

K and θ , Davidson et al. (1969) showed that

$$J = K_s / (1 + mK_s t/d) \qquad \text{——(1.6)}$$

where K_s is the saturated conductivity, d the soil depth and m the slope of the K-$\log_e(\theta)$ function. It can be seen in Fig.1.3 that Davidson et al. (1969) found Eq.1.6 to successfully predict drainage in the relatively uniform Yolo loam and Miller silty clay. The poorer agreement in the Cobb loamy sand was attributed to the non-homogeniety of the soil profile. This physically-based relationship of drainage to storage is an improvement on the empirically 'calibrated' relationship (Eq.1.5) arrived at from the drainage time recession curve, but neither approach is applicable to layered soils. In Chapter 4 the relationship between J and W is investigated for layered soils.

1.2.4 SUMMARY

Much remains to be done in the area of water balance research so that the field soil water status as a function of time can be predicted. In this thesis three aspects of the field water balance of a soil with a coarse underlay are investigated; well-watered crop evapotranspiration, maximum field profile water storage and drainage.

The accuracy of the Penman and Priestley-Taylor estimates of ET is examined by comparison with ET measured using the Bowen ratio-energy balance method over a range of climatic conditions and for a variety of well-watered crops.

A theory is derived to determine the maximum field water storage in soils underlain by a coarse-textured layer. Also the relationship between the drainage flux and the profile water storage is investigated for such layered soils.

The main part of the study was conducted over the winter-spring-early summerperiods of 1974 and 1975 so

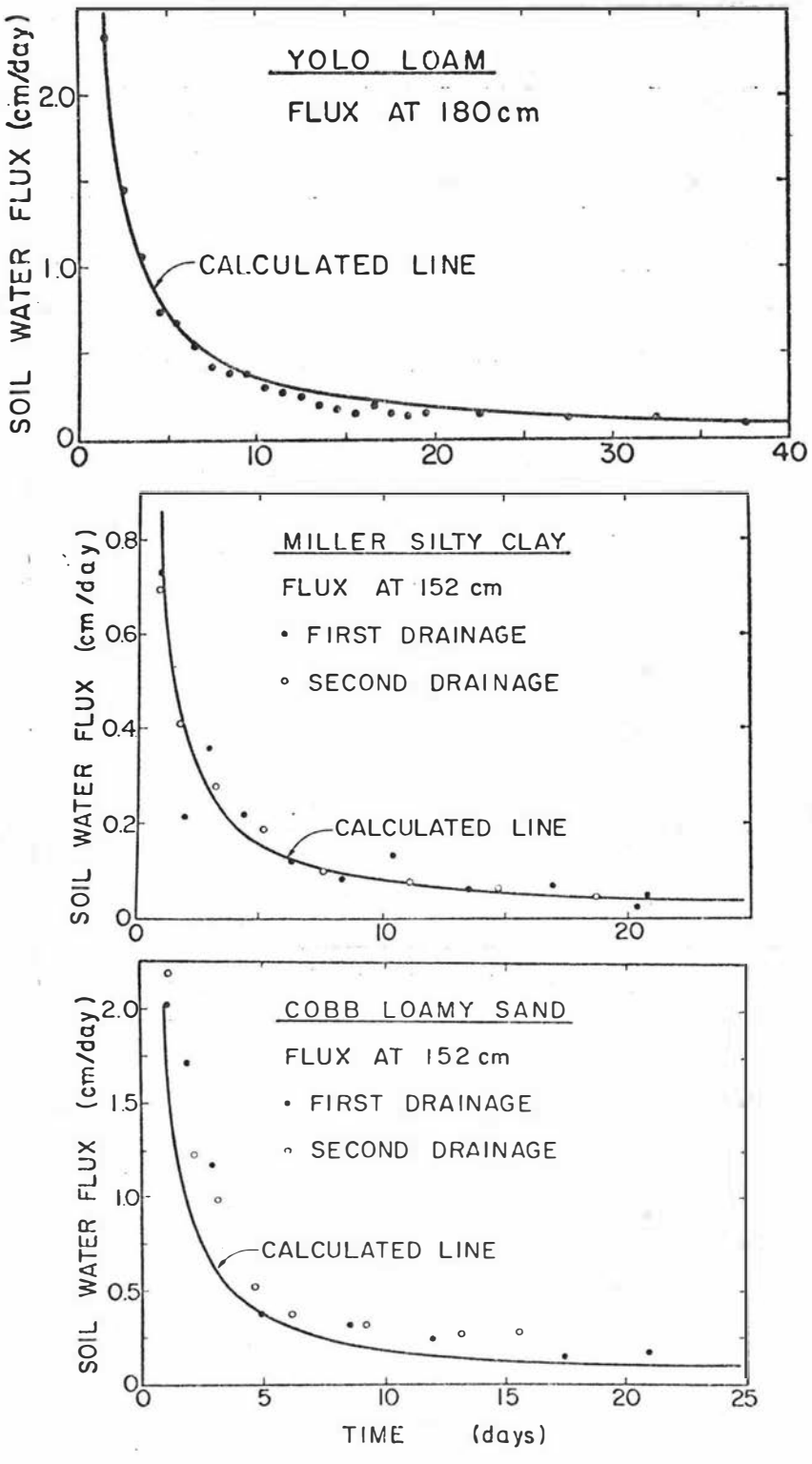

Fig.1.3 Comparison of predicted drainage flux (Eq.1.6) with that measured for the Yolo loam, Miller silty clay and Cobb loamy sand. (After Davidson et al. 1969).

that maximum water storage and drainage could be effectively studied, and so that it would be possible to determine the accuracy of empirical means of estimating well-watered ET rates over a range of climatic conditions.

Oats were selected for this study because they grow well during the cool season in the Manawatu. The use of an annual crop, rather than a perennial pasture subjected to defoliation made long-term measurement of the physical and biological environment easier. Oats may have value as a cool season complementary forage crop to summer grown maize thus giving high annual yields per hectare (Kerr and Menalda, 1976).

In testing empirical ET estimation procedures for well-watered full-cover crops it is useful to obtain data over a wide range of climatic conditions and surface roughness to form a wide empirical base. By using an oats crop sown in autumn it is possible to measure the ET from a well-watered full-cover crop, from the middle of winter through into early summer. Soil water tensiometer pressure potentials at 40 cm depth never fell below -250 cm so the crop was not water-limited.

1.3 MATERIALS AND METHODS

The soil of the 1 hectare plot on which the study was conducted is a Manawatu fine sandy loam and is situated on the No.1 Dairy Unit, Massey University. The soil profile description is given in detail in Appendix III. The profile can be broadly subdivided into 0-50 cm of fine sandy loam, underlain by 40 cm of fine sand, with gravelly coarse sand below 90 cm.

In 1974 a crop of oats (*Avena sativa* L. cv. Mapua) was planted on 26 April, and harvested on 21 November yielding 13,200 kg/ha of dry matter. In 1975 the oats (cv. Achilles) were planted on 7 May and harvested on 15 November yielding 12,400 kg/ha. A description of the crop development and management for the 1974 oats crop, on which ET measurements were made, is given in Appendix IV.

Specific details on soil, site and crop factors are given in the materials and methods section of each chapter. Detailed error analysis of the Bowen ratio method is given in Appendix I. The calibration of the neutron probe is discussed in Appendix II.

CHAPTER 2

MEASURED AND PREDICTED EVAPOTRANSPIRATION FROM WELL-WATERED CROPS

2.1 INTRODUCTION

Evapotranspiration data are important in many agricultural studies. The quantity of water lost by a surface is useful in the interpretation of crop yields, in the understanding of watershed hydrology, in the planning of irrigation schemes, and in the development of schedules that attempt to optimize the amount of irrigation water applied. Continual direct measurement of ET is not easy, thus empirical means of estimation are often used. Presently the two main methods of ET estimation are based on the work of Penman (1948) and Priestley and Taylor (1972).

Penman's formula has been both studied and applied extensively. It may be written

$$ET = [s/(s+\gamma)](R_n - G) + [\gamma/(s+\gamma)] f(u) VPD \qquad \text{——(2.1)}$$

where s is the slope of the saturation vapour pressure-temperature function, γ the psychrometric constant, R_n the net radiation, G the soil heat flux (usually assumed zero), VPD the average daily vapour pressure deficit and f(u) an empirically determined wind function. The radiation-based first term is the "equilibrium evaporation rate" (Slatyer and McIlroy, 1961) and the second term, for which several forms of the function f have been proposed, may be termed the convective term since it attempts to account for the turbulent transfer of vapour. Equation 2.1 has been found to give reasonable estimates of ET from vegetation in many situations (Tanner and Pelton, 1960). However Penman's (1956) comment that the method 'has been used, rather than tested is particularly applicable in New Zealand, so in this chapter measured ET is compared with Penman predictions.

In recent years the ET estimation method of Priestley and Taylor (1972), where ET is considered to be proportional to the equilibrium evaporation rate (ET_{eq}), has been used because of its simplicity and accuracy. It may be

written

$$ET = \alpha ET_{eq} = \alpha[s/(s+\gamma)](R_n - G) \qquad \text{——(2.2)}$$

where α is an empirically determined constant, which for well-watered surfaces in non-advective situations is constrained by

$$1 \leq \alpha \leq (s+\gamma)/s \qquad \text{——(2.3)}$$

From data obtained over land and open water surfaces Priestley and Taylor found α to have a mean value of 1.26. Subsequent research over crops has returned values of α from 1 to 1.4 (Tanner and Jury, 1976). Equation 2.2 has been empirically modified further to account for non energy-limited ET (Davies and Allen, 1973), advective enhancement (Jury and Tanner, 1975) and changes in leaf area (Tanner and Jury, 1976). Although somewhat conservative, α is not a universal constant and may vary with period of integration, location, season or crop. Davies and Allen (1973) stated that "the value of α at low temperatures could not be examined due to the dearth of spring and fall data" hence the applicability of overseas data to the lower temperature and R_n conditions often experienced in New Zealand is not known. The majority of studies presenting data have been conducted in U.S.A. or Canada.

Thus the use of measured ET data to evaluate α and determine its value for a range of seasons and crops would be worthwhile and enable assessment of the usefulness of the Priestley and Taylor method in such climates as experienced in New Zealand.

This study examines values of α for oats (Avena sativa L. cv. Mapua) over a wide range of conditions: from winter days with R_n as low as 0.47 mm/day (water equivalent) and average temperatures as low as 5 C, through to early summer with R_n as high as 6.6 mm/day and average temperatures up to 19 C. Few data have been presented showing the stability of α on a day-to-day or seasonal basis, which determines the accuracy of short

and long term ET predictions by this method.

It is important to remember that the character of the evaporating surface limits the accuracy of all purely meteorologically-based ET estimation procedures, because of variations in the resistance offered by the crop to the transport of water vapour. This present study is concerned only with ET estimation from well-watered crops. Such a procedure is useful because in most irrigated situations, where ET estimates are most commonly used, this constraint is fulfilled. Also, most current crop yield-water use models are based on the divergence of ET away from the well-watered rate (Hanks, 1974).

2.2 EXPERIMENTAL METHODS AND MATERIALS

The Bowen ratio apparatus used to measure ET has been described by Kerr et al. (1973). The unit was placed above the oat crop so that the wet and dry bulb gradients were measured over 60 to 75 cm, with the bottom sensor less than 20 cm above the crop canopy. The unit was shifted slightly in late September to avoid lodged areas that occurred upwind from the sensors. The siting of the instrument enabled the fetch-height ratio to be 70 in the dominant westerly wind direction. The lowest ratio was to the south-east, being 22. The crop possessed a leaf area index (LAI) of at least four and so was considered full-covered (Tanner and Jury, 1976), and was 40 cm high when ET measurements began. It reached a final height of 122 cm, with a final LAI of 12 (Appendix IV).

Net radiation was measured 75 cm above the crop with a polythene-shielded net radiometer. Incoming solar radiation was measured using a thermopile pyranometer. Calibration of both instruments in the field against a Linke-Feussner pyrheliometer was carried out at the conclusion of the study.

Three soil heat flux plates were placed in the soil at a depth of 5 cm, whilst heat storage in the 0 to 5 cm layer was calculated calorimetrically from the temperature change measured at 1.5 cm by 3 diodes. A constant soil heat capacity of 1.7 J cm^{-3} C^{-1} was assumed as variation in the surface soil water content was small. Total soil heat flux was obtained by summing the flux and the storage change.

Half-hourly Bowen ratio-energy balance data were collected on 105 days between 4 July and 11 November 1974, with 70 days data being sufficiently complete to enable daily ET totals to be computed. Data were gathered part of the time (24 days) with a Hewlett Packard 2012 B data logger, scanning every minute from dawn to dusk and punching directly to paper tape. Subsequently a PDP 11/10 mini-computer was used to compute the half hour averages which were punched to paper tape. Inconsistent data and data when the Bowen ratio (β) fell below -0.5, were edited out. Linear interpolation was used to estimate values for missing points between data, provided the gap did not exceed two half-hour means. Integrated values of the measured variables and energy balance computations were found for both 24-hour and daylight (when incoming short wave radiation exceeded 1 Wm^{-2}) periods. The error in the Bowen ratio-energy balance measurements of ET is considered, on the basis of an error analysis (Appendix I) to be less than 11%, this being similar to that found by Fritschen (1965), Tanner (1960) and Blad and Rosenberg (1974). The error in R_n was estimated, by comparison of two radiometers, to be 5%.

The 24 hour ET total was considered to be the same as the daylight ET total, that is nocturnal ET was assumed to be zero. Dewfall, measured as negative ET on two nights with positive values of β, was found to be 0.11 and 0.23 mm. The latter was one of the heavier dew falls observed. Consequently dewfall was estimated to be less than about 0.1 mm/night and so ignored.

Nocturnal evaporation was considered negligible also, as positive vapour pressure gradients observed on several nights were an order of magnitude less than typical daylight values. Monteith (1956, 1963) suggested that the nocturnal latent heat flux above a crop is usually small (<0.2-0.4 mm/night).

In the application and testing of the ET estimation procedures, it was necessary to use standard meteorological data. For this purpose mean temperature, saturation vapour pressure deficit (VPD), windspeed and rainfall data from the Grasslands Division, D.S.I.R., meteorological site about 1 km away were used. The daily mean temperature ($\bar{T}$) was estimated as $(T_{max} + T_{min})/2$. Assuming the vapour pressure to be diurnally constant, the wet (T_w) and dry bulb (T_d) temperatures recorded in the Stevenson screen at 0900 hours were used to compute the mean daily VPD from

$$VPD = e_s(\bar{T}) - [e_s(T_w) - \gamma(T_d - T_w)] \qquad \text{——(2.4)}$$

where e_s ($\bar{T}$) is the saturation vapour pressure at temperature $\bar{T}$. The psychrometer constant was taken as the fully ventilated value of 0.66 mb C^{-1}. Although γ is often assumed to be 0.8 for Stevenson screen measurements, it is of little consequence in Eq.2.4 since usually $(T_d - T_w) < 2.5$ C.

ET measurements for extended periods were found from the drainage lysimeter using the water balance equation for the period 0 to τ,

$$ET = RF - J + W_0 - W_\tau \qquad \text{——(2.5)}$$

where RF is rainfall, J drainage and $W_0 - W_\tau$ the change in soil water storage. Data over five periods of a month or longer were obtained in this way. The lysimeter covered an area of 2 m^2 and was 1 metre deep. Daily drainage from the lysimeter was measured by monitoring the outflow of water as detailed in Chapter 4. This to a reasonable approximation simulates the drainage occurring in the field. If the periods selected for determination of ET by Eq.2.5 begin and end at the

cessation of a drainage event, $W_o - W_\tau$ can be ignored. So for four of the periods it was possible to find ET as RF-J. The end of the period September-October 1975 did not coincide with the cessation of a drainage event, so $W_o - W_\tau$ was estimated using neutron probe data from an adjacent area. The absolute error in the measurement of ET by Eq.2.5 was estimated as $\pm$ 0.05 (RF). This value includes error due to both measurement and the use of RF data from a site 1 km away. Comparison of 47 daily RF values measured above the crop with those measured at the meteorological site showed a mean difference of 1.8%. In the computation of ET the surface was assumed to always be well-watered. The high frequency of rainfall, it is considered, ensured that the soil surface was sufficiently wet, all the time, before full crop cover was attained.

The form of Penman's equation used was essentially that which he gave in 1956

$$ET_p = [s/(s+\gamma)](R_n - G) + [\gamma/(s+\gamma)][0.266\,VPD(0.5 + 0.0052u)] \quad \text{---(2.6)}$$

where the VPD is in mb, and u is the average wind speed in km/day at a height of 5.5 m. This equation is one of the commonly used Penman formulations, and no significant improvement based on single height meteorological data has since been developed. The values of s and γ were evaluated at the mean daily temperature, as is usual when applying Penman's equation.

Wind speed was measured 75 cm above the crop. The wind speed gradient required in van Bavel's (1966) formulation of Penman's convective term was computed using the fact that the wind speed is zero at height z_0, the surface roughness. The surface roughness was estimated on the basis of a regression established between z_0 and crop height by periodic wind profile measurements during adiabatic profile conditions.

In determining the Priestley and Taylor estimates for the oats the 24-hour or daylight value of ET_{eq} was

computed by summing the appropriate half hour ET_{eq} values. The estimates were not significantly different from those found using $s/(s+\gamma)$ computed from the daily mean temperature and the (R_n-G) for the respective periods, as the function $s/(s+\gamma)$ is a slowly varying function of temperature. The soil heat flux was included in the ET_{eq} term for the oats data. On a 24 hour and daylight basis the average $|G/R_n|$ was 4.6% and 6.8% respectively. Therefore G can be ignored if an equation of the form

$$ET = \alpha[s/(s+\gamma)]R_n \qquad \text{——(2.7)}$$

is used with $(s/(s+\gamma))$ calculated at the mean daily temperature. Since Eq.2.7 is applicable only to full-cover crops G is usually small so can be ignored. The summer data (J.P. Kerr and J.S. Talbot, unpublished data; Kerr *et al.* 1973) for paspalum, pasture, and lucerne used ET_{eq} estimates based on Eq.2.7.

2.3 RESULTS

The regression of ET estimates using Eq.2.6, against the measured ET is shown in Fig.2.1. Penman's equation provides reasonable daily ET estimates, although somewhat underestimating ET under low radiation conditions. The accuracy was 15-20% on a daily basis, and is similar to that obtained by Tanner and Pelton (1960). However from Fig.2.2 it can be seen that the measured ET is just as strongly correlated with 24 hour ET_{eq} data, suggesting that the considerable effort in measuring wind speed and VPD to determine Penman's convective term is not warranted. The convective term (C) can be found from measurements of $(ET-ET_{eq})$. However measurement errors in ET ($\pm$ 11%) and ET_{eq} ($\pm$ 5%) result in an error in C of, say δ, which can be shown to be $\sqrt{(0.11\ ET)^2 + (0.05\ ET_{eq})^2}$. In fact the Penman convective term fell within the range $C \pm \delta$ on only 21 of the 61 days for which this comparison was

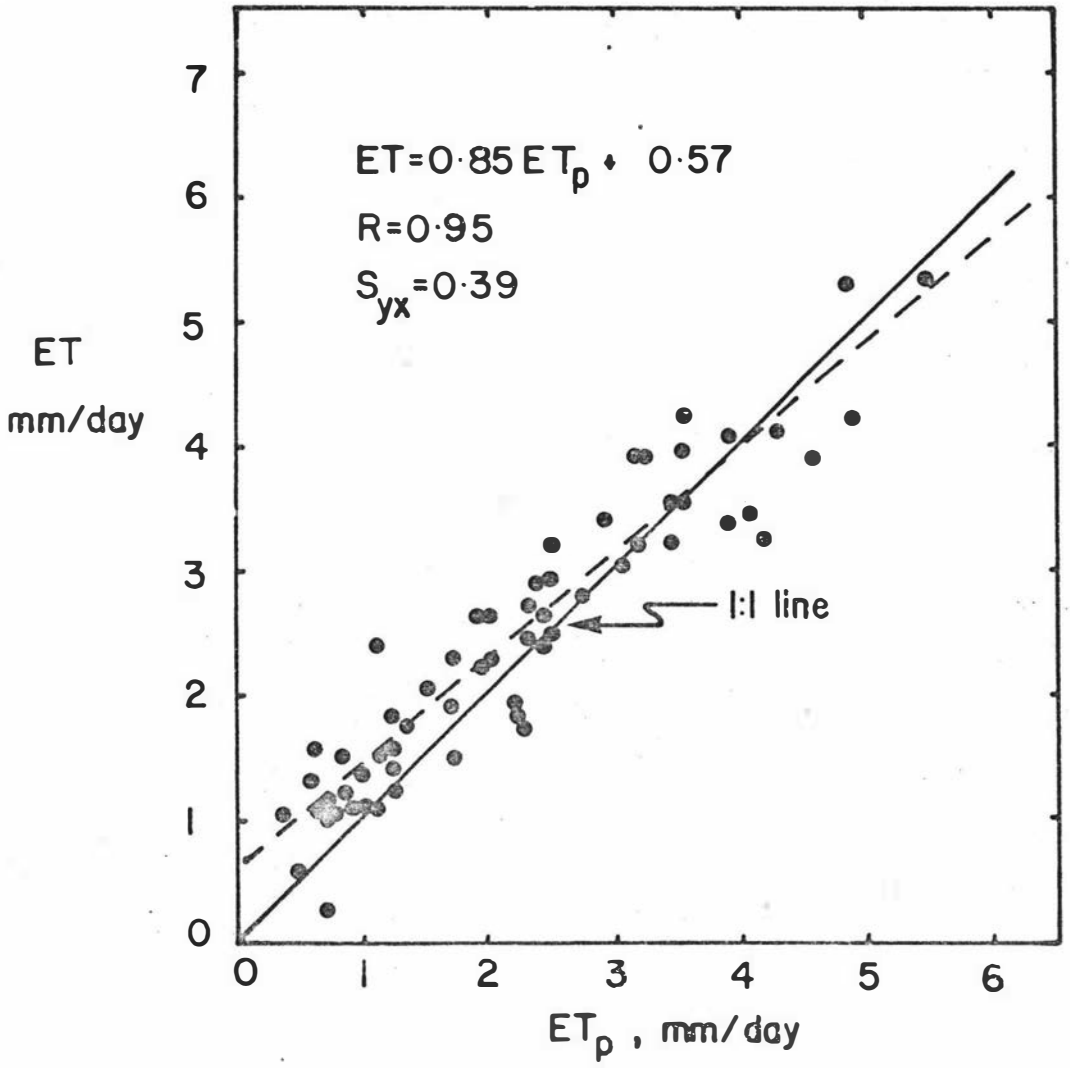

Fig.2.1 Comparison of measured evapotranspiration (ET) against computed Penman estimates (ET_p), for oats. The correlation coefficient (R) and standard error of the estimate (S_{yx}) apply to the linear regression equation.

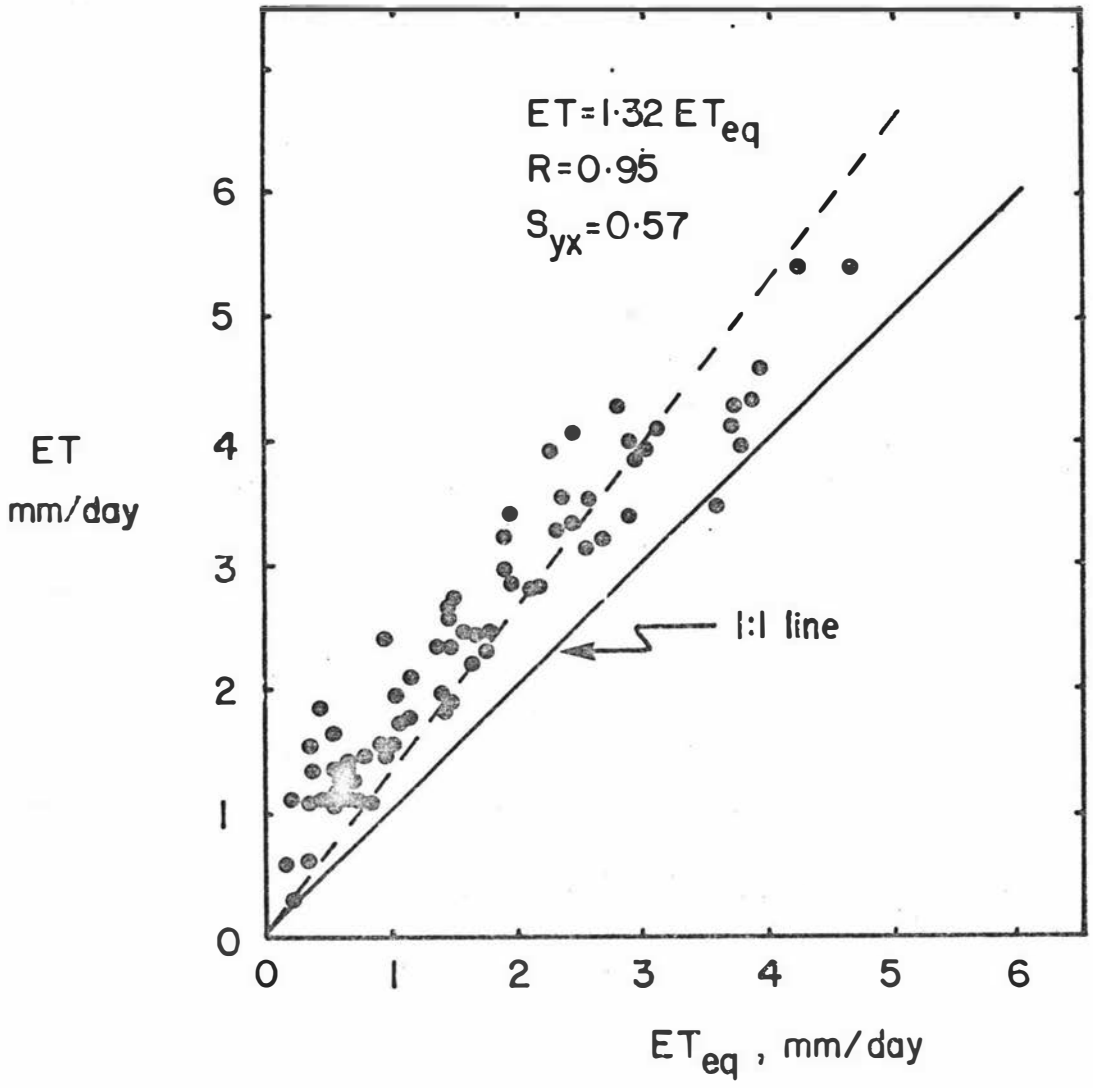

Fig.2.2 Comparison of measured ET against the 24 hour value of the equilibrium evaporation rate (ET_{eq}) for oats, S_{yx} calculated for the regression line constrained through the origin.

carried out. Little improvement resulted from the use of the more complex convective term, based on turbulent transfer along an adiabatic wind profile using the wind speed gradient measured above the crop, as suggested by van Bavel (1966). It appears that in general attempting to model the complicated convective process is not warranted for ET estimation purposes; use of the correlation between ET and ET_{eq} is simpler and just as effective.

From the regression of ET on ET_{eq}, α is found as the slope of the regression constrained through the origin. Davies and Allen (1973) state that in the determination of α, the period of integration is not important, whereas Tanner and Jury (1976) found that for crops the daylight and 24-hour values of α can differ by up to 15%, the latter being larger. Comparison of Figs.2.2 and 2.3 show the daylight value of α to be 8% less than the 24 hour value in the present study. For a shallow arctic lake however, Stewart and Rouse (1976) found there to be no difference between half hourly values of α and the 24 hour value.

The regression of ET against the 24 hour ET_{eq}, constrained through the origin produced a relatively high standard error of the estimate (S_{yx}) of 0.58 mm/day, compared to a normal linear regression which significantly reduced it to 0.36 mm/day. The relative error ($S_{yx}/\bar{ET}$) in estimating the daily value of ET from the regression in Fig.2.3 is 17%. Equation 2.2 can be expanded to give

$$ET = \alpha\, ET_{eq} \qquad \text{——(2.8)}$$

$$= \alpha\, ET'_{eq} + \alpha ET''_{eq} \qquad \text{——(2.9)}$$

where the single and double primes refer to the daylight and nocturnal periods, respectively. As indicated above, dewfall is likely to be relatively small and would not

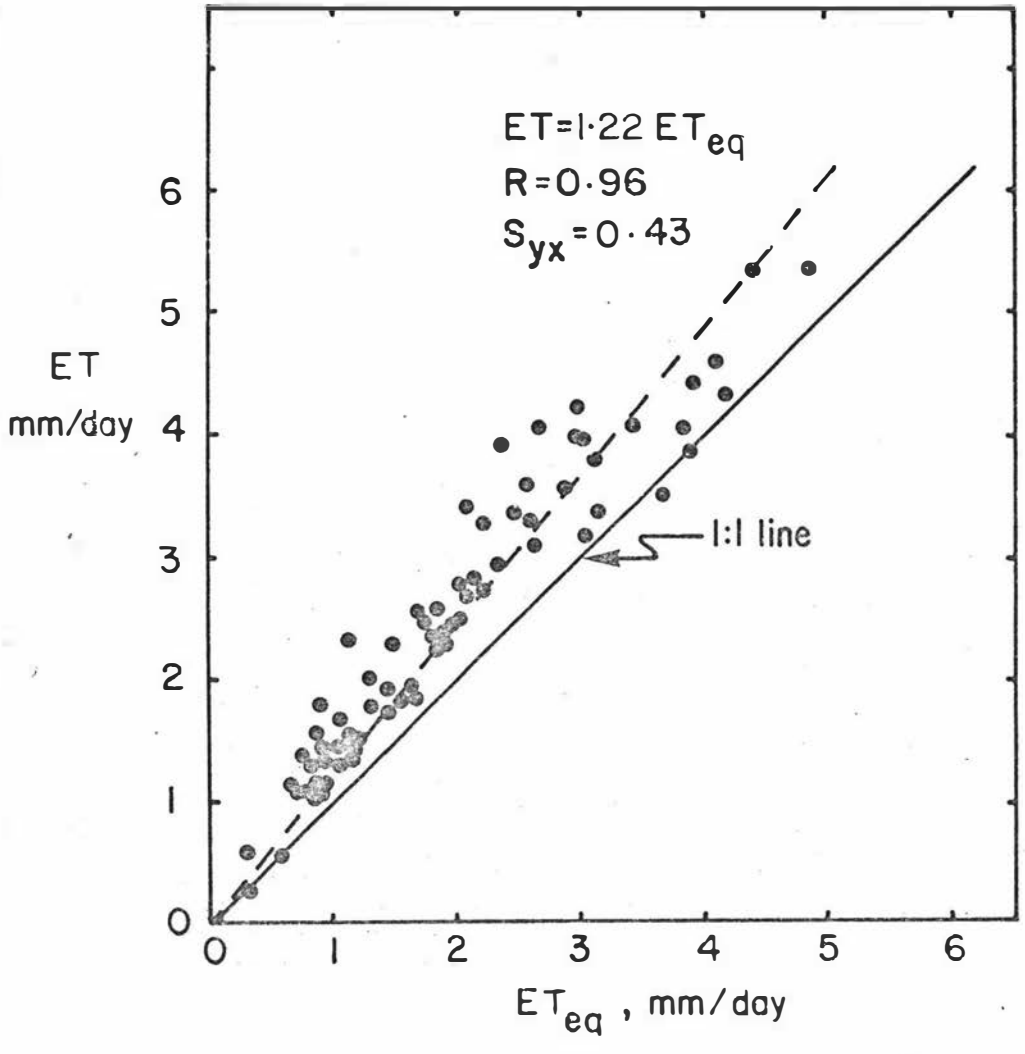

Fig.2.3 Comparison of measured ET against the daylight ET_{eq}, for oats.

account for the deviation of the regression line through the origin at low R_n in Fig.2.2. When R_n is low, 24-hour R_n is significantly less than the daylight R_n, as will be the respective ET_{eq} values. The daylight and 24-hour ET values are considered to be equal. Consequently Priestley and Taylor's model of ET being proportional to ET_{eq} may not hold over 24 hours in such circumstances, since the nocturnal value of α may not be the same as the daylight value (c.f. Eq.2.9). Under high R_n conditions the proportionality will tend to hold as ET''_{eq} will be relatively less significant. The daylight regression is virtually unchanged when a normal linear regression is fitted, verifying that this proportionality holds.

For most long term ET estimation purposes, measurement of R_n is impractical. It is better to use the regression based on daylight values of ET_{eq} as it is easier to model the daylight values of R_n if using a previously established regression of R_n on the more easily measured or computed incoming short wave radiation ($K\downarrow$). Fig.2.4 shows the daylight and 24-hour regressions of R_n on $K\downarrow$. The value of S_{yx} is reduced from 0.48 to 0.29 mm/day if the daylight, rather than the 24 hour regression is used.

The daylight value of α can be seen in Fig.2.5 to be effectively constant throughout winter, spring and early summer. For reasons discussed above the 24-hour value of α was found to vary from 1.80 in winter to 1.24 in early summer. As expected, for a well-watered surface in the absence of advection, the value of α tends to remain within the interval $[1,(s+\gamma)/s]$, as shown in Fig.2.5, although there is a reasonable amount of scatter. Part of this scatter can be attributed to measurement errors in ET and ET_{eq} resulting in an error in α of approximately $\pm$ 12%.

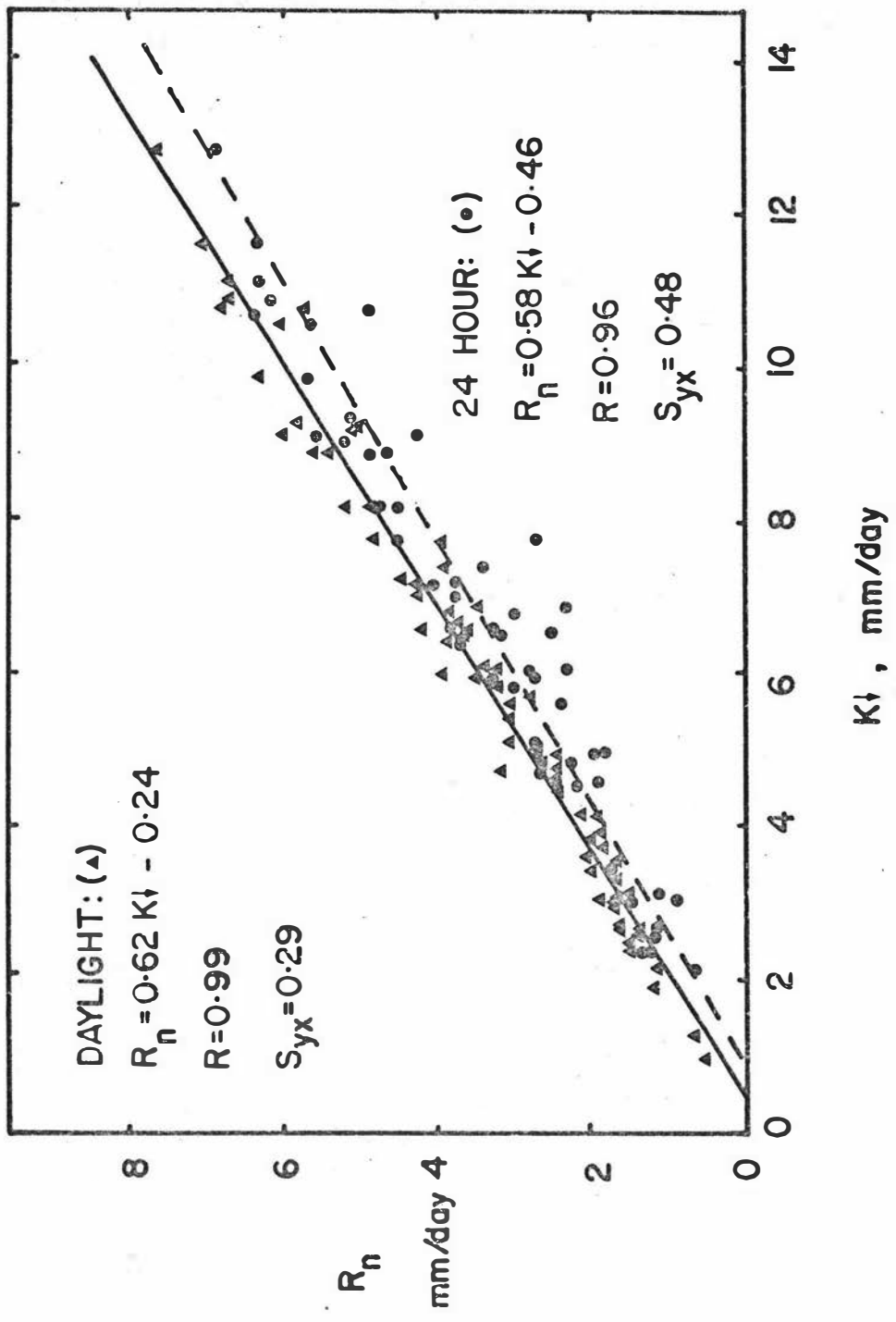

Fig.2.4 Regression of incoming solar radiation (K↓) against the net radiation (R_n) measured over oats. Both the 24 hour and daylight regressions are shown.

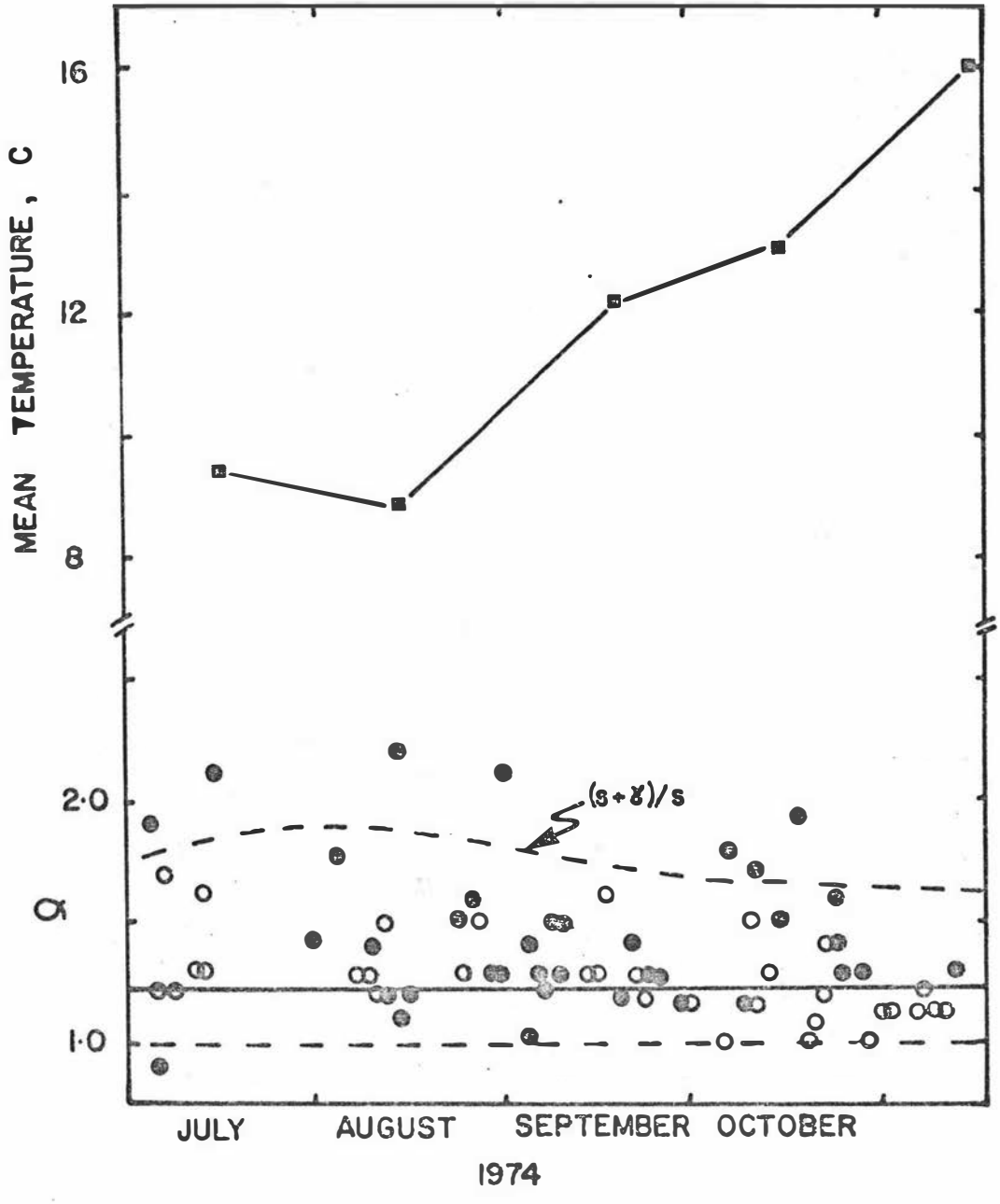

Fig.2.5 Ratio of daylight ET/ET_{eq} (i.e. α) for oats from winter to early summer. Days when free water was noted on the crop are indicated (●). The mean monthly temperature is shown. The limits on α of 1 and $(s+\gamma)/s$ suggested by Eq.2.3 are also shown (---).

Another cause of the variation in α may be the presence or absence of free water on the leaves. In Fig.2.5 those days on which free water was observed to have remained on the leaves for at least 3 hours during daylight are indicated. The α values tend to be higher on such days. Modifying Monteith's (1965) empirical expression gives

$$\alpha = ET/ET_{eq} = [(s+\gamma)/s.\log_{10}(25/r_s)^{1/2}] \qquad \text{—(2.10)}$$

This equation gives some indication of the likely magnitude of the effect of the crop resistance (r_s) on α. Kerr and Beardsell (1975) showed that for a paspalum pasture the presence of dew lowered r_s from about 1.0 to approximately 0.5 sec/cm. Applying this result in Eq.2.10, at a temperature of 10 C suggests that free water on the leaves would, in this case, raise α from 1.26 to 1.53. This result is in general agreement with the range of α found for the oats (Fig.2.5). However other factors will also influence α, such as the varying interaction between the radiant heating of the crop and the air temperature, resulting in varying convective transfer. Albeit, to a reasonable approximation α may be considered constant (α = 1.22) over the study period.

Figure 2.6 shows that the ET data obtained independently from the lysimeter and that predicted by 1.22 ET_{eq} are in reasonable agreement, allowing for the uncertainty of the measured values.

Calculations of monthly ET by Penman's equation for May through October for both 1974 and 1975 (J.D. Coulter pers.comm.) are given in Table 2.1 with the estimates based on 1.22 ET_{eq}. As R_n data were unavailable, Coulter used sunshine hour data with de Lisle's (1966) constant to find $K\downarrow$ and assumed an albedo of 0.25, and used Brunt's (1932) longwave radiation formula to calculate R_n. The two estimates are in quite reasonable agreement,

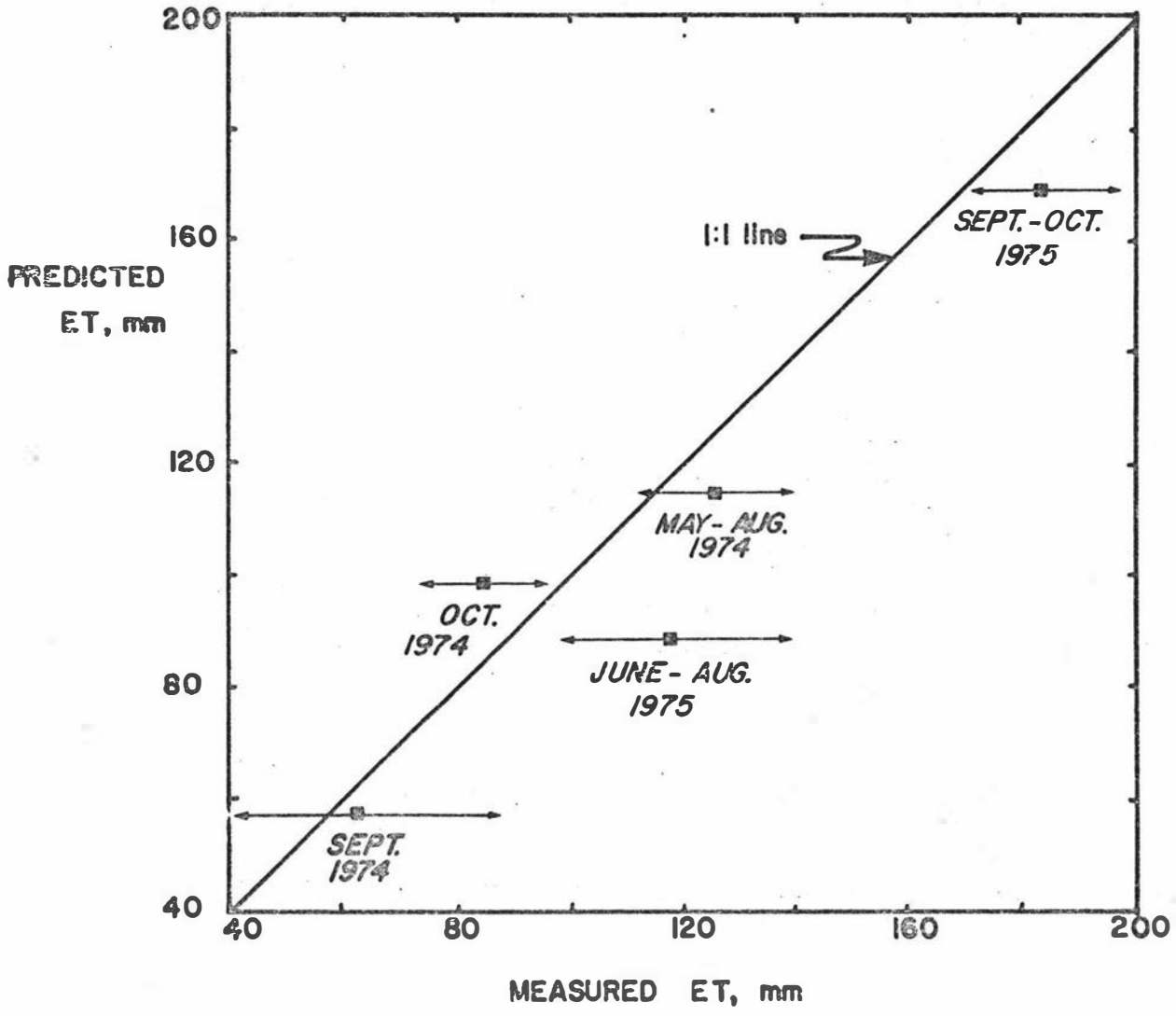

Fig.2.6 Predicted ET (1.22 ET_{eq}) for selected periods against the ET measured from a water balance applied to the lysimeter growing oats. The error band is $\pm$ 0.05 (rainfall) over the period.

Table 2.1 Comparison of monthly values of 1.22 ET_{eq} and Penman estimates of evapotranspiration (ET_p) for Palmerston North

Month	1974		1975	
	1.22 ET_{eq}	ET_p^*	1.22 ET_{eq}	ET_p^*
May	35.3	34.4	33.4	35.4
June	27.0	21.4	25.3	18.0
July	22.4	23.5	27.5	22.2
August	41.3	34.7	36.9	36.2
September	57.3	58.3	58.3	57.7
October	89.6	86.0	97.0	101.6
TOTAL	272.9	258.3	278.4	271.1

* J.D. Coulter, pers. comm.

especially under higher radiation conditions when errors in estimating long wave radiation would be relatively less important.

However, Coulter's (1973a) Palmerston North data for the ratio ET_p to ET_{eq} imply α to be 4.0 in July, dropping to 1.41 in October. As some of these values are beyond the range indicated by Eq.2.3 he considers this as "confirming the important role of advection ... generally in winter". However the measured data presented in Fig.2.5 show in general far lower values of α, and very few "advective days". It is likely that the high α values inferred by Coulter (1973a) are an artifact, perhaps due in part to the underestimation of R_n by Brunt's (1932) equation under low radiation conditions.

This far only data for α relating to oats from winter through to early summer have been presented, and it is necessary to verify that this method of ET estimation has value for other crops in other seasons. Data from Bowen ratio-energy balance measurements previously obtained over well-watered paspalum, pasture and lucerne during summer near Palmerston North, combined with the oats data for winter, are shown in Fig.2.7. The resulting value of α (1.21) is similar to the value previously found, thus suggesting that reasonable estimates of daily ET ($S_{yx}/\overline{ET}$ = 19%) may be obtained for well-watered crops using such a procedure unless severe advection occurs. As most ET estimation procedures are used to compute water requirements for irrigation scheduling, ET totals for approximately weekly periods are of more importance than daily values. Grouping the data into 7 day totals reduces the error from 19% to a more acceptable level of 8%. Although it is to be expected that as the fetch becomes very large, α will tend to approach unity (McNaughton, 1976), in most situations, particularly in New Zealand, this condition will not be reached and so α is generally greater than unity and probably about 1.2.

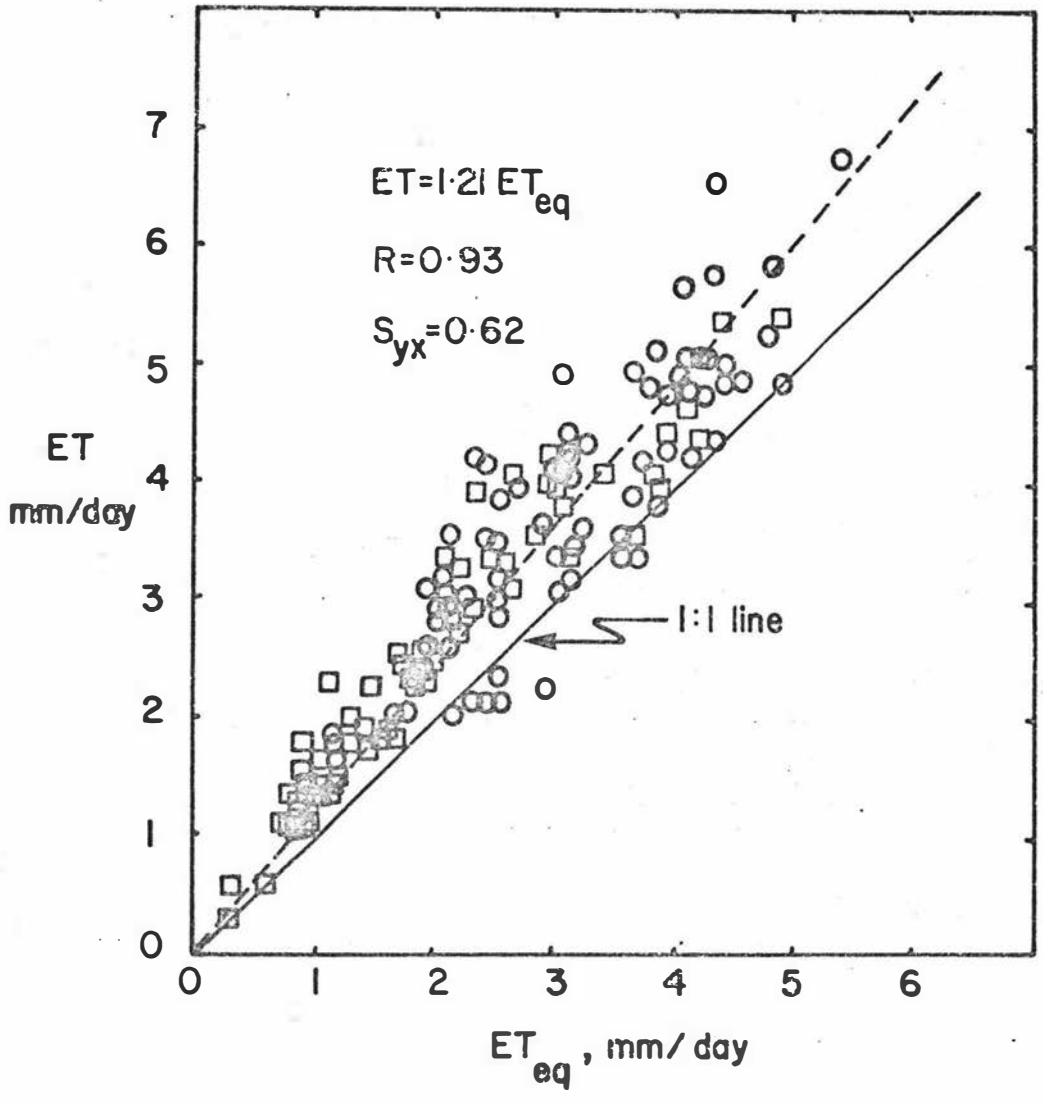

Fig.2.7 Comparison of measured ET over oats (□) and lucerne, paspalum or pasture (0) against the daylight ET_{eq}.

2.4 CONCLUSIONS AND SUMMARY

Penman's equation was found to provide reasonable estimates of daily ET under the climatic conditions experienced during the growth of an oats crop in winter. However a closer analysis revealed that this was almost entirely due to the significant correlation between ET and the ET_{eq} term in the Penman equation. The convective term tended to be small and positive and the substantial effort involved in its computation did little or nothing to improve the efficacy of the method.

The ET estimation procedure of Priestley and Taylor, based on the correlation between ET and ET_{eq}, was simpler and just as accurate. Values of the daylight Priestley-Taylor coefficient (α) over oats were found to be constant throughout the season, although possessing a day-to-day variability of 17%. Summer data over paspalum, pasture and lucerne in combination with the winter data over oats gave a similar overall value for α. Nocturnal evaporation or dewfall was considered negligible. Calculation of ET from the regression on ET_{eq} from daylight rather than 24 hour data resulted in a lower standard error and removed seasonal variation in α. Under low R_n conditions when nocturnal re-radiation is more significant, no fixed proportionality between ET and ET_{eq} was found when 24-hour ET_{eq} data was used. Also in applying such an ET estimation procedure values of R_n will be generally based on a relationship with solar radiation or sunshine hours (de Lisle, 1966), and the accuracy of such estimates is greater when only the daylight period is considered. Because only temperature and solar radiation data are required, Priestley and Taylor estimates of ET could be applied to well-watered crops more easily and in a greater number of locations within New Zealand than Penman estimates.

CHAPTER 3

WATER RETENTION IN SOIL UNDERLAIN BY A COARSE-TEXTURED LAYER

3.1 INTRODUCTION

Storage of water in the root zone of field soils is of importance to both dryland and irrigated agriculture. As discussed in Chapter 1, the upper bound of available water storage, usually termed "field capacity", is an elusive quantity. The concept is more tenable for coarse than fine-textured soils, because in such soils the hydraulic conductivity drops more rapidly with decreasing pressure potential, causing the water flux to decrease more rapidly. Miller (1969) showed that permeable soils underlain by a coarse layer exhibit a distinct field capacity, in that, after wetting the water content profile fairly rapidly approaches a quasi-static equilibrium, as is evident in Fig.1.2.

The fact that soils underlain by a coarse-textured stratum, such as coarse sand or gravels, store more water at field capacity than their uniform counterparts has long been known (Alway and McDole, 1917). Later the experiments of Moore (1939) explained this phenomenon on the basis of the relative shape of the hydraulic conductivity-pressure potential curves. Much experimental work has subsequently been carried out into the effects of coarse layers on water storage at field capacity (Robins, 1959; Eagleman and Jamison, 1962; Miller, 1963, 1969, 1973; Miller and Bunger, 1963; Unger, 1971; Poulovassilis et al. 1974; Brown and Duble, 1975). Using the observation that the pressure potential within the soil above the coarse layer decreased by 1 cm for each centimeter increase in elevation, Miller and Bunger (1963) were able to use water retentivity curves to predict successfully field capacity in layered soil situations. Subsequently Miller (1969, 1973) measured the effect of the soil depth and coarseness of the underlay on water retention. He concluded that

"the amount of water held by a layered soil increases as the underlying particles become coarser ....(and) it decreases with elevation above the layer" (Miller, 1969, p.28).

In the literature, only limited reference appears to have been made about the effect of the shape of the water retentivity curve of the overlying soil on the amount of water retained. Although Poulovassilis *et al.* (1974) hinted at such a relationship by stating that " ..... the water lost by Layer 1 (i.e. the upper layer) depends on the difference between the layers, as far as their moisture characteristics and conductivities are concerned ...." (p.213), they did not comment on its form. Also the observations of Alway and McDole (1917) and Miller (1973) indicated that enhanced water retention depended on the soil type as well as its height above the coarse-textured layer.

Thus there exists a need for a theory to describe water retention in layered soils. The only attempt at a theoretical treatment of the subject has been by Miller (1969) based on the similarity theory of Miller and Miller (1956). The basis of the similarity theory is the scaling of the pressure potential function (ψ) by

$$L_1 \psi_1 = L_2 \psi_2 \qquad \text{——(3.1)}$$

and the diffusivity function (D) by

$$D_1/L_1 = D_2/L_2 \qquad \text{——(3.2)}$$

where L_1 and L_2 are the characteristic lengths. Thus Miller (1969) could calculate the functions D_2 and ψ_2 for a hypothetical underlay relative to a reference coarse underlay (D_1, ψ_1, L_1) by varying the characteristic length (L_2). Use of a finite difference numerical scheme for simulating drainage thus enabled him to calculate the effect of the coarseness of the underlay (L_2) on the water storage in the profile, relative to the soil underlain by the reference underlay. This approach,

although illustrative, is of little practical use because of the difficulty in measuring the characteristic lengths.

In this chapter, a theory is derived that incorporates the factors involved in determining the water storage and permits analysis of their relative effects. The theory is applied to predict the retention of water in situ by a Manawatu fine sandy loam, which consists of finer textured soil overlying a coarse layer. Similar coarse layers underlie a number of other important agricultural soils in New Zealand, such as the aeolian or alluvial deposits of fine material on coarse Quaternary outwash gravels or volcanic lapilli.

3.2 THEORY

The water retentivity curve of a soil can be described by modifying the expression developed by Brooks and Corey (1966) to yield

$$\theta(\psi) = \begin{cases} \theta_s(\psi_e/\psi)^{\lambda} & \psi \leq \psi_e \quad \text{——(3.3a)} \\ \theta_s & \psi > \psi_e \quad \text{——(3.3b)} \end{cases}$$

where θ is the volumetric water content, θ_s the porosity, ψ the pressure potential and ψ_e is the air entry pressure potential. To simplify the subsequent analysis ψ is expressed in units of energy per unit weight. The parameter λ, termed by Brooks and Corey (1966) the pore size distribution index, describes the shape of the unsaturated portion of the water retentivity curve (Fig.3.1) and depends upon the soil texture and structure. In the following analysis only the unsaturated case (i.e. $\psi \leq \psi_e$) is considered as the saturated case ($\psi > \psi_e$) is the same as the simple unsaturated case of $\psi \leq \psi_e$ when $\lambda = 0$.

Consider first the case of a uniform non-layered soil. Following saturation permeable soils tend to

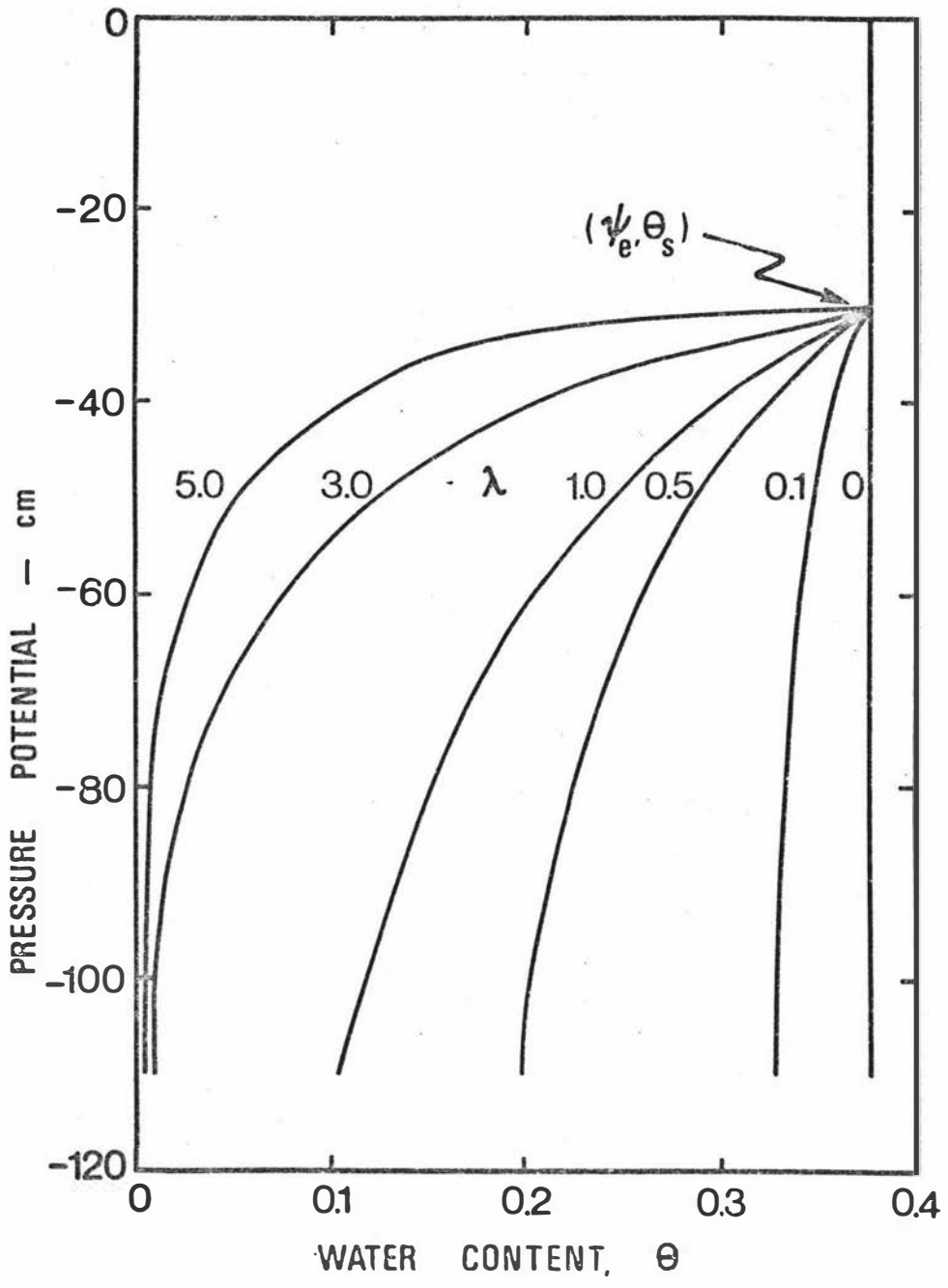

Fig.3.1 Variation in the water retentivity curve due to changing the value of the pore size distribution index λ .

drain to a uniform pressure potential (Gardner, 1960; Davidson et al. 1969). Let ψ_c be the pressure potential at which K, the hydraulic conductivity becomes very small, and hence drainage effectively ceases. Then in a uniform soil of depth z_i when drainage has ceased

$$\psi(z) = \psi_c \qquad 0 \leq z \leq z_i \qquad \text{—(3.4)}$$

consequently by Eq.3.3.

$$\theta(z) = \theta_s(\psi_e/\psi_c)^{\lambda} \qquad 0 \leq z \leq z_i \qquad \text{—(3.5)}$$

that is the water content is uniform with depth. Since the water stored in the profile is given by

$$W = \int_0^{z_i} \theta(z)\, dz \qquad \text{—(3.6)}$$

then the water stored in a uniform profile (W_u) is given by

$$W_u = \theta_s(\psi_e/\psi_c)^{\lambda} z_i \qquad \text{—(3.7)}$$

However, should the same soil be underlain at depth z_i by a coarse-textured stratum, then drainage will cease at a wetter pressure potential, ψ_i at z_i (Fig.3.2). Immediately above this interface, since there is negligible flux it follows that $\partial\psi/\partial z = 1$ (Miller, 1969, 1973). This unity pressure potential gradient is considered to apply only until the pressure potential reaches ψ_c at some depth, z^*. Above z^* the effect of the layering is negligible because the K (ψ) relationship is steep. Therefore, for $z < z^*$ the pressure potential profile becomes that of a uniform soil, namely $\partial\psi/\partial z = 0$. The depth z^* can be defined by

$$z^* = \begin{cases} 0 & z_i \leq \psi_i - \psi_c \qquad \text{—(3.8a)} \\ \psi_c + z_i - \psi_i & z_i > \psi_i - \psi_c \qquad \text{—(3.8b)} \end{cases}$$

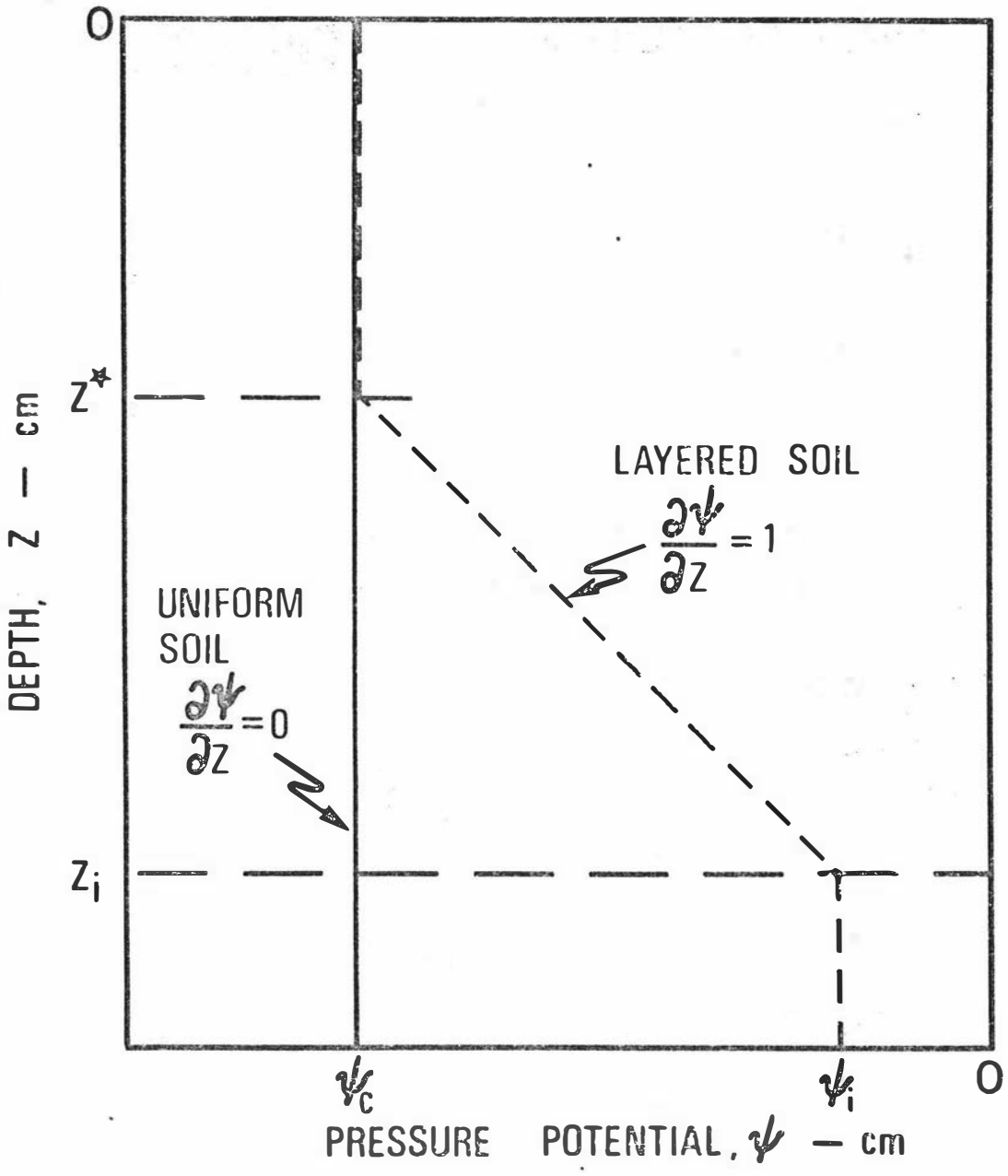

Fig.3.2 The pressure potential profile in a layered soil and in a uniform soil at the cessation of drainage.

so, in the layered case

$$\psi(z) = \begin{cases} \psi_i - z_i + z & z \geq z^* \quad \text{——(3.9a)} \\ \psi_c & z < z^* \quad \text{——(3.9b)} \end{cases}$$

Consequently the water content profile is given by

$$\theta(z) = \begin{cases} \theta_s[\psi_e/(\psi_i - z_i + z)]^{\lambda} & z \geq z^* \quad \text{——(3.10a)} \\ \theta_s[\psi_e/\psi_c]^{\lambda} & z < z^* \quad \text{——(3.10b)} \end{cases}$$

The water stored in a layered profile (W_L) is found using Eqs.3.6 and 3.10 as

$$W_L = \theta_s\left[\int_0^{z^*} (\psi_e/\psi_c)^{\lambda} dz + \int_{z^*}^{z_i} (\psi_e/(\psi_i - z_i + z))^{\lambda} dz\right] \quad \text{——(3.11)}$$

It is now possible to calculate the increase in water storage due to layering (ΔW). Since

$$\Delta W = W_L - W_U \quad \text{——(3.12)}$$

use of Eqs.3.7 and 3.11 in Eq.3.12 gives after integration

$$\Delta W = \begin{cases} \theta_s(-\psi_e)^{\lambda}\left[\left\{(-\psi_i)^{1-\lambda} - (z_i - \psi_i - z^*)^{1-\lambda}\right\}/(\lambda - 1) + (z^* - z_i)/(-\psi_c)^{\lambda}\right] & \lambda \neq 1 \quad \text{——(3.13a)} \\ \theta_s \psi_e\left[\log_e(\psi_i/(\psi_i - z_i + z^*)) + (z^* - z_i)/\psi_c\right] & \lambda = 1 \quad \text{——(3.13b)} \end{cases}$$

It can be shown that ΔW is continuous and positive for all $\lambda \geq 0$. This function predicts the increase in water retained at the cessation of drainage, due to layering, and incorporates the parameters that serve to control this increase: the character of the overlying soil, the depth to the layer and the coarseness of the underlay.

In some cases however, such a simple situation of uniform soil overlying a coarse underlay does not occur, rather, textural and structural changes occur within the soil.

These changes, whilst not significantly affecting water flow, do alter the storage capacity of the soil. These situations can be analysed similarly. If secondary layering occurs at z_L, it is possible to define the water content profile as follows

$$\theta(z)=\begin{cases}\theta_{s_2}[\psi_{e_2}/(\psi_i-z_i+z)]^{\lambda_2} & 0\leq z\leq z_L \text{ and } z\geq z_2^* \qquad \text{—(3.14a)}\\ \theta_{s_1}[\psi_{e_1}/(\psi_i-z_i+z)]^{\lambda_1} & z_L<z\leq z_i \text{ and } z\geq z_1^* \qquad \text{—(3.14b)}\end{cases}$$

where the subscripts 1 and 2 refer to the different soil layers. This enables an almost identical derivation leading to an expression for W_L. The resulting equation for ΔW is just a simple extension of Eq.3.13.

Consider ΔW as a function of the shape of the water retentivity curve of the overlying soil described by λ, the underlying coarse strata characterised by ψ_i and the depth to the interface z_i. The elements θ_s and ψ_e are assumed constant, and values for use in Eq.3.13 were taken from the Manawatu fine sandy loam data described later. Figs.3.3 and 3.4 show the interrelations of ΔW, λ, ψ_i and z_i predicted by Eq.3.13. Any textural or structural variations in the overlying soil, which alter λ, can be seen in Figs.3.3 and 3.4 to have a marked effect on ΔW. Poorly structured clayey soils ($\lambda\cong 0$) and very coarse-textured ($\lambda>5.0$) soils gain little extra water storage in layered situations, whereas the greatest increase occurs for sandy soils ($\lambda\cong 1$). It is possible to determine the maximal value of λ numerically. The resulting λ_{max} values are shown in Figs.3.3 and 3.4, and indicate that, given the fixed parameters θ_s, ψ_e, ψ_c and $z_i \geq 25$ cm, then $0.7<\lambda_{max}<1.4$ for $-100\leq\psi_i\leq -30$ cm. That is sandy soils in layered situations, tend to have larger values of ΔW.

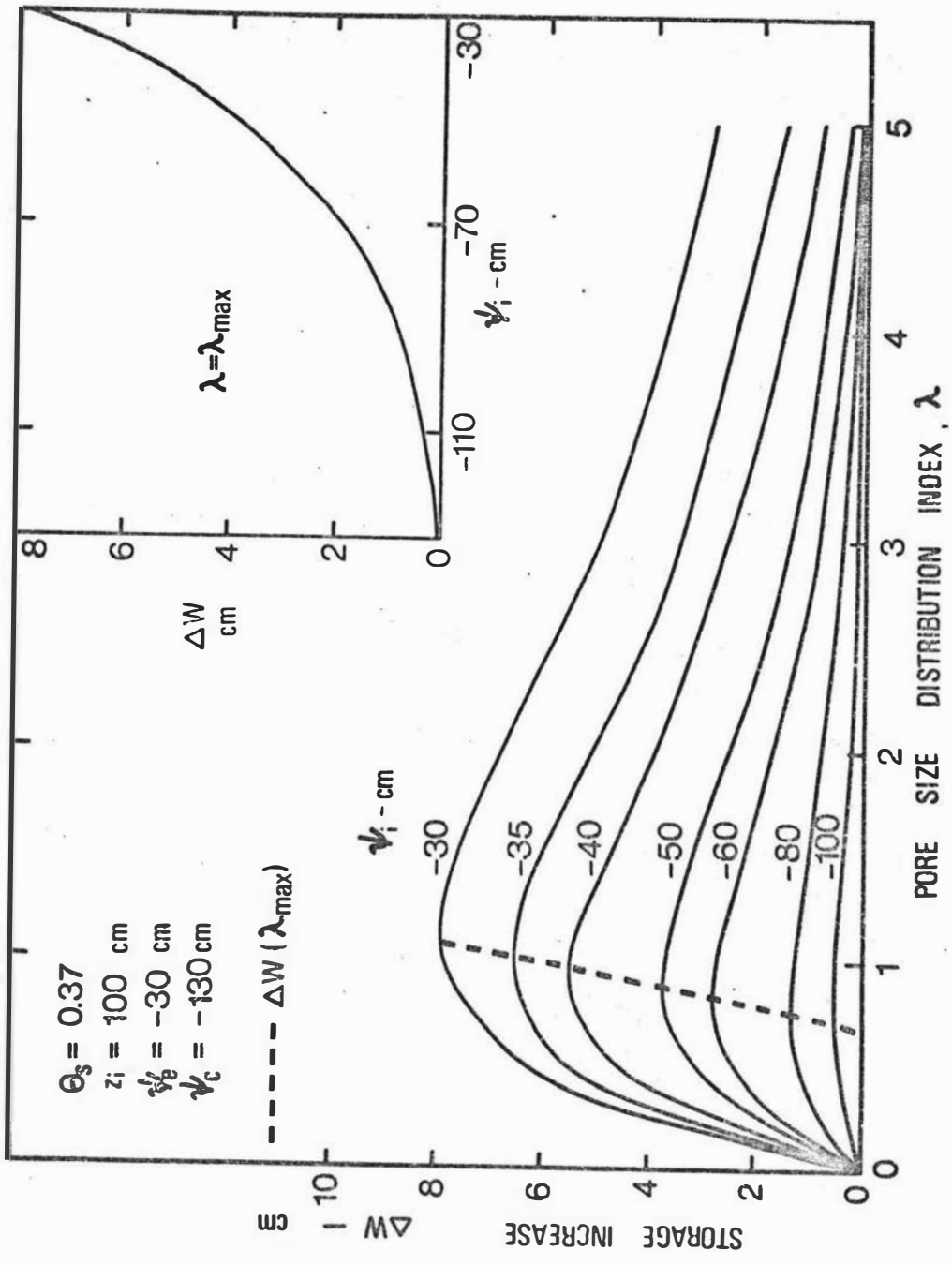

Fig.3.3 The increase in storage ΔW, as a function of the pore size distribution index λ, for varying ψ_i, the cut-off potential in the underlay. Inset. The increase in storage as a function of ψ_i for $\lambda = \lambda_{max}$.

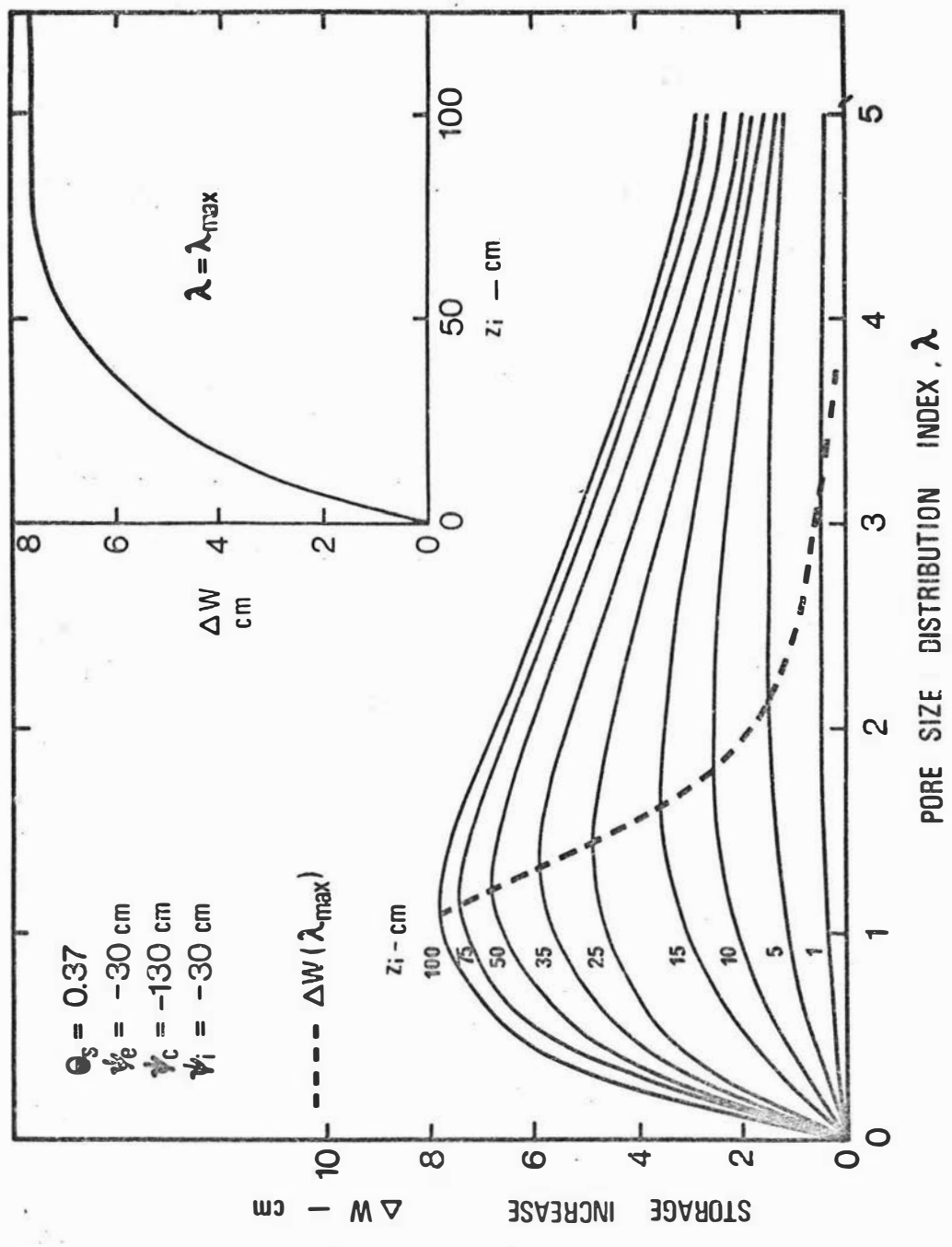

Fig.3.4 The increase in storage ΔW, as a function of the pore size distribution index λ, for varying z_i, the soil depth. Inset. The increase in storage as a function of z_i for $\lambda = \lambda_{max}$.

The effect of varying ψ_i, the cut-off pressure potential in the coarse underlay at which drainage effectively ceases, is also depicted in Fig.3.3 where $\Delta W\ (\psi_i)$ is shown for $\lambda = \lambda_{max}$. The sensitivity of ΔW to slight changes in ψ_i for high values of ψ_i is striking. Changing ψ_i from -30 to -50 cm halves ΔW. As the soil profile becomes more uniform, i.e. ψ_i approaches ψ_c, the effect of layering on the amount of water retained becomes very small.

From Fig.3.4 it can be seen that deep soil profiles (i.e. large z_i) enable the textural and structural variations described by λ to express their influence more than for shallow profiles. Also, the graph of $\Delta W\ (z_i)$ for $\lambda = \lambda_{max}$ shows that only small increases in ΔW occur for $z_i > 50$ cm. In fact, doubling the soil depth from 50 cm to 100 cm increases ΔW by only 16%. This demonstrates the known fact that most of the increased storage in layered soils is in the region immediately above the interface.

In the case where secondary layering occurs at z_L, Fig.3.5 shows that the main contribution to ΔW, as expected from Fig.3.4, comes from the zone immediately above the interface at z_i. In fact in this case it matters little what value λ_2 assumes.

The theoretical expressions derived for W_U, W_L and ΔW show that the shape of the water retentivity curve of the soil overlying the coarse stratum is a major factor controlling the field capacity of layered soils. Further, the theory clarifies the role that soil depth and coarseness of the underlay play in water retention in such soils. It serves as a useful basis for the analysis and interpretation of field data, since Eqs.3.7, 3.11 and 3.13 can be applied easily to field situations.

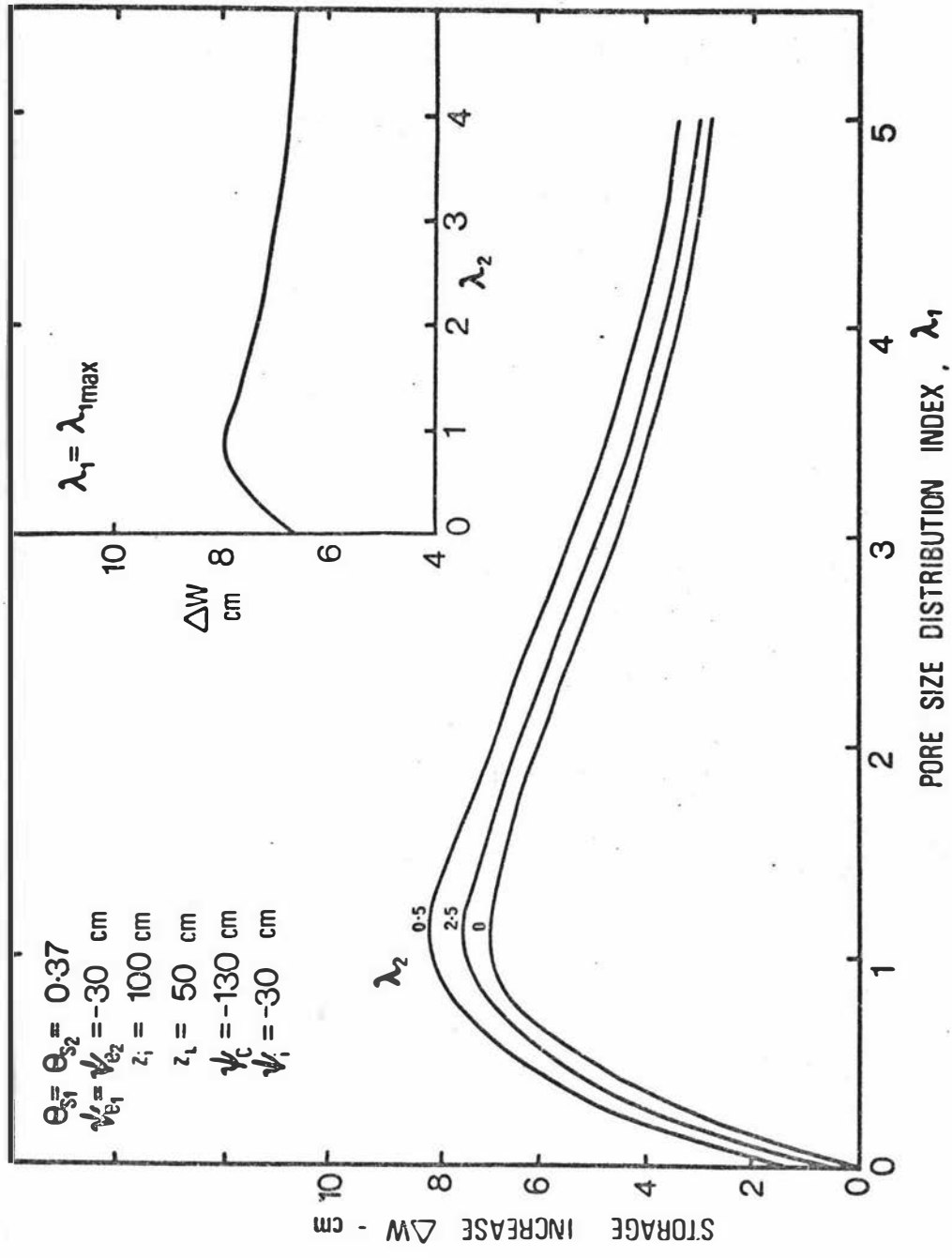

Fig.3.5 The increase in storage ΔW, in a soil with secondary layering at depth z_L. The subscript '1' refers to the soil $z_L < z \leq z_i$ and '2' to the soil $0 \leq z \leq z_L$. Inset. The increase in storage as a function of λ_2 for $\lambda_1 = \lambda_{1max}$.

3.3 EXPERIMENTAL METHODS AND MATERIALS

Most of the work to date has involved experimental studies of the effect of varying the depth and coarseness of the underlay in artificially constructed soil profiles. The paucity of research on naturally occurring layered soils *in situ* is in part due to the inapplicability of "flooded-plot" experiments (Rose *et al.*, 1965) because of significant horizontal flow of water that occurs in such soils during these experiments (Miller, 1963).

As discussed in Appendix III the profile of the Manawatu fine sandy loam may be subdivided into three elements. The first 50 cm consists of a fine sandy loam, which is underlain to a depth of 90 cm by a fine sand, and beyond 90 cm by a gravelly coarse sand. The physical characteristics of these profile elements are given in Table 3.1. The soils of the Manawatu series typically are made up of these three elements, although there is variation in the depth of the layers (Cowie, 1972). To a first approximation spatial variation in water storage can be accounted for by variations in z_i and z_L (Appendix III).

Haines' method (Vomocil, 1965) was used to obtain the water retentivity data for pressure potentials greater than -150 cm. Equations of the form given in Eq.3.3 were fitted to the data in this range, and are shown in Fig.3.6. The functions can be seen to fit the data reasonably well, particularly in the portion of the curve required in the subsequent analysis (i.e. $\psi \leqslant \psi_i \cong$ -35 cm). The -1000 cm water contents given in Table 3.1 were determined using the pressure plate apparatus. Linear interpolation of log (ψ) vs log (θ) was used to obtain water contents in the -1000 cm to -150 cm range.

The laboratory hydraulic conductivity data shown in Fig.3.7 were obtained using the long-column method of Childs (1945). Conductivity data at low pressure

Table 3.1 Physical characteristics of a Manawatu fine sandy loam

Depth (cm)	Texture	θ_s	θ at ψ = -1000 cm	ψ_e (cm)	λ	K_s (cm/day)
0-50	Fine sandy loam	0.37	0.17	5.2	0.06	110
50-90	Fine sand	0.38	0.05	28.7	0.94	251
> 90	Gravelly coarse sand	0.27	0.04	8.8	1.16	784

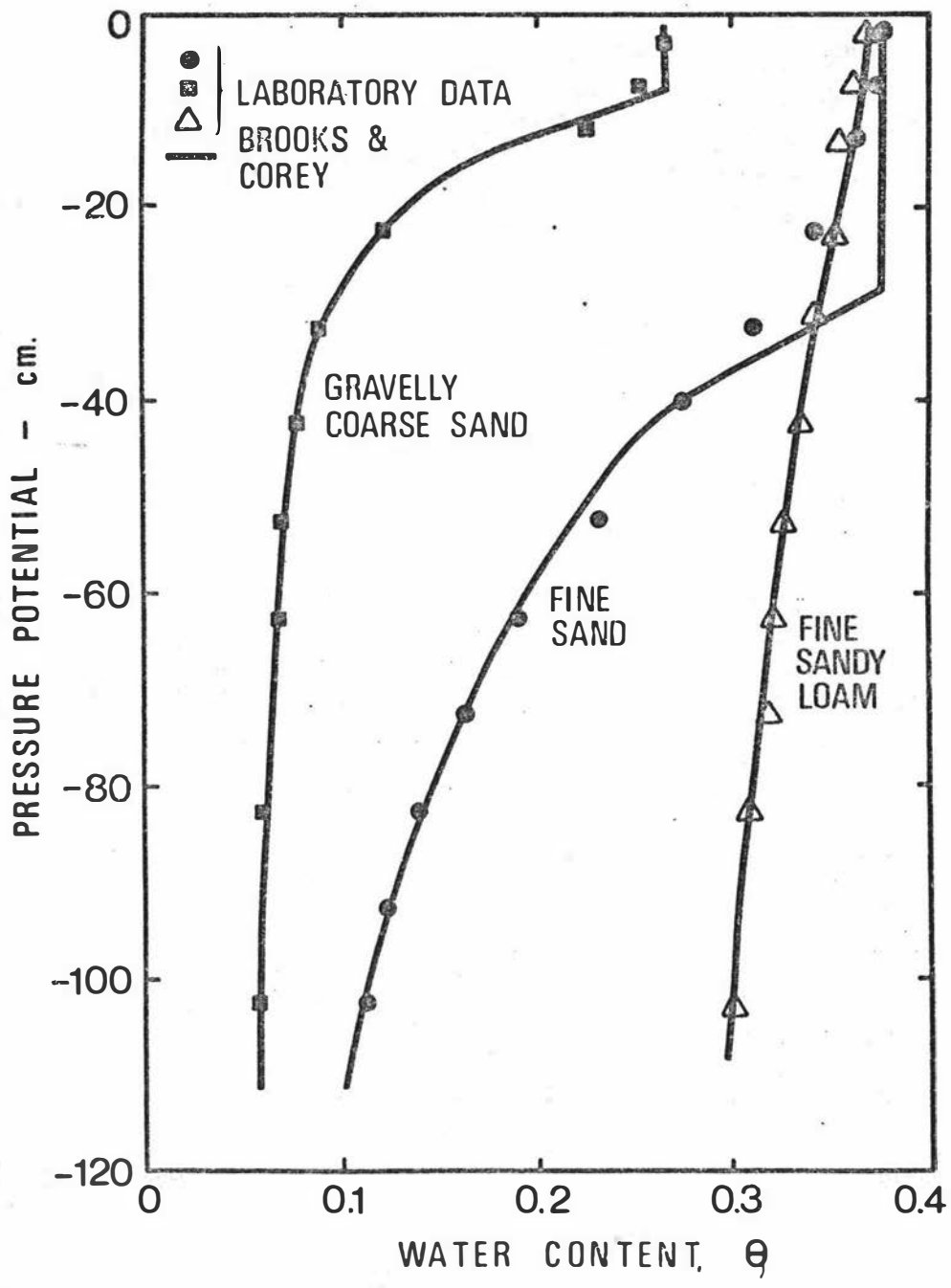

Fig.3.6 Drying water retentivity curves for the three profile elements of a Manawatu fine sandy loam.

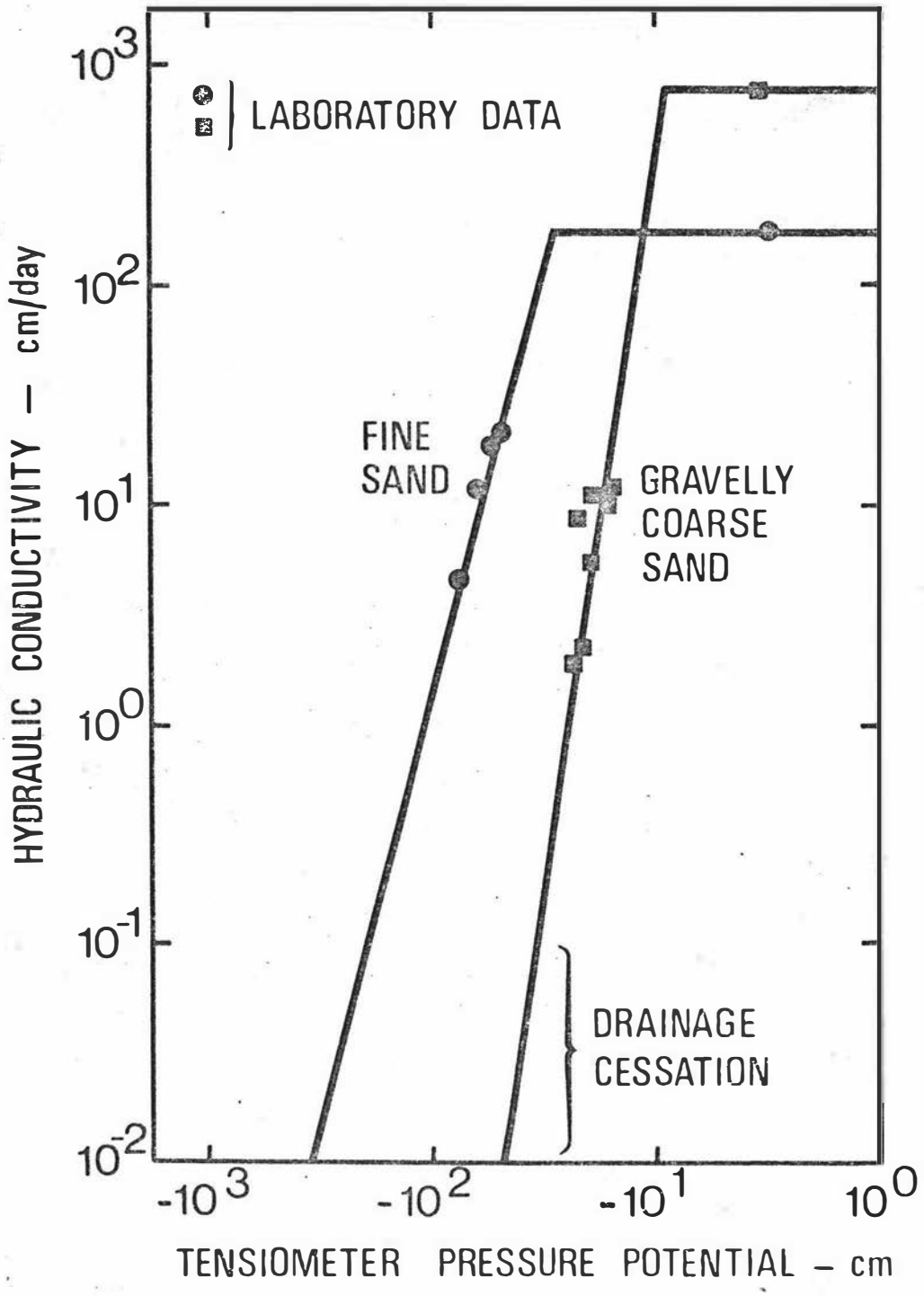

Fig.3.7 Hydraulic conductivity curves for two of the profile elements of a Manawatu fine sandy loam. Drainage is considered to become negligible when $K < 10^{-1}$ cm/day.

potentials were obtained using the theory of Brooks and Corey (1966) as the basis for extrapolation. From Eq.3.3 Brooks and Corey (1966) predict that the conductivity function is given by

$$K(\psi) = \begin{cases} K_s(\psi_e/\psi)^{\eta} & \psi \leq \psi_e \quad \text{——(3.15a)} \\ K_s & \psi > \psi_e \quad \text{——(3.15b)} \end{cases}$$

where K_s is the saturated hydraulic conductivity and η is given by $(2 + 3\lambda)$. In this present study η was estimated by a least squares regression, constrained through (K_s, ψ_e). However the values of η found this way did not vary significantly from $(2 + 3\lambda)$.

Tensiometer pressure potential was measured in the long-column and at two sites in the field with mercury-manometer tensiometers with 10 mm diameter ceramic tips. The pressure potential data were corrected by 8 cm to account for the capillary suppression of the mercury in the manometer tubing (internal diameter 1.2 mm). Water content profiles in the field were measured by a Troxler 1265 neutron probe, in 2 access holes. A field calibration curve was established following the technique of Rawls and Asmussen (1973) (Appendix II).

3.4 RESULTS

Miller (1969) considered that drainage becomes negligible when K falls below 0.1 to 0.01 cm/day. Because of the steepness of the K (ψ) relationship at these conductivity values, it is of little consequence which value is selected. On this basis it is estimated that the gravelly coarse sand effectively ceased to conduct water once the potential fell to -30 to -40 cm(Fig 3.7 Fig.3.8 shows five days after heavy winter rainfall that the

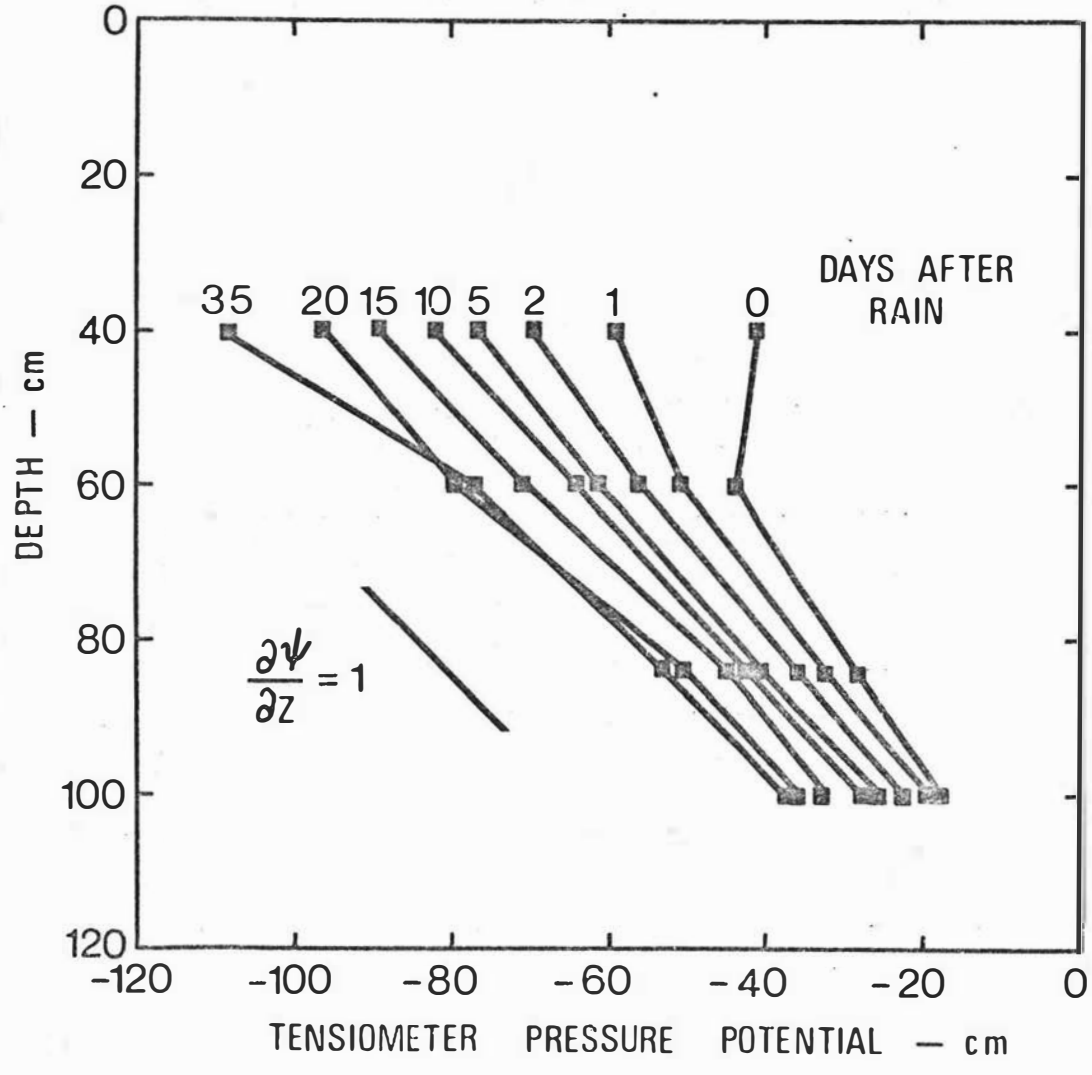

Fig.3.8 Field tensiometer pressure potential data showing the decline in potential for a Manawatu fine sandy loam following a heavy winter rain of 29 mm. Over the subsequent 35 day period, evapotranspiration losses of 70.5 mm were offset by 19 small rainfalls totalling 66.2 mm.

pressure potential in the gravelly coarse sand was -26 cm, and it eventually attained a steady state value of -35 cm, which is in good agreement with the predicted cut-off potential. Thus the cut-off potential ψ_i may be determined in the field by following the decline in the tensiometer pressure potential following heavy rain or irrigation. It can be shown that in general W_L and ΔW are fairly insensitive to changes in ψ_c. Thus, ψ_c can be set equal to one of the commonly accepted approximations for ψ at field capacity in a uniform soil, namely -100 to -350 cm. Having estimated ψ_i and ψ_c and established the parameters in the Brooks and Corey expression for the water retentivity curve of the soil, it is possible to establish $\theta(z)$ and hence W_L and ΔW for a layered soil.

With the extension to account for secondary layering above the coarse stratum, Eq.3.10 may be used to describe field capacity in the Manawatu fine sandy loam. The calculated water content profile is shown in Fig.3.9a together with the profile calculated for a soil with the gravelly coarse sand layer absent, but otherwise identical. The increased water storage due to layering is 5.5 cm which is a 31% increase over the storage of 175 cm without the coarse stratum. This is water enough for 10-30 days of transpiration. In Fig.3.9b the calculated water content profile is compared with four individual field moisture profiles determined using the neutron probe 10-15 days after heavy winter rain. Considering the smoothing that is inherent in the use of a neutron probe (Cannell and Asbell, 1974), this agreement is very satisfactory. The formation of iron accumulations and mottling immediately above the discontinuity at 90 cm provides evidence that the soil is near saturated there for significant periods of time (Veneman *et al.*, 1976) (Table A3.1).

It is interesting to note that secondary layering in a Manawatu fine sandy loam results, fortuitously,

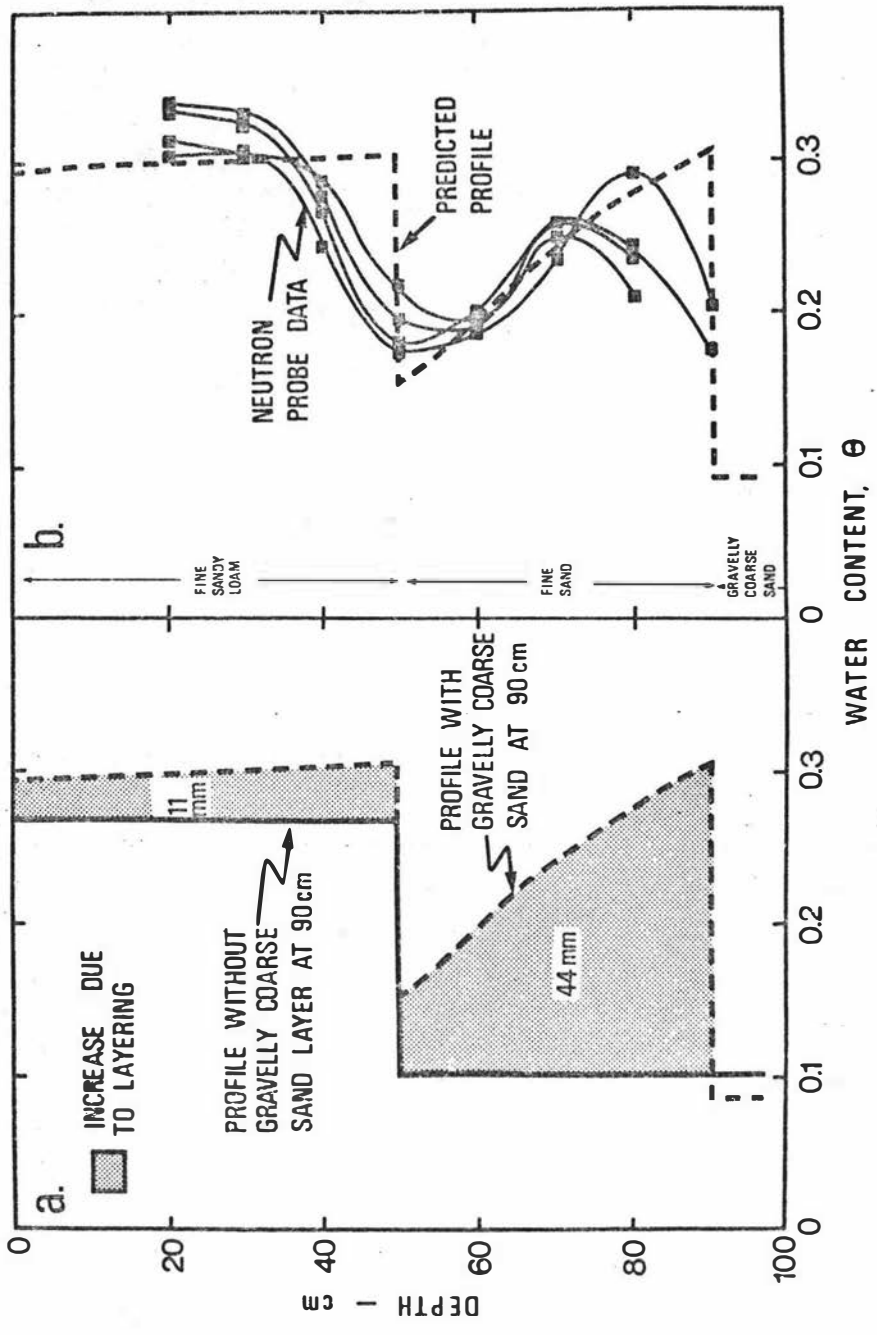

Fig.3.9a Predicted profiles of water content in a Manawatu fine sandy loam, with and without the gravelly coarse sand layer.

Fig.3.9b Field neutron probe data for a Manawatu fine sandy loam compared with the predicted profile of water content.

in near-maximal additional water storage. In this soil, the important region immediately above the coarse layer is occupied by a fine sand with $\lambda = 0.94$, which is very close to λ_{max} (Fig.3.3). For this reason 4.4 cm (80%) of the extra storage occurs in the 40 cm of fine sand above the coarse gravelly sand, as expected from Fig.3.5. Were the secondary layering inverted so that the fine sandy loam ($\lambda = 0.06 \ll \lambda_{max}$) was immediately above the coarse layer, a value for ΔW of 2.0 cm for the whole profile is predicted. This illustrates the importance of λ in the determination of ΔW.

Miller (1969) presented data on the magnitude of the error in the estimation of W_L if the water content at a pressure potential of -340 cm is used, as shown in Table 1.1. Had the -340 cm water content been used to compute W_L for the Manawatu fine sandy loam, the estimate would be 9.5 cm less than actual field capacity. In this chapter, it is shown that W_L may be found using Eq.3.11 without reference to hydraulic conductivity data.

3.5 SUMMARY AND CONCLUSIONS

Coarse-layered soils are free draining in the saturated state yet impede water transmission in the unsaturated state, making them particularly valuable for agriculture. A theoretical framework has been established enabling the analysis of the "field capacity" water retention in coarse-layered soils. It has been shown that the shape of the water retentivity curve of the soil overlying the coarse stratum is a major factor controlling the water stored in the soil profile.

Further, the theory clarifies the roles which soil depth and coarseness of the underlay play in

increasing water retention in layered soils. Field data from a layered soil are presented and application of theory to the field situation is illustrated. The theory can be applied without reference to hydraulic conductivity data.

CHAPTER 4

DRAINAGE FLUX IN PERMEABLE SOIL UNDERLAIN BY A COARSE-TEXTURED LAYER

4.1 INTRODUCTION

Although the drainage flux as a term in the water balance equation is often assumed negligible, or found as the residual when the other terms are evaluated, it can be a significant part of the water balance in permeable soils. Further, a knowledge of this flux is of relevance in leaching studies in assessing the losses of ions from the root zone or their accumulation in groundwater (Jury et al. 1976).

Presently, much remains to be achieved in the development of readily applicable ways of measuring or calculating the drainage flux. Attempts to measure drainage in the field directly with flux meters (Cary, 1973) have met with qualified success, but their practical value has yet to be demonstrated. If the hydraulic conductivity-pressure potential relation is known and the gradient in pressure potential measured, the drainage flux may be calculated (La Rue et al. 1968; van Bavel et al. 1968). However spatial variability in soil water properties means that extensive replication is usually necessary (Nielsen et al. 1973). Also the requirement of frequent pressure potential readings makes this method unsuitable for most long term water balance or leaching studies.

Alternatively, finite-difference or finite-element solutions of the flow equation have been used to predict changes in soil water content during infiltration or drainage in both laboratory soil columns (Hanks and Bowers, 1962) and in the field (Wang and Lakshminarayana, 1968). Subsequently these solutions have been developed so as to include effects due to layering in the profile, hysteresis, root uptake and salt movement. However such solutions need detailed and accurate soil physical data as well as a large computer. They are often difficult and costly to obtain especially if flux data for an extended period are to be computed.

The reasonable success in the estimation of field drainage that has been achieved by using simplified analytical solutions was discussed in Chapter 1. In a permeable, uniform soil profile Black et al.(1969), by assuming zero pressure potential gradient during drainage, showed the flux of water at the base of the profile to be a function of the storage of water in the soil above. However Davidson et al. (1969) using this approach found for the less uniform Cobb loamy sand the agreement was poorer as shown in Fig.1.3. They suggested that reliable estimates of drainage in such heterogeneous soils require detailed conductivity and retentivity data so as to enable numerical simulation. Black et al. (1969) are more optimistic stating that although "the drainage situation will be quite different in layered soils ..... the general approach may apply ..... That is, it may be possible to describe drainage as a simple function of profile storage".

In this chapter drainage from a Manawatu fine sandy loam is investigated. The soil has a moderate saturated conductivity throughout and is underlain by a coarse-textured layer (Table 3.1). Field data, and theory coupled with basic physical data for such a profile, are used to test a simple model that relates the drainage flux to the water storage in the soil above the coarse-textured layer.

4.2 THEORY

The vertical flux of water through a soil may be described by

$$J = -K(\psi)[\partial\psi/\partial z - 1] \qquad \text{——(4.1)}$$

where J is the water flux, K the hydraulic conductivity, ψ the pressure potential and z the soil depth. For a soil underlain by a deep homogeneous coarse layer it is reasonable to assume that $\partial\psi/\partial z = 0$ and so, $J = -K(\psi)$ below the interface (Eagleman and Jamison, 1962). During

drainage, the flux in the overlying soil must be less than or equal to K_i, where the subscript 'i' refers to the coarse underlay below the interface. Further, if water is moving downward the pressure potential gradient will be less than unity. Thus in the overlying soil it follows that

$$1 > \partial\psi/\partial z \geq 1 - [K_i(\psi)/K_f(\psi)] \qquad \text{——(4.2)}$$

where the subscript 'f' refers to the finer textured soil above. For soil underlain by an unsaturated coarse layer it is expected that K_i/K_f is small, and so by Eq.4.2, $\partial\psi/\partial z \cong 1$ above the interface. Though the assumption that $\partial\psi/\partial z = 1$ (i.e. the no-flux condition) in the overlying soil during drainage is obviously impossible in the limit, it can be used to predict the pressure potential in the soil above the coarse underlay during drainage.

Now for any value of the pressure potential in the coarse underlay (ψ_i) it is possible to find a wetting and drying drainage flux $[J_i = K_i(\psi_i)]$ and also a water content profile in the soil above the interface at depth z_i using an equation similar to Eq.3.9, namely

$$\psi(z) = \psi_i - (z_i - z) \qquad \text{——(4.3)}$$

and the appropriate wetting or drying water retentivity curve. By integrating the water stored above the coarse-textured layer at each pressure potential, two relationships between the flux (J_i) and the profile water storage (W) can be found, one for wetting and one for drying. So it follows that in soils of moderate saturated hydraulic conductivity underlain by a coarse-textured stratum a relationship between J_i and W exists. If the effects of hysteresis are small, a unique relation between J_i and W can be expected.

4.3 MATERIALS AND METHODS

The soil used for this study was a Manawatu fine sandy loam as described in Chapter 3 and in more detail in Appendix III. Hysteretic water retentivity data for

the two lower profile elements, and draining retentivity data for the fine sandy loam, were measured using Haines' apparatus (Vomocil, 1965), and are presented in Fig.4.1. These data are different to the drying curve data presented in Fig.3.6 as the main wetting and drying envelopes are included. Undisturbed core samples were used for the top two layers, but repacked loose material had to be used for the gravelly coarse sand. Scanning curves within the main hysteresis loops were calculated using the procedure described by Mualem (1974). Field water retentivity data for the fine sand and fine sandy loam were obtained using simultaneous tensiometer and water content measurements. These are shown also and are in reasonable agreement with the laboratory data. Field data could not be obtained for the gravelly coarse sand underlay because of the difficulty of inserting neutron probe access tubes to sufficient depth in the underlay.

Hydraulic conductivity data are shown in Fig.4.2. The fine sand and gravelly coarse sand data are the same as in Fig.3.7. The saturated conductivity of the fine sandy loam was found by maintaining a shallow free water surface over two undisturbed cores 140 cm^3 in volume and monitoring the steady-state efflux. Conductivity data at low pressure potentials on the main drying curve from saturation for the fine sandy loam were obtained using the theory of Brooks and Corey (1966) as the basis for extrapolation (Eq.3.15) from the measured values of K_s and ψ_e (Table 3.1). Water content profiles in the field were measured at 10 cm depth increments by the neutron probe at two sites. Comparison with gravimetric sampling showed that the water content measured by the neutron probe at 10 cm depth provided a reasonable estimate of the mean water content of the 0 to 15 cm zone (Appendix II).

Drainage was found by monitoring the outflow of water from the lysimeter described in Chapter 2. For selected periods the drainage was also calculated from the water balance equation using neutron probe, rainfall

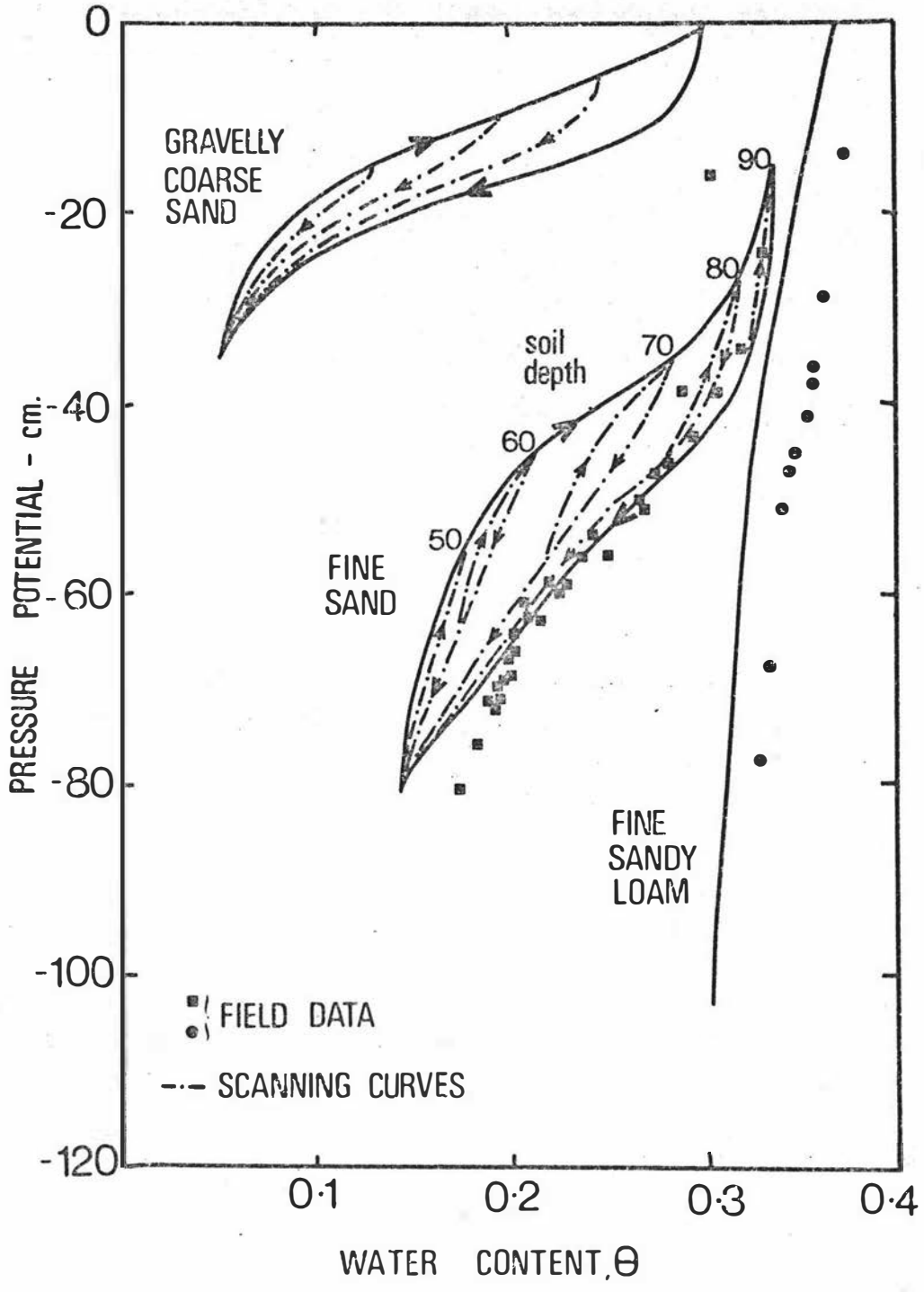

Fig.4.1 The water retentivity curves for the three profile elements of a Manawatu fine sandy loam. Measured hysteresis loops (→) and computed scanning curves (·→·) are shown for the gravelly coarse sand and fine sand. The scanning loops for various soil profile depths are shown for the fine sand. Field data for the fine sand (●) and fine sandy loam (■) are also presented.

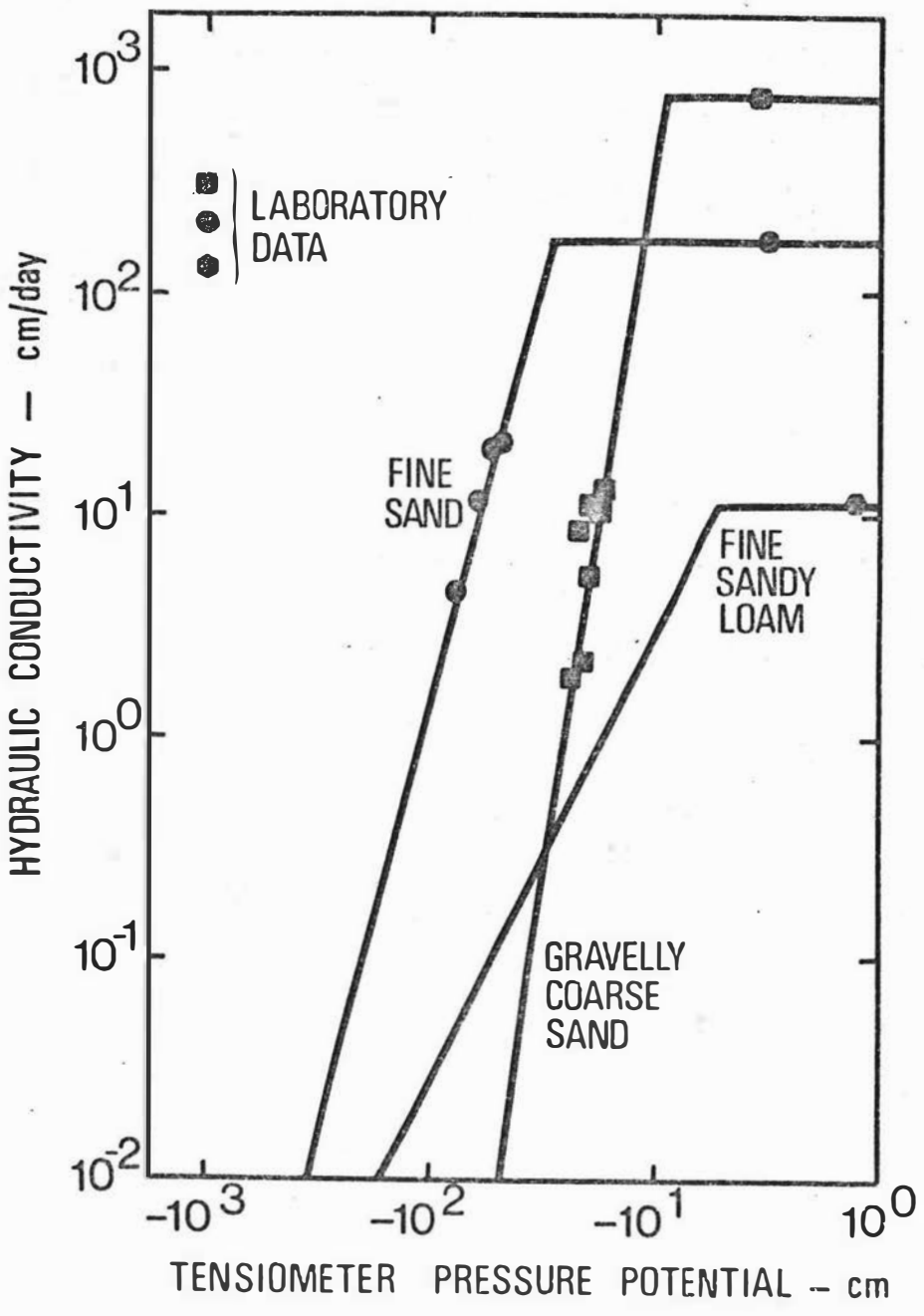

Fig.4.2 Hydraulic conductivity curves for all three profile elements of a Manawatu fine sandy loam.

and evaporation data. The layering found in the field was replicated in the 1 m soil profile in the lysimeter when it was filled five years prior to this study. Nine ceramic plates, each 46 cm^2 in area and of air entry value approximately -20 cm of water were situated in the gravelly coarse sand about 8 cm below the fine sand interface, and the daily drainage was considered to be the amount of water removed by these plates following the application of a suction of -40 cm of water for 2 hours. A potential of about -20 cm at the base of the lysimeter is within the range of the pressure potentials measured in the gravelly coarse sand outside the lysimeter, as shown in Figs.3.8 and 4.4. Tensiometer pressure potential data within the lysimeter were found to be in fairly close agreement (5 to 10 cm) with those measured in the field nearby. Consequently lysimeter drainage measurements are thought to be reasonably representative of drainage in the adjacent field. The lysimeter would tend to underestimate drainage at lower pressure potentials, but as the flux at this stage is small it is of little consequence.

The drainage model described later is applied over two 6 month periods to the Manawatu fine sandy loam. To enable computation of the profile water storage, evapotranspiration and rainfall data are also required. Evapotranspiration (ET) was estimated following the method of Priestley and Taylor (1972). The value of α used in this chapter was based on the data presented in Fig.2.2. It was assumed that the surface was always well-watered, an assumption discussed in Chapter 5. To obtain ET_{eq} in 1974 R_n was measured above the crop, however in 1975 it was estimated from the regression of R_n on solar radiation found from the 1974 data (Fig.2.4) and using solar radiation data from the meteorological site. RF was also measured at the meteorological site.

4.4 RESULTS AND DISCUSSION

In the Manawatu fine sandy loam the gravelly coarse sand underlay is homogeneous and deep, therefore it is reasonable to assume that $\partial\psi/\partial z = 0$, and so $J = K(\psi)$ below the interface at 90 cm. The expected maximum daily rainfall is of the order of 20 mm; Figs.4.1 and 4.2 show that a flux of 20 mm/day would cause the gravelly coarse sand to wet up to a pressure potential of -15 cm, approximating the maximum mean daily potential expected there. The steepness of the $K(\psi)$ relationship in the gravelly coarse sand means this potential is fairly insensitive to the value of the maximum flux chosen.

For all pressure potentials in the underlay drier than -15 cm it can be seen from Fig.4.2 that for the fine sand $K_i/K_f < 10^{-2}$ and hence by Eq.4.2, $\partial\psi/\partial z \cong 1$. An exception is in the wettest case for the fine sandy loam when K_i/K_f is not small, and $\partial\psi/\partial z$ probably tends to be smaller in this zone. However as the expected pressure potential, at this stage, at the base of the fine sandy loam is -55 cm, K_i/K_f rapidly becomes negligible as the gravelly coarse sand and fine sand drain. On a daily time scale the wettest pressure potential profile to be expected in this soil thus corresponds to an interface pressure potential of -15 cm with $\partial\psi/\partial z = 1$ in the soil above.

The conductivity of the gravelly coarse sand falls steeply with decreasing pressure potential, and if it is assumed that the flux of water is negligible when $K_i(\psi)$ is less than about 10^{-1} cm/day (Miller, 1969), Fig.4.2 shows drainage becomes negligible when a pressure potential of -30 to -40 cm is attained at the interface as already noted in Chapter 3. Again, from Eq.4.2, it can be expected that $\partial\psi/\partial z = 1$ in the soil above. In Fig.3.8 is shown the tensiometer pressure potential measured in the field following a winter rainfall event. The data show this distinct wettest and driest envelope.

The pressure potentials at 100 cm depth, in the gravelly coarse sand, are within the expected values and $\partial\psi/\partial z$ in the soil above approaches one. An exception occurs on the day of the rain in the fine sandy loam, but this is expected since K_i/K_f is not yet sufficiently small. This is of little consequence as the steep retentivity curve in the fine sandy loam means that only relatively small amounts of water are lost from it during drainage, the major contribution being from the fine sand layer.

In computing the water content profile from pressure potential data it is necessary to account for the effect of hysteresis in the fine sand. As water initially enters the fine sand it is wet up along the wetting curve indicated in Fig.4.1, until the potential reaches approximately

$$\psi(z) = -15 - (90 - z) \qquad \text{——(4.4)}$$

Due to the steepness of the retentivity curve hysteresis is ignored in the fine sandy loam (Fig.4.1). Using the appropriate moisture characteristic data with Eq.4.4 it is possible to predict the wettest expected water content profile. This is shown in Fig.4.3 with the two wettest water content profiles measured during winter. When the inability of the neutron probe to resolve discontinuities in the water content profile (Cannell and Asbell, 1974) is considered, the predicted and measured values are in reasonable agreement.

The driest expected profile corresponds to a pressure potential profile approximated by

$$\psi(z) = -35 - (90 - z) \qquad \text{——(4.5)}$$

and in the fine sandy loam corresponding water contents are easily found from the non-hysteretic retentivity curve. However in the hysteretic fine sand, the moisture content corresponding to $\psi(z)$ is found using the appropriate drying scanning curve beginning on the

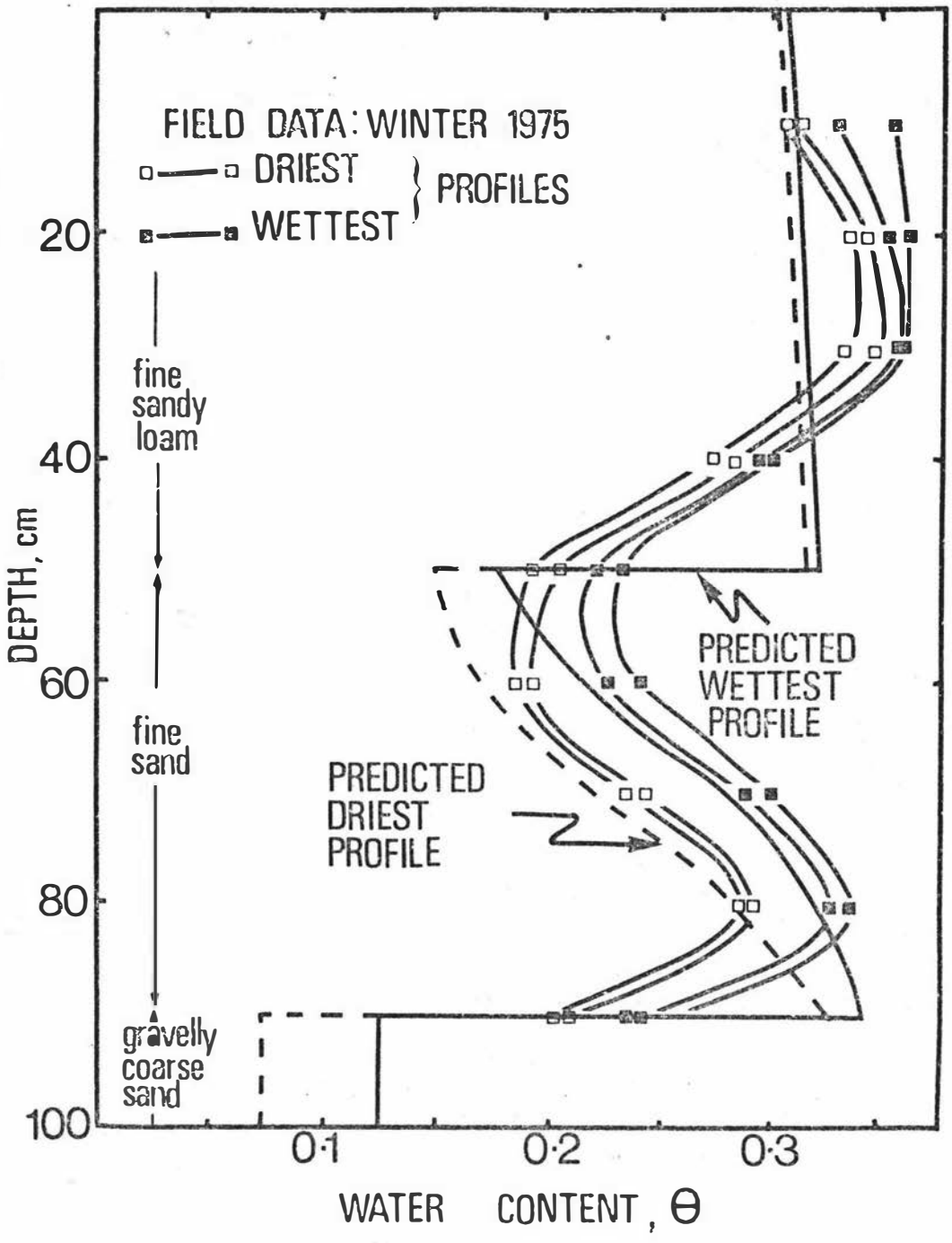

Fig.4.3 Predicted wettest and driest profiles (ignoring evapotranspiration) of water content in a Manawatu fine sandy loam. The two wettest and driest neutron probe water content profiles recorded between May and September 1975 are also shown.

wetting curve at $[-15-(90-z)]$, as shown in Fig.4.1 for 5 depths in the soil. The predicted driest profile (in the absence of evaporation) is also shown in Fig.4.3 and again there is reasonable agreement with the two driest profiles measured by the neutron probe in winter when ET was small. Upon rewetting the fine sand will wet up along the wetting scanning curve beginning at $[-35-(90-z)]$ back to $[-15-(90-z)]$, completing the loop. That the pressure potential in the gravelly coarse sand, in the absence of significant ET, tends to be bounded by -15 cm in the wettest case and -35 cm in the driest case is shown in Fig.4.4.

In Fig.4.4, Eq.4.3 can be seen to quite successfully predict the pressure potential at two depths in the overlying soil, given the pressure potential in the gravelly coarse sand. As already discussed on days of heavy rain the pressure potential in the fine sandy loam tends to be greater than predicted. Since in the Manawatu fine sandy loam, for any ψ_i both $\psi(z)$ in the soil and K_i (ψ_i) in the underlay are known, it is possible to determine J_i (W). The wetting and drying storage-flux relationships resolved in this way are shown in Fig.4.5. As there is little difference between the two curves a unique relationship for J (W) can be assumed with little error. This is a result of the relatively small variation in ψ in the fine sand (Fig.4.4) giving a narrow envelope between the wetting and drying curves, despite the wide envelope between the main wetting and drying curves (Fig.4.1). Further the scanning loop between -15 and -35 cm in the gravelly coarse sand is narrow, so that hysteresis in its hydraulic conductivity-pressure potential relationship is quite small. In the application of this relationship the drying curve was used.

If only drainage contributes to the change in W then

$$dW/dt = J_i = f\ (W) \qquad \text{——(4.6)}$$

where t is time and f (W) is the solid line in Fig.4.5.

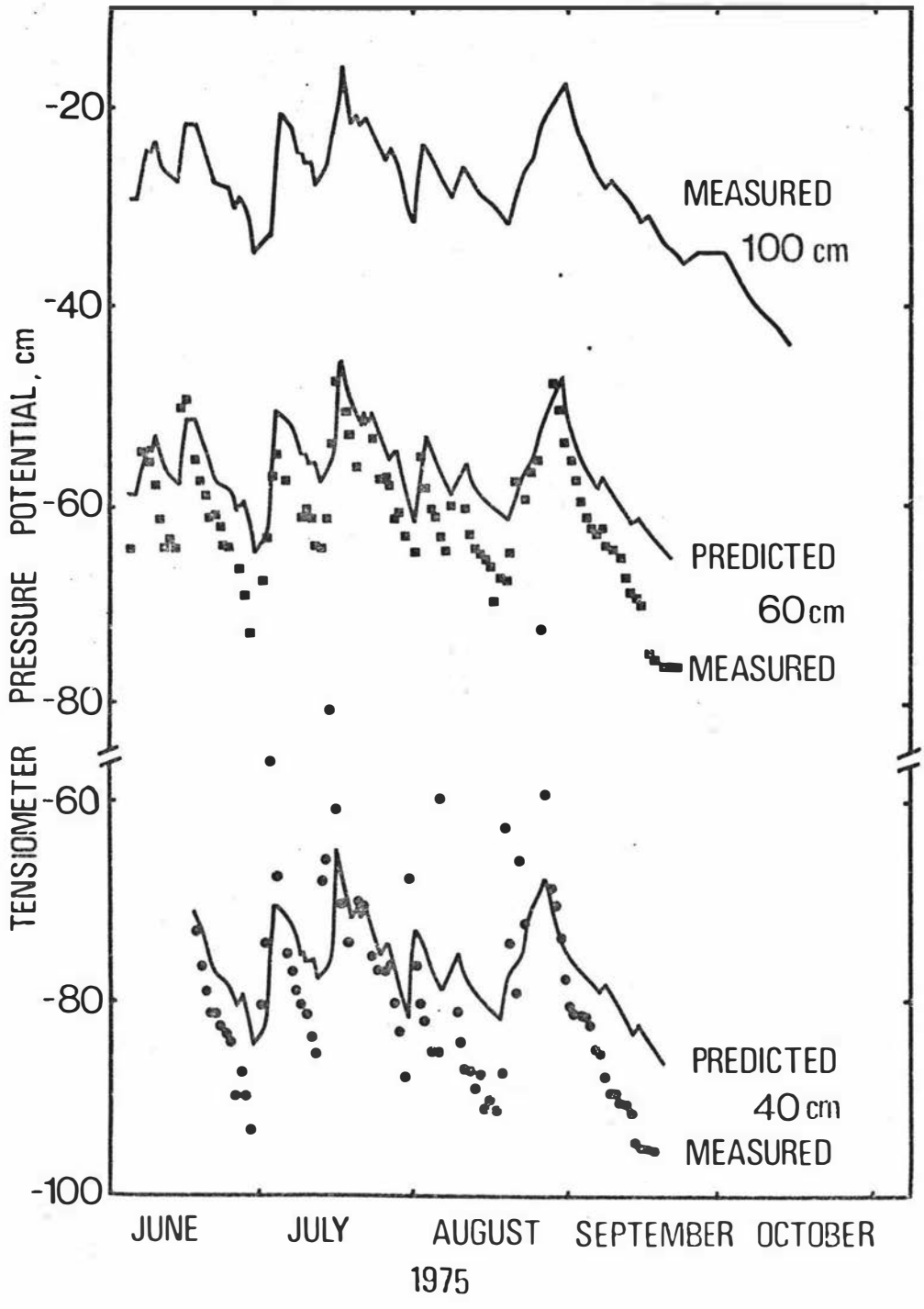

Fig.4.4 Measured tensiometer pressure potential in the gravelly coarse sand at 100 cm depth during the winter of 1975 and predicted tensiometer pressure potential in comparison with field measurements at depths of 40 cm and 60 cm in the soil profile.

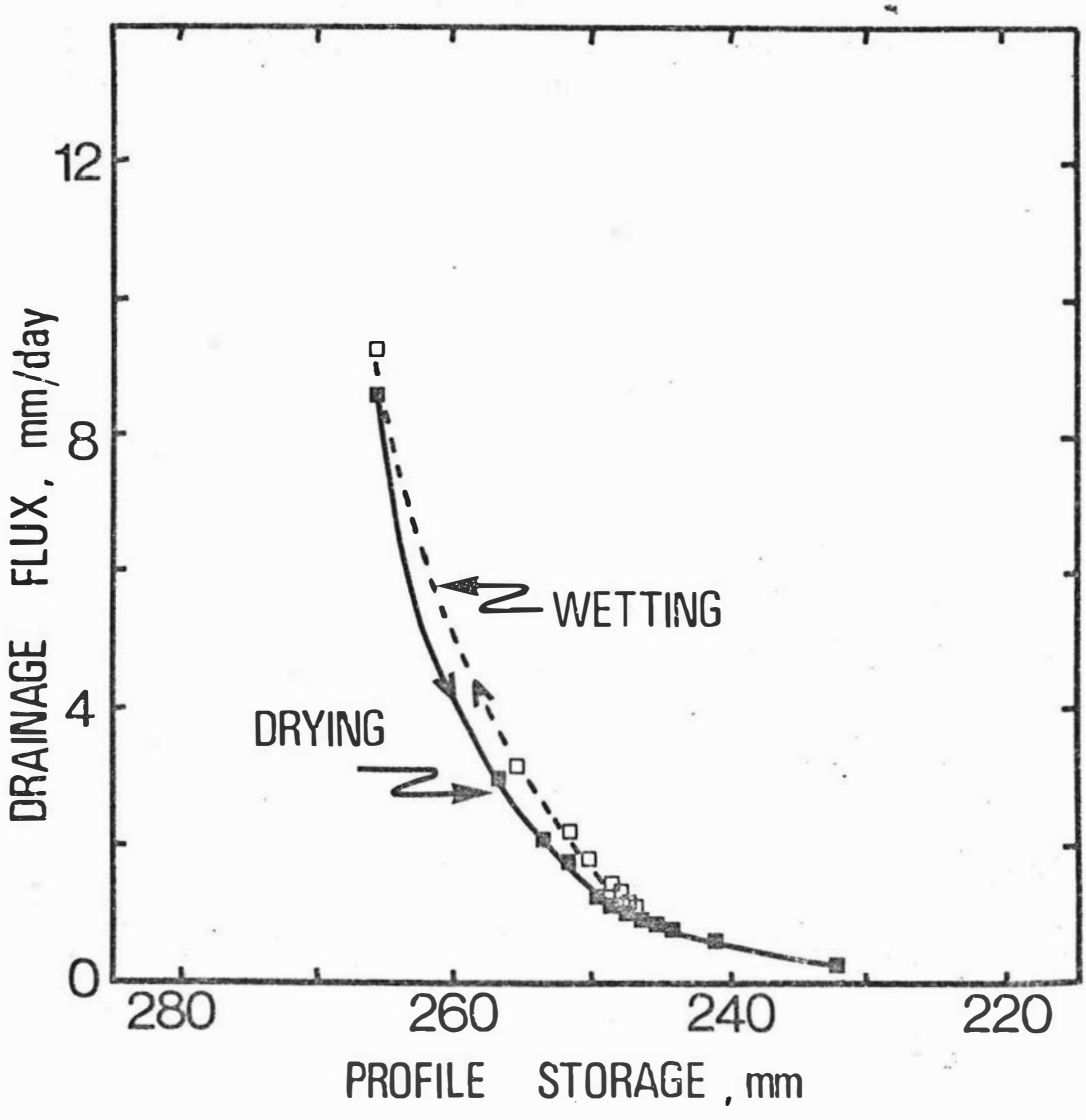

Fig.4.5 Predicted wetting and drying drainage flux - profile water storage relationships for a Manawatu fine sandy loam.

It is possible to solve Eq.4.6 numerically using a finite difference approximation of dW/dt, with f (W) evaluated at the midpoint of the interval in W. Thus it is possible to obtain the decline in W and J with time, from the previously discussed maximum value of W. The predicted decline in W with time is shown in Fig.4.6 to be in agreement with the water storage decline measured by the neutron probe during two rain free periods following days with heavy rain (>17 mm). Changes in storage due to water losses by evapotranspiration were accounted for in the field data. The variability in the field measured storage data is to be expected since W is a function of the depth to the coarse layer, and for a Manawatu fine sandy loam a 5 cm variation in this results in a 10 mm change in W (see Fig.A3.2). However the changes in storage with time are similar at each site.

The predicted flux-time relationship is compared in Fig.4.7 with that calculated from the field neutron probe data and also the mean curve established for four winter drainage events from the lysimeter. As expected the agreement with the lysimeter is better over the first 6 days when the pressure potential is still quite high. Also within the accuracy possible for fluxes calculated from neutron probe data, the recession curve found this way is compatible with that predicted. The predicted amount of water lost between days 1 and 9 is 20.3 mm which is comparable to the 24.6 ($\pm$ 3.7) mm drained from the lysimeter and the 25.8 mm measured by the neutron probe.

While the J (W) relationship derived assumes only the drainage flux to be responsible for decreasing the soil water storage, evapotranspiration also removes water from the soil profile. If the soil is bare the water extracted by evapotranspiration will come from near the surface and so deep drainage will be little affected, as demonstrated by Davidson *et al.* (1969). This water loss must subsequently be replaced by rainfall

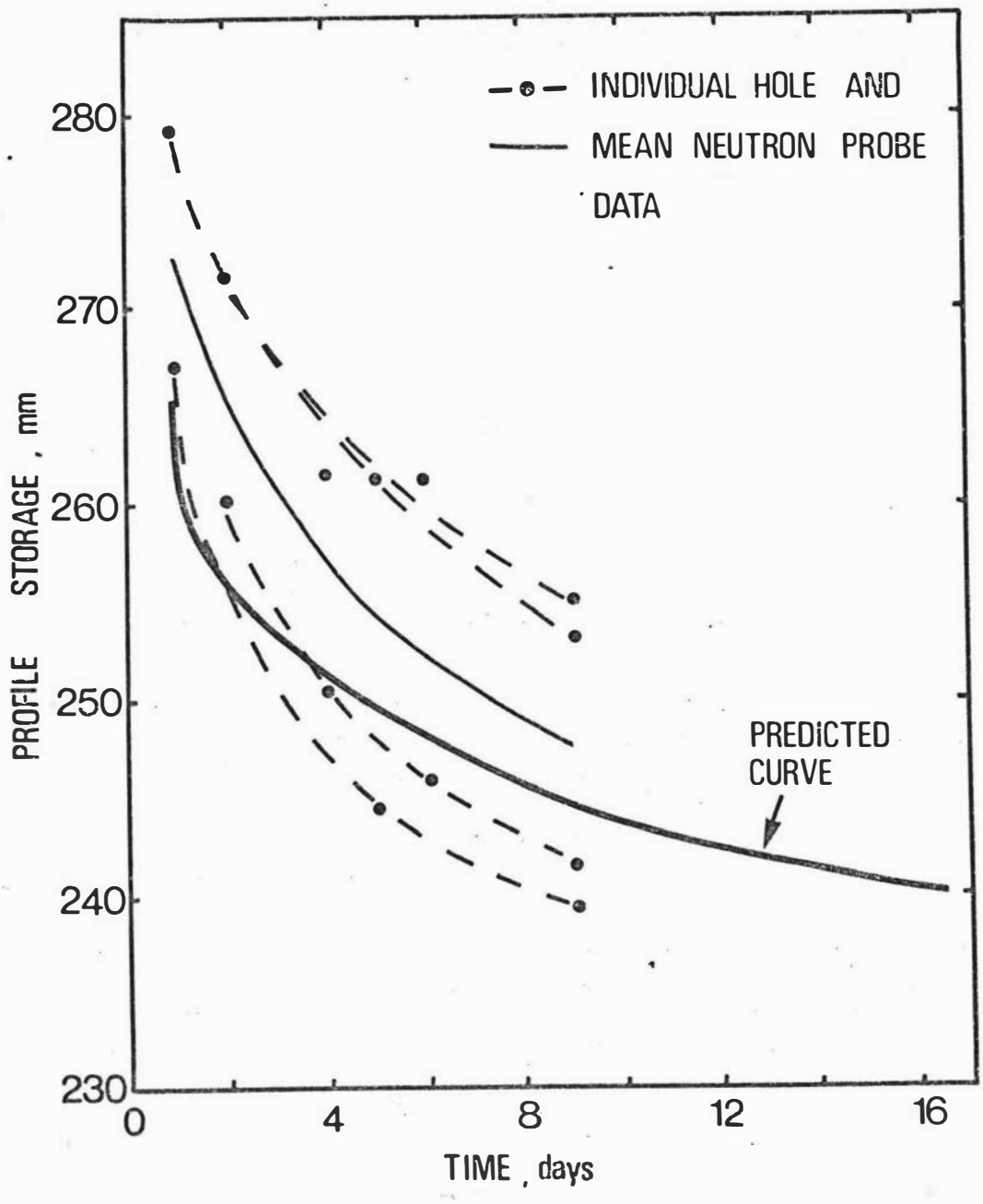

Fig.4.6 Predicted decline in profile water storage with time in comparison with that measured by the neutron probe at two sites following two heavy winter rainfalls.

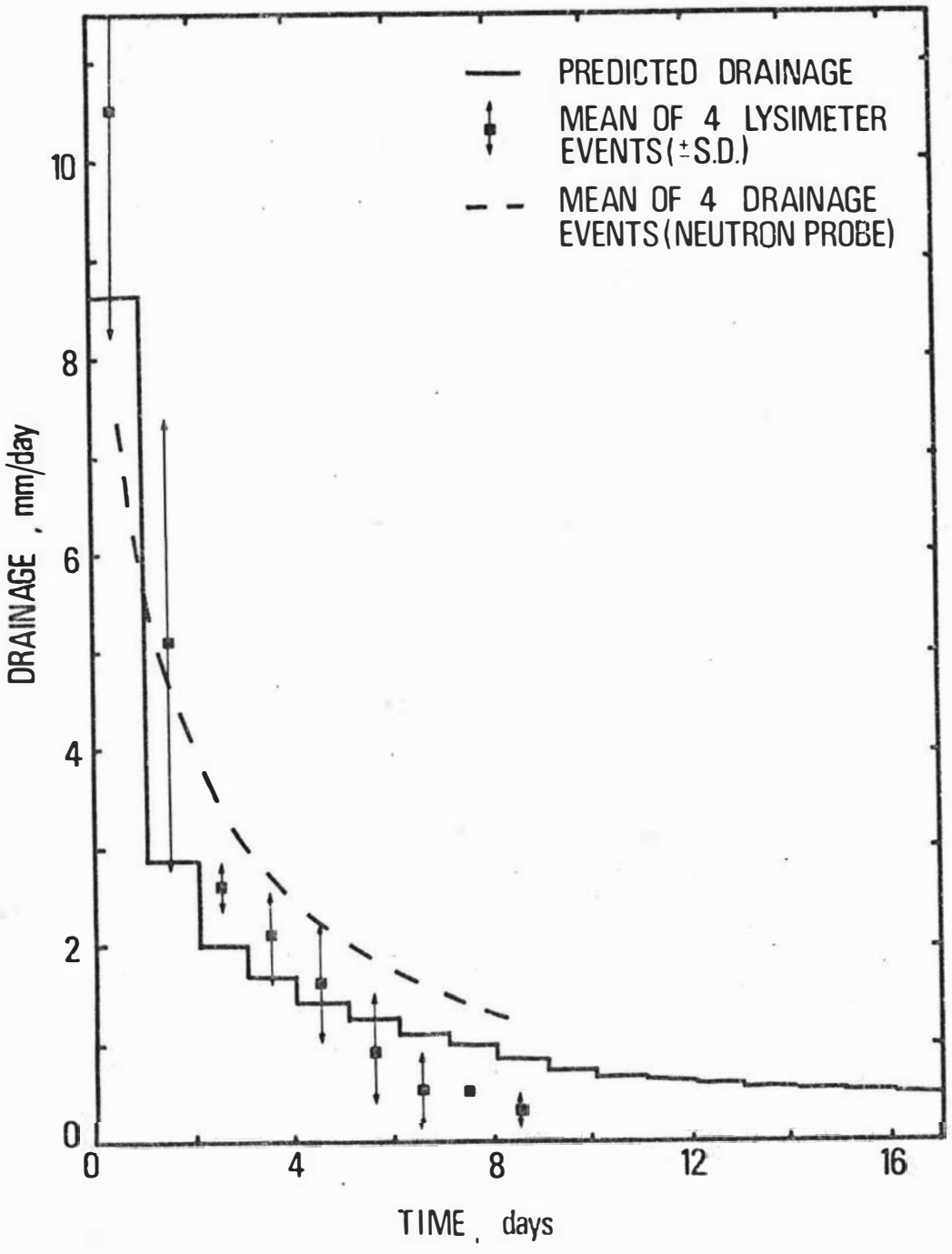

Fig.4.7 Predicted decline in drainage flux with time in comparison to the drainage flux computed from the neutron probe data in Fig.4.6, and the mean of that measured by the lysimeter over four drainage events.

or irrigation before drainage is affected. During the present study however an oats crop was actively growing. In this case, as the hydraulic conductivity of the soil above the coarse underlay remains relatively high during and after drainage, equilibrium conditions should be approached during simultaneous ET and drainage. Consequently ET and drainage are treated as additive in their influence on W, and so J. Hence the storage in the profile on any given day (W_d) is computed as

$$W_d = W_{d-1} - ET_{d-1} + RF_{d-1} - J_{d-1} \qquad \text{——(4.7)}$$

where $J_{d-1} = f(W_{d-1})$ and RF_{d-1} is the rainfall of the previous day. Drainage was generally about 70% of the rainfall, and so it matters little which way ET is treated. Thus the J (W) relationship established was used as a basis for a drainage model for the Manawatu fine sandy loam. It is assumed that on any day the storage exceeds 265 mm, the drainage on that day is the storage excess (W-265) plus the drainage predicted for a storage of 265 mm, namely 8.6 mm. This is reasonable as J (W) is nearly vertical when $W > 265$. Drainage below 0.2 mm/day is ignored.

The predicted drainage for May to November 1974 and a similar period in 1975 can be seen in Figs.4.8 and 4.9 to be in reasonable agreement with that measured from the lysimeter, in terms of both the timing and amount of drainage. Within the bounds of variability in the data, the changes in profile water storage measured by the neutron probe also can be seen to verify the applicability of the model (Fig.4.8). The model can be expected to work in any soil with a coarse-textured stratum at some depth, and a saturated hydraulic conductivity of at least say 50 mm/day throughout the profile above. In such situations the unsaturated hydraulic conductivity of the coarse-textured stratum controls the rate of drainage at all times, except possibly during and immediately after very heavy rain. During drainage and in the quasi-equilibrium condition

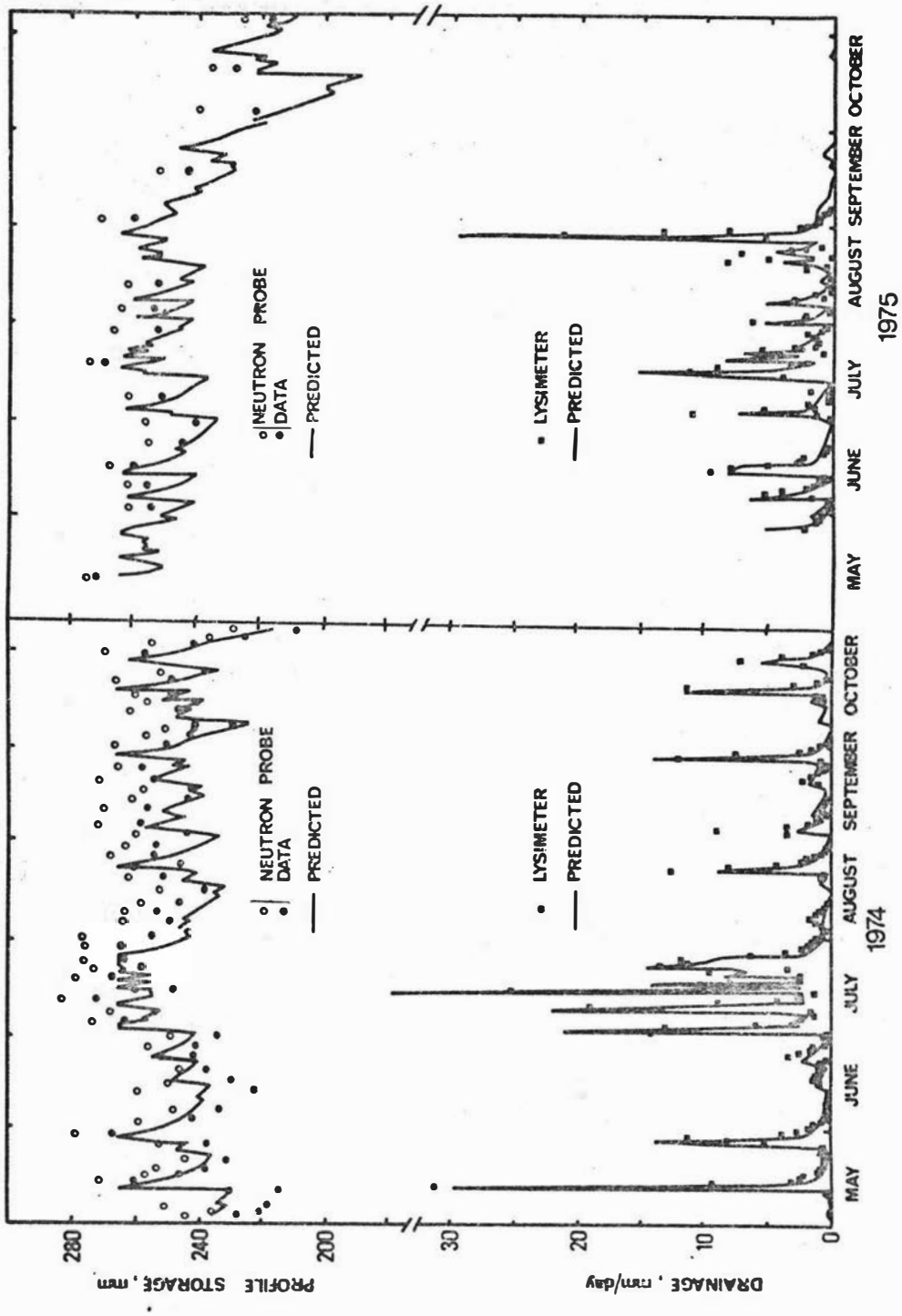

Fig.4.8 Neutron probe profile water content data at two sites, in comparison with that predicted for 1974 and 1975.
Drainage flux predicted in comparison with that measured by the lysimeter in 1974 and 1975.

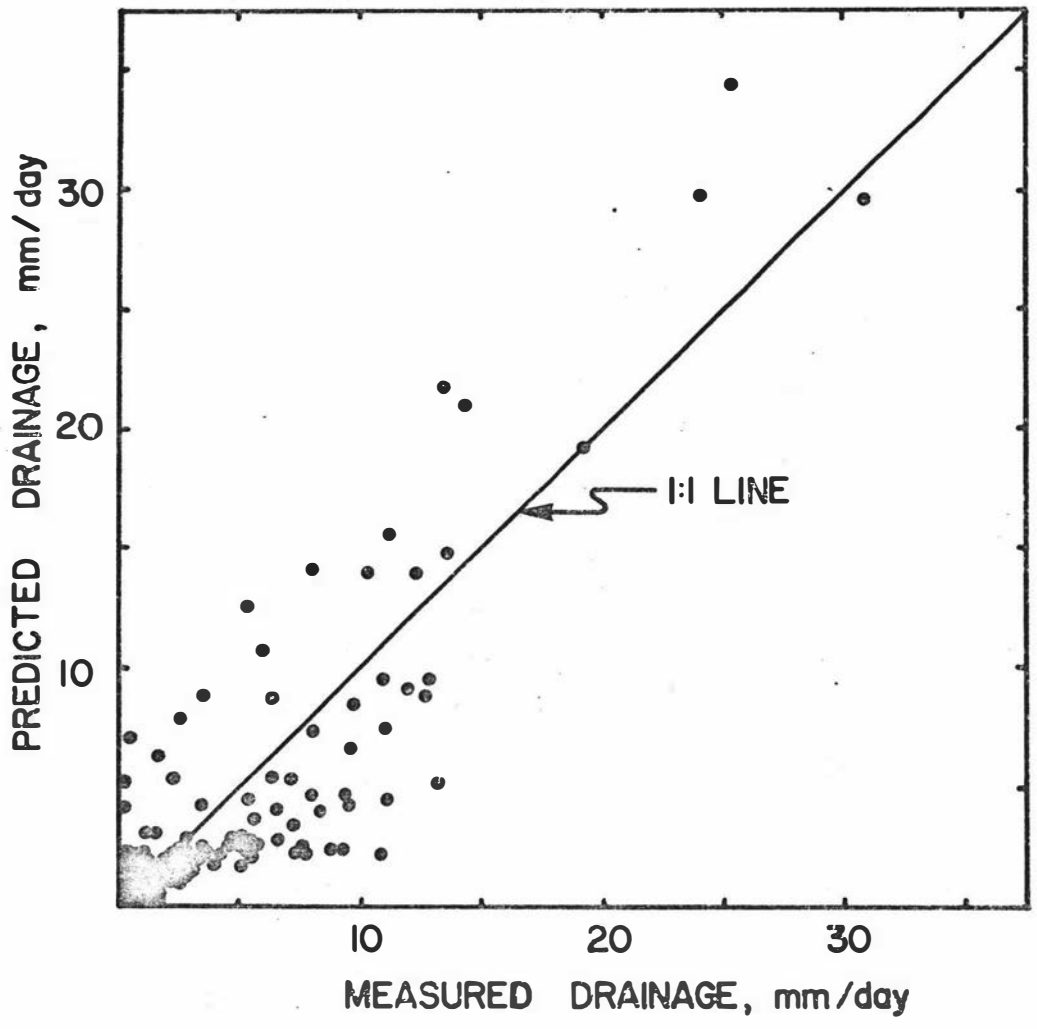

Fig.4.9 Predicted drainage in relation to that measured by the lysimeter, for both 1974 and 1975.

following, the hydraulic conductivity of the soil above the coarse stratum remains relatively high. Thus, unless the profile has been dried out by evapotranspiration, the time lag between a rainfall input and the corresponding adjustment of the drainage rate will be small, usually less than a day. This contrasts with the situation in a uniform profile, where a much longer response time is usual. In the uniform Plainfield sand, Black et al. (1969) found it took about 2 days for an increase in storage to affect the drainage rate at 1.5 m depth.

This simple model can also be used as an analytical tool, when applied to a soil that satisfies all the necessary conditions outlined. In the Manawatu fine sandy loam, with both fine sandy loam and fine sand layers above the gravelly coarse sand, the model predicts that it takes 6.7 days for the drainage flux to drop to 1 mm/day, following wetting of the profile. Over this period the soil loses 20.3 mm of water. Hypothetically however, if the gravelly coarse sand was still at 90 cm depth but overlain by only fine sand, it is predicted that to attain a drainage rate of 1 mm/day would take 15 days and 50 mm of water would have been removed during drainage. Although drainage persists for longer from fine sand it is this type of soil that undergoes the greatest increase in water storage due to the layering, by virtue of the shape of its retentivity curve as shown in Figs.3.3 and 3.4 and discussed in Chapter 3.

Alternatively if the gravelly coarse sand were at a depth of 20 cm under fine sand it would only take 4.3 days for the drainage rate to drop to 1 mm/day, with a drainage loss of only 13 mm. The existence of a coarse-textured stratum in a permeable profile does not necessarily mean a rapid cessation of drainage, but rather the time course of the drainage recession depends on the nature of both the overlying soil and the underlay, and the depth to the interface.

The model of Black et al. (1969) was applied to a 90 cm deep soil of uniform fine sand. The initial condition chosen was the soil wet to $\psi = -15$ at 90 cm with $\partial\psi/\partial z = 0$. The decline in profile water storage is shown in Fig.4.10 in comparison to that predicted by Eq.4.6 for 90 cm of fine sand wet up to $\psi = -15$ at 90 cm with $\partial\psi/\partial z = 1$, but underlain by gravelly coarse sand. It can be seen layering results in more water being stored in the profile when quasi-equilibrium is reached (c.f. Figs.3.3 and 3.4) and causes the drainage recession curve to be much flatter, with the flux becoming < 1 mm/day more quickly.

4.5 CONCLUSION

The theory proposed by Black et al. (1969), that the drainage flux can be treated simply as a function of soil water storage, would appear to work even better in permeable soils with a coarse-textured stratum at depth than in the uniform permeable soils for which it was first proposed. In such layered soils the hydraulic conductivity of the coarse-textured underlay usually controls the drainage flux at all times ensuring $\partial\psi/\partial z \cong 1$, whilst the soil above maintains a high hydraulic conductivity. Thus, firstly, the total potential gradient in the overlying soil will approach zero during drainage, in contrast to the unit gradient of a uniform profile and secondly, the response in the drainage flux to an input of water at the soil surface will usually be more rapid than in a uniform soil. While the drainage flux is controlled by the conductivity of the coarse stratum, the drainage-storage relation is determined by the depth and the water retentivity of the soil above the stratum, as well as the pressure potential-conductivity relation of the underlay.

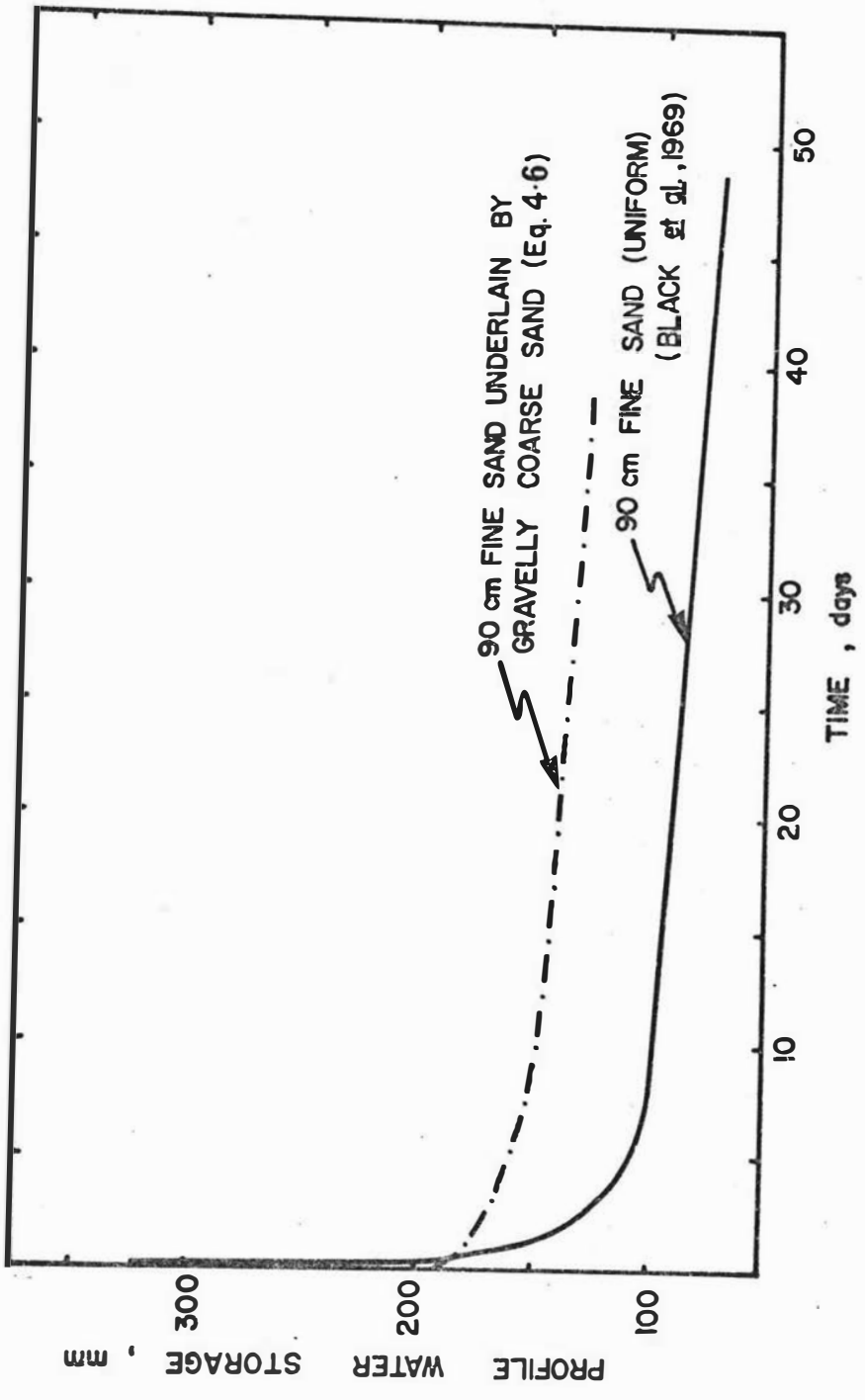

Fig.4.10 The decline in profile water storage for a uniform soil of fine sand, predicted using the model of Black et al. (1969) in comparison to the decline predicted for a fine sand underlain by a layer of gravelly coarse sand, using Eq.4.6 .

If the relationship between pressure potential and water content in the overlying soil and the relation between the hydraulic conductivity and pressure potential in the coarse underlay are known, simple theory may be used to derive a relation between the drainage flux and the water storage for a permeable soil underlain by a coarse stratum. Hysteresis effects in the water retentivity curve of the soil and in the hydraulic conductivity curve of the underlay would be expected to cause some hysteresis in the drainage-storage relation. However in the soil profile studied this was small enough to ignore, despite a pronounced hysteresic envelope between the main wetting and drying retentivity curves of the soil immediately above the coarse layer.

CHAPTER 5

CONCLUSIONS AND SUMMARY

5.1 THE OVERALL WATER BALANCE

An analysis of daily ET, soil water retention, and drainage for a crop of oats grown in winter on a layered soil in the Manawatu has been presented in the preceding chapters. In this final chapter the overall water balances during the 1974 and 1975 growing seasons are considered, and the results of the investigation are summarized.

Table 5.1 shows the components of the water balance for monthly periods. During crop establishment in the May-June period ET was assumed to be equivalent to that of a well-watered surface. The high number of rain days that occurred (> 10 per month) would ensure that the soil surface was sufficiently wet all the time, and that this assumption was valid. The water balance data are based on an initial storage (W_0) measured by the neutron probe. The average rainfall data show that both the 1974 and 1975 seasons were wetter than normal. The monthly rainfall totals between years have a mean difference of 61 mm. For ET between the years there was a mean monthly difference of only 5 mm. Year to year variation in ET is much less than for rainfall (Tanner, 1967). Because of this consistency, year to year variation is often ignored in the monthly ET values used in approximate water balance studies (Coulter, 1973b). The strong dependence of J on RF causes monthly totals of drainage to vary markedly between years. Over the May-October periods outlined, approximately 60% of the rainfall was lost as drainage, and about 40% as ET. Drainage during the summer period is unlikely. As the mean annual rainfall is 1000 mm, the annual drainage loss will be about 30-35% of the rainfall input. ET will account for the remaining 65-70%.

Table 5.1 Estimates of the components of the water balance of oats grown in the Manawatu during 1974 and 1975. The figures in brackets are the values of the components in terms of % rainfall. Also shown is the mean rainfall (1941-1970). All values in mm.

1974	Measured RF	Predicted ET	Predicted J	Predicted $W_0 - W_\tau$	Mean RF
May*	119	36	71	13	86
June	47	21	24	2	99
July	237	27	218	-7	91
August	72	47	32	-7	84
September	118	62	45	12	69
October	126	92	39	-6	89
TOTAL	720	285(40%)	428(59%)	7(1%)	518

* Period 5 May - 31 May only

1975					
May*	101	22	94	-15	
June	77	29	49	0	
July	130	33	85	12	
August	143	47	101	-5	
September	51	64	19	-32	
October	83	91	1	-9	
TOTAL	585	285(49%)	348(60%)	-49(9%)	

* Period 12 May - 31 May only

As has been shown, the daily drainage flux from a soil is intimately related to the physical properties of the entire soil profile. But once the soil profile is fully rewetted ($W = W_{max}$), overall during winter, if the profile saturated hydraulic conductivity is high, since W tends to W_{max}, $J \cong RF-ET$. That the layered Manawatu fine sandy loam possesses a sufficiently high value of K_s is evidenced in July 1974 when a massive 218 mm (92% RF) was lost as drainage.

Whether a soil is underlain by a coarse-layer below the root zone or not makes no difference to the value of W_{min}, the minimum profile water content that occurs during a dry summer. However the value of W_{max} for a coarse-layered soil is greater by ΔW than that of a uniform soil. Consequently when the soil is rewet in autumn or early winter the storage in a uniform soil will reach W_{max} and begin draining before a similar soil underlain by a coarse layer. This results in the drainage component of a layered soil being ΔW less than that of the uniform soil. During a dry spring-summer period under dryland conditions, since in a layered soil $W_{max}-W_{min}$ is ΔW greater than for a uniform soil, ET will be approximately ΔW greater in the water balance of the layered soil.

Under irrigation the increase in W_{max} caused by the coarse-textured layer means that irrigation need be applied less frequently. In the Manawatu fine sandy loam ΔW was found to be 55 mm, which is water enough for an additional 10-30 days plant use during the growing season. Because of the size of W_{max} the soil may be irrigated to a value of less than W_{max} without fear of a shortage of soil water and so allowing for the chance of recharge by rainfall, thus minimising the risk of drainage loss.

Applied water balance studies require good estimates of both W_{min} and W_{max} as well as estimates of ET for a well-watered crop. The results presented in Chapter 2 confirm that simple, yet accurate methods of calculating ET for well-watered crops, based on physical principles, and requiring only meteorological data, are available. Conversely, in Chapter 3, it was shown that simple estimates of W_{max} based on standard laboratory measurements may be quite inaccurate, particularly in non-uniform soil profiles. A theory that predicts W_{max} in layered soils was presented and successfully applied to the Manawatu silt loam.

Often in water balance studies when $W \geq W_{max}$ it is assumed that J = RF-ET on a daily basis. However it is sometimes necessary to account for drainage more realistically. In Chapter 4 it was shown that a simple relationship could be developed, and used to predict the drainage in the coarse-layered Manawatu fine sandy loam. This was not significantly affected by hysteresis.

The highly variable components of soil water movement and storage are important in applied water balance studies. This work provides relatively simple models for estimating W_{max} and drainage fluxes in permeable soils underlain by a coarse-textured stratum.

5.2 SUMMARY OF RESULTS

1. ET estimates from meteorological data using either Penman's equation or Priestley and Taylor's procedure were found to be 15-20% accurate on a daily basis in comparison to Bowen ratio-energy balance ET measurements, and about 10% accurate over weekly periods.

2. If only the daylight period was considered, the empirical coefficient in Priestley and Taylor's procedure was found to be constant (α= 1.21) over a range of crops and climatic conditions. Under

low net radiation conditions, significant nocturnal long-wave radiation loss not associated with a vapour flux was considered to be the reason for the lesser success of Priestley and Taylor's method over the 24 hour period. Fair agreement was found between the daylight Priestley and Taylor estimates and ET measured using the water balance of a drainage lysimeter over periods greater than a month.

3. A theoretical framework was established to enable analysis of the maximum profile water retention in soil underlain by a coarse layer. As well as the depth of the overlying soil and the coarseness of the underlay, the shape of the water retention curve of the overlying soil plays a major part in controlling the quantity of water stored in the soil profile. Water storage in sandy soils is more affected by the occurrence of a coarse-textured underlay, than finer- or coarser-textured soils.

4. In the Manawatu fine sandy loam, coarse layering at 90 cm depth was found to increase the profile water storage 55 mm above that of a hypothetically similar soil without the coarse layer. Good agreement was obtained between the quasi-equilibrium profile of water content predicted by the theory and profiles of water content measured in the field by neutron probing after drainage had ceased.

5. It was shown that for certain layered soils it is possible to develop simple theory relating the drainage flux to the water stored in the overlying soil. This theory also enables the pressure potential profile in the soil to be predicted during drainage. Significant hysteresis, in both the water retentivity curve of the overlying soil and to a lesser extent in the hydraulic conductivity-

pressure potential curve of the coarse layer, was shown to be of little consequence. A unique relationship between the drainage flux and profile storage could be assumed.

6. The drainage theory was shown to be applicable to the Manawatu fine sandy loam. Drainage predicted by the model was in agreement with that measured by the lysimeter, and the predicted soil water storage was found to be similar to that measured by neutron probing. The theory was also used to show that soils underlain by a coarse layer have a much flatter drainage recession curve compared to that of a similar uniform soil. This results in the greater water storage capacity of layered soils.

APPENDIX I

ERROR ANALYSIS OF THE BOWEN RATIO-ENERGY BALANCE METHOD OF ET ESTIMATION

A1.1 INTRODUCTION

In the Bowen ratio-energy balance method evapotranspiration (ET) is calculated from the energy balance equation

$$ET = (R_n - G)/(1 + \beta) \qquad \text{——(A1.1)}$$

where the Bowen ratio $\beta = H/ET$, where R_n is the net radiation, G the soil heat flux, and H the sensible heat flux. R_n, G, H and ET are in units of equivalent depth of water (mm), having divided through by the latent heat of vapourization of water. Using the aerodynamic equations for heat and mass transfer, and assuming similarity of the diffusivities of H and ET it can be shown that

$$\beta = \gamma \Delta T / \Delta e \qquad \text{——(A1.2)}$$

where γ is the psychrometric constant, and ΔT and Δe are the temperature and humidity differences between two levels above the evaporating surface. It is possible to measure ΔT by use of temperature sensors and Δe by wet bulb psychrometers. Following Fuchs and Tanner (1970) Eq.A1.2 can be rewritten to give

$$\beta = \gamma \Delta T / [(s + \gamma^*) \Delta T_w] \qquad \text{——(A1.3)}$$

where s is the slope of the saturated vapour pressure-temperature curve, γ^* the psychrometer constant (as distinct from the thermodynamically defined psychrometric constant), and ΔT_w the difference in the wet bulb temperature between the two levels.

Eq.A1.3 relates to a psychrometer assembly where the value of ΔT_w is measured at the same dry bulb temperature (Slatyer and Bierhuizin, 1964). A similar isothermal block arrangement was used in this study and has been previously described by Kerr et al. (1973).

Errors in the measurement of ΔT and ΔT_w can be seen to affect β via Eq.A1.3. Similarly error in γ^* can result in error in the value of β. Errors in the measurement of β and $R_n - G$ affects the value of ET computed by Eq.A1.1.

In this Appendix the magnitude of these errors is examined and their effect on ET determined.

A1.2 THEORY

Fuchs and Tanner (1970) analysed the effect of errors in the measurement of ΔT, ΔT_w, R_n-G, and s on the accuracy of determination of ET, on the basis of maximum error calculations. Hence, using the symbol 'δ' to denote the error in a quantity, they wrote the relative error in ET from Eq.A1.1 as

$$\delta ET/ET = (\delta R_n + \delta G)/|R_n - G| + \delta\beta/|1+\beta| \qquad \text{——(A1.4)}$$

Determination of the probable error however is more realistic, whereby the error in a quantity is given as the square root of the sum of squares of the maximum error in each variable (Topping, 1966). Hence, as Sinclair (1972) has suggested the relative error in ET can be found as

$$\delta ET/ET = \sqrt{(\delta R_n^2 + \delta G^2)/(R_n - G)^2 + [\delta\beta/(1+\beta)]^2} \qquad \text{——(A1.5)}$$

On this basis considering the error in ΔT, ΔT_w and γ^* the relative error $\delta\beta/(1+\beta)$ can be found from Eq.A1.3 as

$$\delta\beta/(1+\beta) = [\beta\gamma/(1+\beta)] \sqrt{(\delta\Delta T/\Delta T)^2 + (\delta\Delta T_w/\Delta T_w)^2 + [\delta\gamma^*/(s+\gamma^*)]^2} \qquad \text{——(A1.6)}$$

The quantity $\delta\Delta T$ represents the error in measurement of the temperature gradient which can be given as

$$\delta\Delta T = \sqrt{\delta T_d^2 + \delta T_d^2} \qquad \text{——(A1.7)}$$

where δT_d is the maximum error involved in the measured temperature T_d. Similarly for wet bulb psychrometers

$$\delta\Delta T_w = \sqrt{2}\,\delta T_w \qquad \text{——(A1.8)}$$

Equations A1.5 and A1.6 provide a basis for analysing the errors in ET due to the contribution of measurement errors from the various sources. This measurement error analysis procedure does not account for the inadequacy of the steady-state and one-dimensional assumptions inherent

in the determination of ET by Eq.A1.1. As shown by Rose et al. (1972) this assumption can introduce errors up to 18% in daily ET under very non-steady state conditions. Under steady-state conditions the accuracy was less than 5%. Similarly errors due to the failure of the assumption of similarity between the diffusivities of heat and mass are ignored. These Campbell (1973) concluded could lead to errors of up to 10%.

A1.3 RESULTS

A1.3.1 ERROR CONTRIBUTION DUE TO THE PSYCHROMETER CONSTANT

In a perfect psychrometer the change in latent heat content per unit volume when the vapour pressure rises from e to saturation at T_W $[e_s(T_W)]$ is equal to the amount of heat lost as the air cools from T_d to T_W. Hence it can be shown that

$$e = e_s(T_w) - [Pc_p/L\varepsilon](T_d - T_w) \qquad \text{——(A1.9)}$$

or

$$e = e_s(T_w) - \gamma(T_d - T_w) \qquad \text{——(A1.10)}$$

where P is the pressure, c_p the specific heat capacity of the air, L the latent heat of vapourization and ε the ratio of the molecular weight of water to air. A good empirical expression for γ is given by the Ferrel's equation (List, 1958), namely

$$\gamma = (6.61 \times 10^{-4})[1 + 0.00115 T_w]P \qquad \text{——(A1.11)}$$

where T_W is in units of C and P in mbar.

However in practice psychrometers may not fulfil the adiabatic or other constraints necessary to arrive at Eq.A1.10. It was necessary then to test the accuracy of the psychrometer assembly used in this study.

From consideration of the energy balance of a wick psychrometer it is possible to show that

$$e = e_s(T_w) - \gamma^*(T_d - T_w) \qquad \text{——(A1.12)}$$

where $\gamma^* = \gamma(1+\Lambda)$ and Λ can be shown to be related to the thermal conductivity of the wick and the diffusion resistance to heat and vapour leaving the wick. Hence Λ is a function of air velocity (u) over the wick for a given psychrometer. Consequently γ^* is also a function of u, unless the psychrometer is fully ventilated and adiabatic conditions apply.

The psychrometer unit used in the field in this study was set up in the laboratory in a way similar to that used in the field, so the form of $\gamma^*(u)$ could be determined. A flow meter was placed in the aspiration line to measure the air flow, as direct measurement of the air velocity over the wet bulb was not possible. The measurement accuracy of the flow meter was 0.1 l/min. Rearrangement of Eq.A1.12 gives

$$\gamma^*/\gamma = (e_s(T_w) - e)/(\gamma[T_d - T_w]) \qquad \text{——(A1.13)}$$

The value of e was that of the ambient vapour pressure in the laboratory, measured with an Assman psychrometer and found to be effectively constant during the experimental run ($< \pm$ 1 mb). The temperatures T_d and T_w were measured on a chart recorder so as to ensure that sufficient equilibration time was allowed for, following changing of the flow rate.

The results are shown in Fig.A1.1 and it can be seen that the aspiration plateau does not begin until a flow rate of about 5 l/min is achieved. A flow of this rate is estimated to produce an air speed of 2.5 m/sec in the chamber just before the wick, which is close to the recommended ventilation rate for psychrometers (Bindon, 1965). The use of different wick and water level configurations in the wet bulb results in a different value of Λ for each run causing some of the scatter in the data, especially at low flow rates. As in the field the unit was operated in the range 1-2 l/min it can be seen that $\gamma^* = 1.75\ (\pm\ 0.3)\gamma$, and $\delta\gamma^* = 0.2$ as $\gamma = 0.66$, in mb/C.

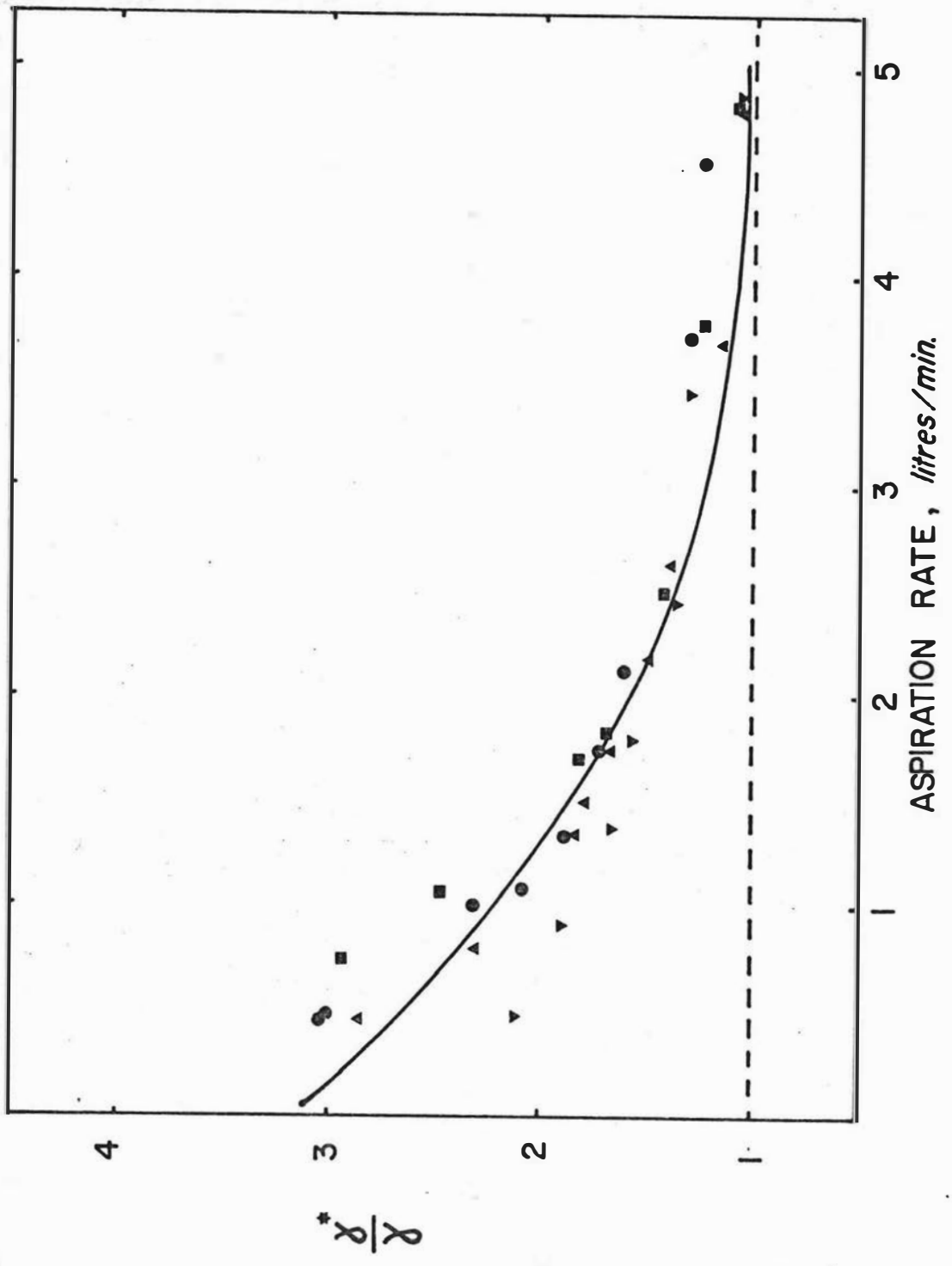

Fig.A1.1 Ratio of the psychrometer to the psychrometric constant as a function of aspiration flow rate, for four different experimental runs.

A1.3.2 TEMPERATURE MEASUREMENT ERROR

To determine β it is necessary that both the wet-bulb and the dry-bulb temperature gradients can be measured. Paired diodes with matching calibration curve slopes were used to estimate both ΔT and ΔT_w. In order to eliminate the errors due to inaccurately determined offsets in the diodes used for the gradient measurement, the sensors were rotated through 180^o every 15 minutes so that error cancellation would occur when the 30 minute average was formed. Thus errors in ΔT and ΔT_w will be similar and arise through recorder resolution, the slopes of calibration curves of the paired diodes not being identical, and short term sampling and scanning rate problems. Since it is not possible to determine accurately the magnitude of such errors it was considered that δT_d and δT_w were of the order 0.05 C. This is of similar magnitude reported by Fuchs and Tanner (1970) using similar diode sensors (δT_d = 0.01 C, δT_w = 0.1 C) and Sinclair (1972) (0.02 and 0.04 C respectively).

A1.3.3 NET RADIATION MEASUREMENT ERROR

The form of Eq.A1.1 means that measurement error in the determination of R_n, can be seen, by Eq.A1.5 to have an effect on the accuracy of resolution of ET by the Bowen ratio-energy balance method. Comparing two net radiometers Fuchs and Tanner (1970) estimated the accuracy in measurement of R_n to be 3%. For estimation of δR_n in this study, a comparison was performed over 45 daily totals of R_n from two separate, but identical polythene-shielded radiometers (Funk, 1959), the output of one was recorded on a data logger and the other on an analogue integrator (Fig.A1.2). The value of the standard error of the estimate of the regression between them was 0.2 mm/day, with the mean R_n, 3.4 mm/day, corresponding to an accuracy of 6%. As this will be in part due to the different modes of integration it is assumed that δR_n is 5%. Since $G \ll R_n$, in fact $G \cong 5\%\ R_n$, even though $\delta G \cong \delta R_n$ it is reasonable in Eq.A1.4 to ignore the effect of δG.

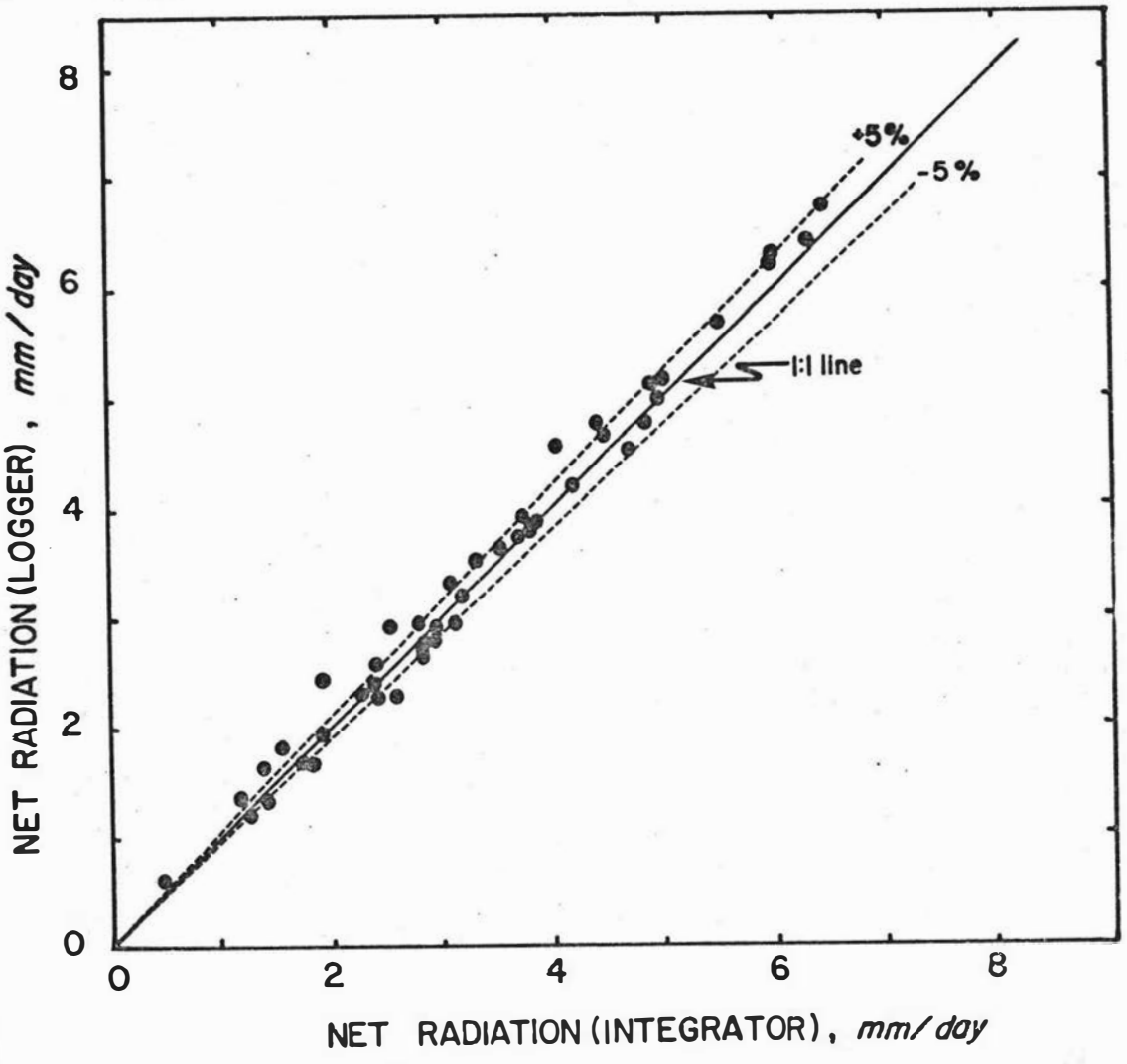

Fig.A1.2 Comparison of daily net radiation measured by two different net radiometers. The daily total of one found by integration of 1 minute sampling on a data logger and the other by analogue integration.

A1.4 DETERMINATION OF THE ERROR IN ET

Having established the errors in T_d, T_W and γ^* it is possible to determine the relative error $\delta\beta/(1+\beta)$ by Eq.A1.6. Given that $\delta T_d = \delta T_W = 0.05$ C, $\overline{\Delta T} = 0.5$ C, $\overline{\Delta T}_W = 0.3$ C and $\delta\gamma^* = 0.2$ it can be shown by Eq.A1.6 that errors emanating from the psychrometer system are in the main due to measurement errors in T_d and T_W. Errors due to variation in the flow rate which alter γ^* are minor. In Eq.A1.6

$$\delta\beta/(1+\beta) = 0.19\beta/(1+\beta) \qquad \text{——(A1.14)}$$

Since throughout this study generally $\beta<1$ this reduces to

$$\delta\beta/(1+\beta) < 0.1 \qquad \text{——(A1.15)}$$

The size of this error term is much larger than that predicted by Sinclair (1972) who suggested it could, in most circumstances, be ignored. However it is of similar order to the error that Fuchs and Tanner (1970) calculated using Pasquill's (1949) measurements over wet pasture.

As δR_n is 5% from Eqs.A1.15 and A1.5, it follows that the error due to measurement in the Bowen ratio-energy balance estimate of ET is

$$\delta ET/ET < 11\% \qquad \text{——(A1.16)}$$

This is of similar magnitude to the differences found between Bowen ratio estimates and lysimeter measurements under non-advective conditions (Fritschen, 1965; Denmead and McIlroy, 1970 and Blad and Rosenberg, 1974).

APPENDIX II

NEUTRON PROBE CALIBRATION

A2.1 INTRODUCTION

The neutron probe used in this study was a Troxler 1265 annular source model. The fast neutron source comprises of 3.7 x 10^9 Bq (100 m Ci) Americium-Beryllium, and the slow neutron detector is a $^{10}BF_3$ filled proportional counter. The slow neutron count was monitored by a Troxler G-200 ratemeter. Polythene is employed in the radiation shield and reference standard. Seamless aluminium irrigation tubing 5.08 cm (2.0") O.D., 4.83 cm (1.9") I.D. was used for the access tubes. The voltage detector plateau was established at 1350 volts prior to use of the probe.

In this Appendix is discussed the procedure by which this probe was calibrated.

A2.2 THEORY

The response of a neutron probe depends on the bulk density of the soil body, its chemical composition, and the constitutional hydrogen content, as well as the volumetric water content found by oven-drying. Calibration may be carried out in the laboratory using soil or artificial media in containers. Alternatively a field technique can be used.

Laboratory results and the use of theoretical models have resolved the effect of the various parameters on the response of neutron probes.

It is possible to show that the energy transfer resulting from a fast neutron (2-11 MeV) colliding with a nucleus, called scattering, is inversely proportional to the relative atomic weight of the nucleus, which is approximately the mass number (IAEA, 1970). Thus hydrogen and low mass number elements are most efficient in the neutron slowing down process. Also the absorption of epithermal neutrons (0.2-2 MeV) into the nucleii of soil

atoms can occur, resulting in a lower thermal neutron flux. Consequently the count rate of thermalized neutrons is greatest for water and hydrogen followed, an order of magnitude lower by the group of elements (B, C, N, O, Mg, Al, Si, K, Ca, Fe). Burn (1965) attributed the disagreement he found between a calibration established in artificial soil and the field calibration, to the significant amounts of potassium and iron in the latter.

Also the presence of constitutional hydrogen affects the response of a neutron probe (Holmes, 1966). Constitutional hydrogen is primarily due to bound water not removed by oven-drying, or to organic matter in the soil. However in sandy or silty soils, low in organic matter, the volumetric content of such hydrogen will be small.

The nature of the effect of bulk density ρ_b on the calibration of the neutron probe is disputed. Holmes (1966) found a tendency for the thermal neutron count rate to decrease with an increase in ρ_b, whereas Ølgaard and Haahr (1968) suggested the rate should increase. Bulk density can affect the count rate in three ways (Ølgaard and Haahr, 1968). Firstly with an increase in ρ_b there tends to be an increase in the volumetric content of bound water. Secondly greater scattering due to the greater number of soil atoms near the detector with increasing ρ_b occurs, even though their effect on slowing down the neutrons is relatively small. Thirdly an increase in ρ_b increases the concentration of absorbing elements. The effect of ρ_b on the count rate of an oven-dry soil will depend on the combined effect of these three processes. Greacen and Schrale (1976) suggest that Holmes' (1966) data is suspect because of his overestimation of the bound water content of his soil and variability in his ρ_b data. Greacen and Schrale (1976) found that the plot of count ratio* against total water content was linear with a residual variability due

---

* Count ratio (C.R.) = thermal neutron cps/cps in radiation shield

to scattering and absorption effects with changing ρ_b. This residual scatter they could reduce by using an empirical relationship based on $\sqrt{\rho_b}$. Variability and measurement error in field data however makes this correction not worthwhile, in most circumstances.

A field technique was chosen for calibrating the present instrument, as the calibration established will implicitly account for the effects outlined above. However this approach requires sufficient replication to provide the desired resolution, in order to overcome measurement errors.

A2.3 EXPERIMENTAL

At each calibration site an access hole was installed using a 4.4 cm auger, removing 5-10 cm long samples for bulk density (ρ_b) and oven-dry gravimetric water content measurements. The hole was reamed out to the correct size with a length of old access tube, and an access tube installed. The neutron probe was then used to establish the count ratio at 5 cm depth intervals down the profile. Surface calibration data for the 0-15 cm depth were obtained by measuring the count ratio at 10 cm depth at two sites and finding the 0-15 cm depth volumetric water content (θ) of two cores, removed within 50-100 cm of the tubes, for a range of water contents (van Bavel and Stirk, 1967).

The bulk density of the soil, a Manawatu fine sandy loam was found to be 1.39 ($\pm$ 0.10) gm/cm^3 from 103 samples obtained over the 0-110 cm profile. Applying the empirical model of Greacen and Schrale (1976) suggests this 7% variation in bulk density will result in only a 3.5% change in the count ratio due to scattering and absorption effects. Since the soil on which this study was conducted is of medium texture and low in organic matter ignoring the constitutional hydrogen content by using oven-dry water contents is considered of little consequence. The value of ρ_b found for each core was

used to change the gravimetric water content into volumetric units (θ). Much of the measurement error in establishing θ will be due to measurement error in the determination of the length of the core. Since the measurement error in the length is considered to be less than 10% it follows that the error in θ from this is also less than 10%. The comparison of θ and C.R. is presented in Fig.A2.1 and an error of 10% in the measurement of θ can be seen to account for much of the variation.

A linear regression through the data yielded the equation

$$\begin{aligned} \theta &= 0.386\ \text{C.R.} - 0.025 \\ R &= 0.90^{****} \\ S_{yx} &= 0.034\ \text{cm}^3/\text{cm}^3 \\ n &= 103 \end{aligned} \qquad \text{——(A2.1)}$$

where R is the correlation coefficient, S_{yx} the standard error of the estimate and n the number of observations. This line is significantly higher (0.025 cm^3/cm^3) than the factory calibration curve. The values of R and S_{yx} are of the same order of magnitude as found in other field calibrations (Rose, 1966; Rawitz, 1969; Rawls and Asmussen, 1973; Păultineau and Apostol, 1974).

The surface calibration data are similar to the depth data and hence Eq.A2.1 was also used to determine the water content in the 0-15 cm zone using the 10 cm C.R. data.

The upward translation of the field calibration curve in relation to the Troxler supplied curve is at variance with the downward translation found by Rawitz (1969) and the rotation of Rawls and Asmussen (1973), both using similar Troxler probes. This emphasises the need to establish independent calibration curves, and this can be achieved using field procedures.

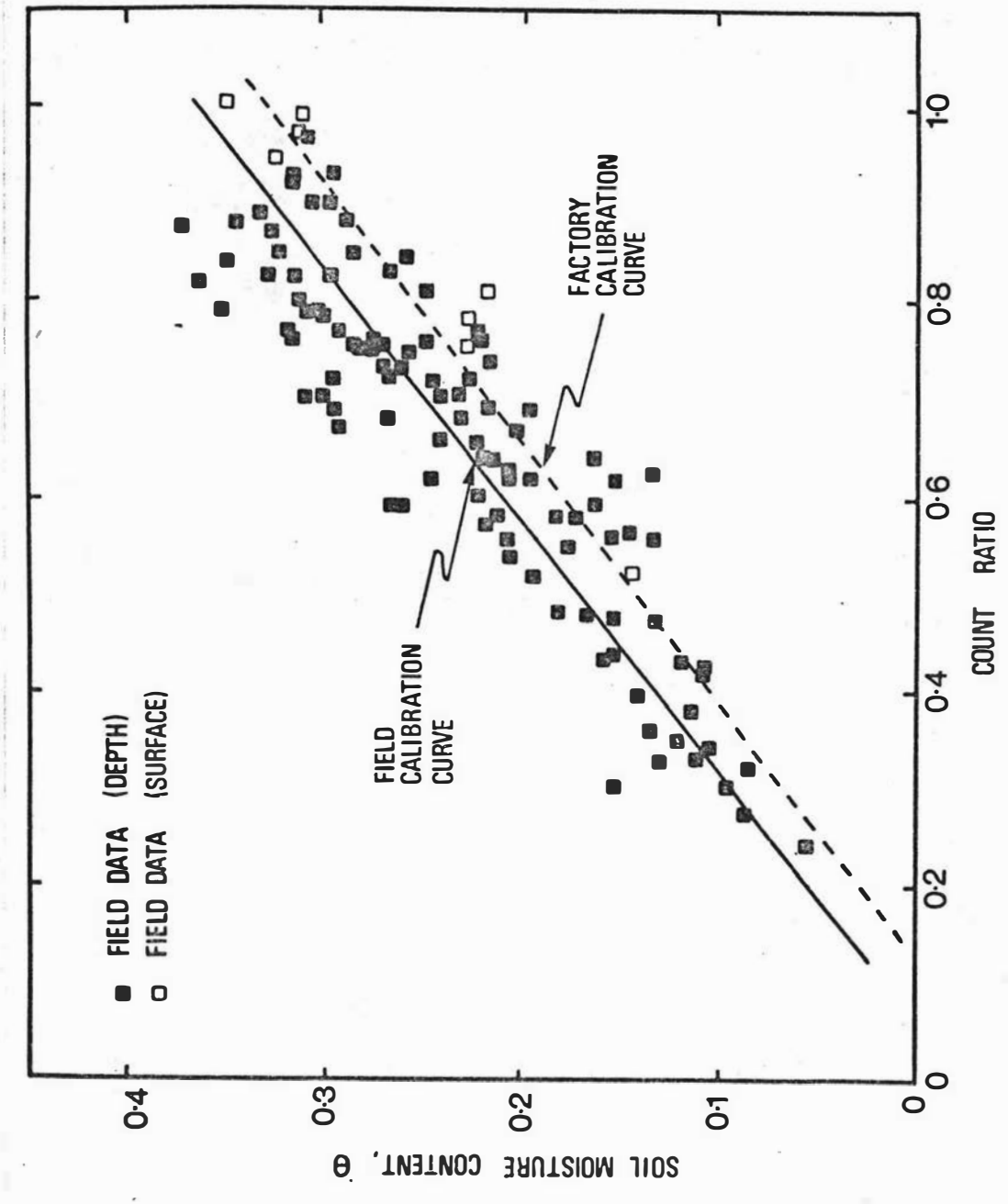

Fig.A2.1 Soil moisture content (cm^3/cm^3) in comparison with the count ratio. Also shown is the calibration curve supplied by Troxler.

APPENDIX III

SOIL PROFILE DESCRIPTION

A3.1 SPATIAL VARIATION (J.D. Cowie, 1971, pers.comm.)

The one hectare plot on which the study was carried out was found to contain 5 different phases of Manawatu fine sandy loam, as resolved by auger bores made on a 30.5 m grid. For most of the area the overall soil profile was found to be similar, i.e. a brown to yellowish brown fine sandy loam overlying an olive to olive grey medium to fine sand on gravelly coarse sand. Although in fine detail the pattern is very variable, due to the presence of complex alluvial banding, and varying depths to the gravelly coarse sand. Many of the bands are of only small lateral extent. Allowing for this variation the soils were grouped, on the basis of the depth to the gravelly coarse sand, and depth of the respective layers. Thus to a first approximation the major variation is due to depth variations rather than textural or structural changes.

A3.2 PROFILE DESCRIPTION (J.D. Cowie, R.H. Wilde, 1974, pers.comm.)

The soil pit to enable the description was dug near the lysimeter, and is shown in Fig.A3.1. Profile description follows Taylor and Pohlen (1970) (Table A3.1). In order to model water retention and flow of water in this soil it was necessary to simplify this description. For such purposes the profile was subdivided as follows: 0-50 cm fine sandy loam, underlain by 40 cm of fine sand with gravelly coarse sand beyond 90 cm. The physical characteristics of these profile elements are given in Table 3.1. As can be seen in Fig.A3.2 the gravelly coarse sand interface varies in terms of its depth and the texture of the underlay immediately under the interface.

Table A3.1 Profile description of the Manawatu fine sandy loam

Horizon	Depth	Description
A	0-23 cm	dark greyish brown (2.5 YR 4/2) fine sandy loam to silt loam; friable, moderately developed medium and fine nutty structure; very few faint grey and reddish brown mottles in lower part of horizon, many roots, distinct wavy boundary.
(B)	23-51 cm	dark greyish brown (2.5 Y 4.2) fine sandy loam; friable; weakly developed nutty structure; few roots; distinct wavy boundary.
C_{11}	51-74 cm	olive grey (5 Y 4/2) fine sand; very friable; weakly developed blocky structure; no roots; distinct wavy boundary.
C_{12g}	74-87 cm	olive (5 YR 4/3) fine loamy sand; very friable; weakly developed medium blocky structure; many distinct fine reddish brown mottles; thin sand layers throughout and thin iron staining at base; sharp wavy boundary.
C_{13}	87-102 cm	olive (5 YR 4/3) medium sand; loose; single grained; very wavy distinct boundary.
D	102 cm (+)	gravelly coarse sand (5 Y 3/2).

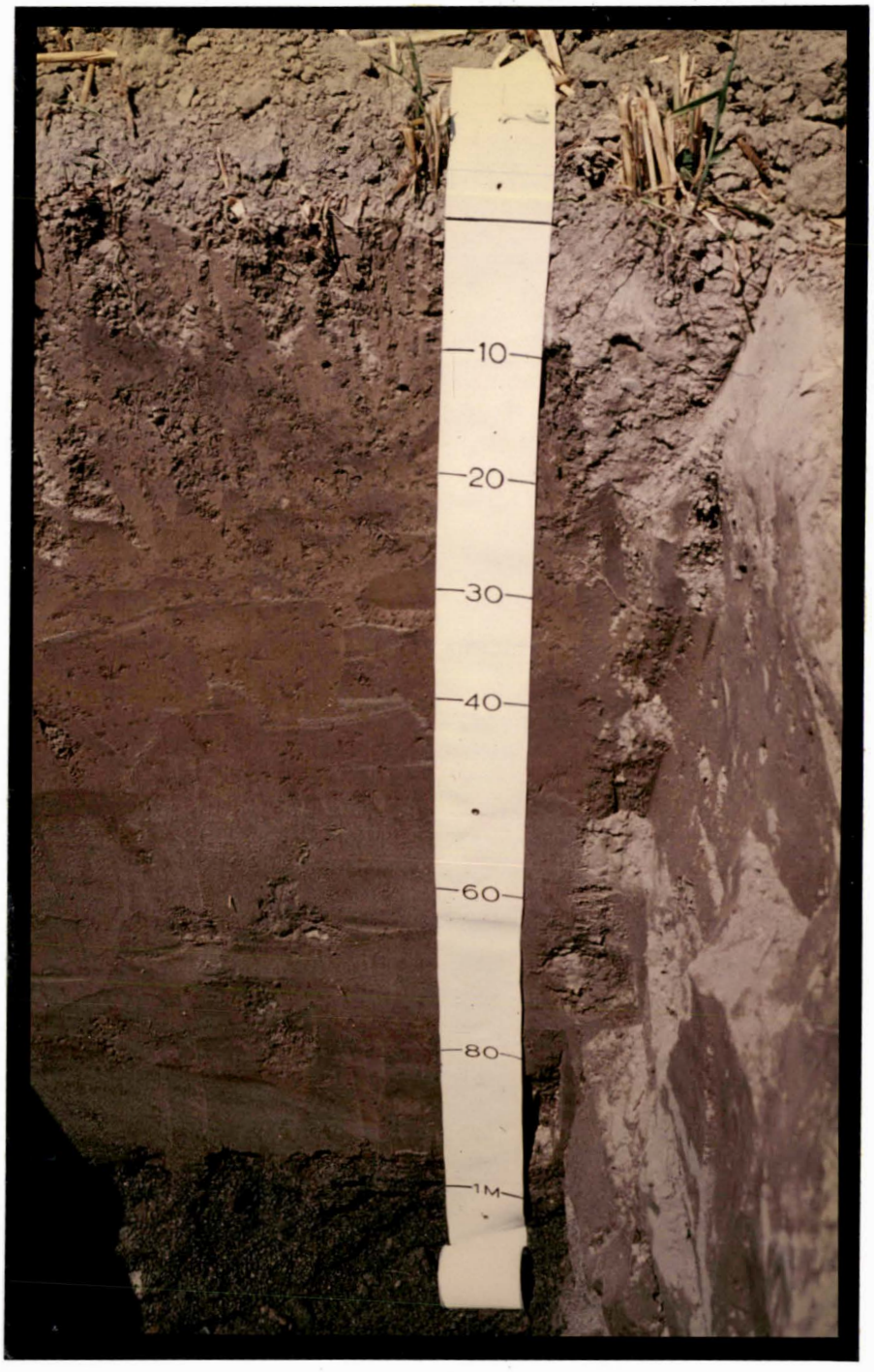

Fig.A3.1 The profile of Manawatu fine sandy loam

Fig.A3.2 The interface between the fine sand and gravelly coarse sand of Manawatu fine sandy loam. The range in height of the interface in this photo is 10 cm.

APPENDIX IV

CROP DESCRIPTION

A4.1 INTRODUCTION

In this Appendix are given details of the development and management of the oats crop over which the Bowen-ratio energy balance ET measurements were made in 1974.

A4.2 CROP AGRONOMY

The experimental area was ploughed out of a ryegrass-clover pasture in early autumn 1974 and given a final cultivation to prepare a good seedbed. On the day prior to planting, urea and Rustica Blue (N:P:K 12:5:14) were both applied at a rate of 250 kg/ha and the paddock was then harrowed. The oats (cv. Mapua 70) were sown on the 26 April at 112 kg/ha with 15 cm row spacing. On August 6 an additional 250 kg/ha of urea (46% nitrogen) was applied by air.

The development of dry matter production of the crop over the growing season is shown in Fig.A4.1 and the height and LAI in Fig.A4.2. These data were obtained by sampling at 4 sites within the crop every 14 days. The sample area was 1 m long and 4 rows wide. By mid-June the crop had achieved a stable plant population of 8×10^6 tillers/ha.

Evapotranspiration was measured over the period 4 July-11 November 1974. Throughout this period LAI $>$ 6 and as the leaves covered the inter-row space the crop was at full-cover. Seedhead emergence began in early November with an associated increase in the dry matter %.

The crop suffered slight barley yellow dwarf virus and lodged in parts during September and contracted Dreschlera (Helminthsporium) and crown rust in October. The areas in which these were severe was limited and it is considered that they had no significant affect on transpiration.

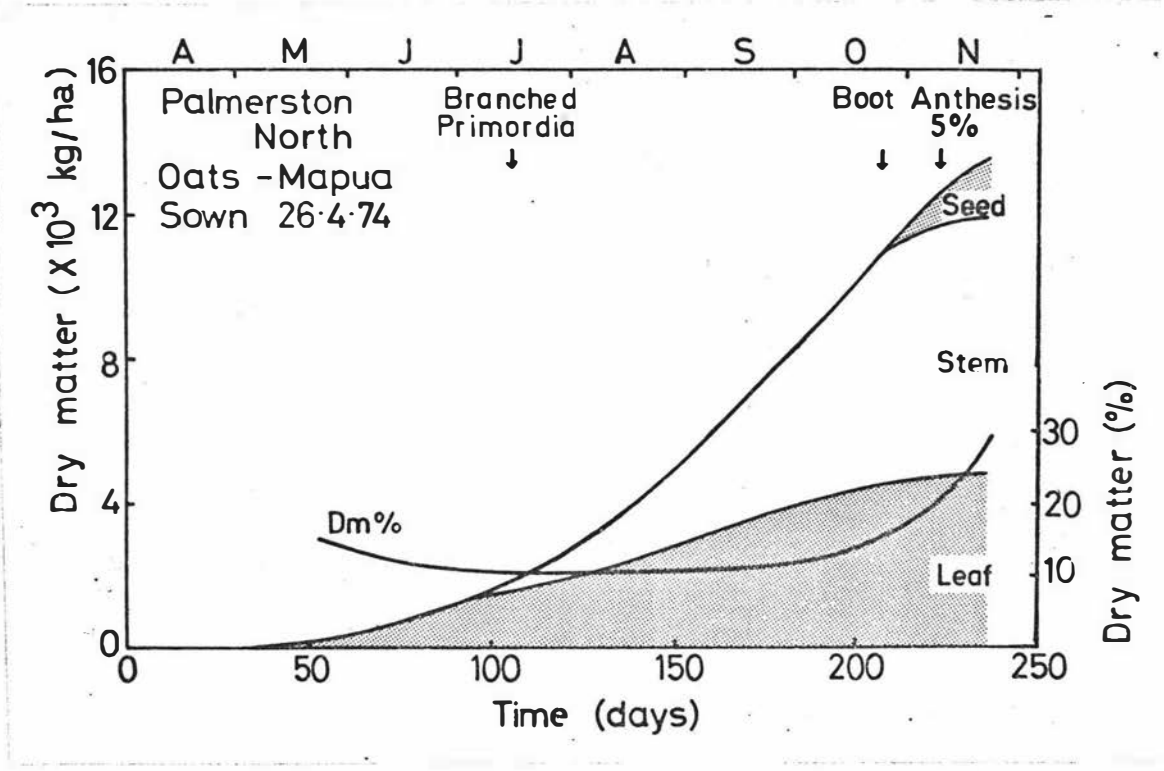

Fig.A4.1 Seasonal changes in yield components and dry matter % (Dm) of total forage, of the 1974 oats crop (After Kerr and Menalda, 1976).

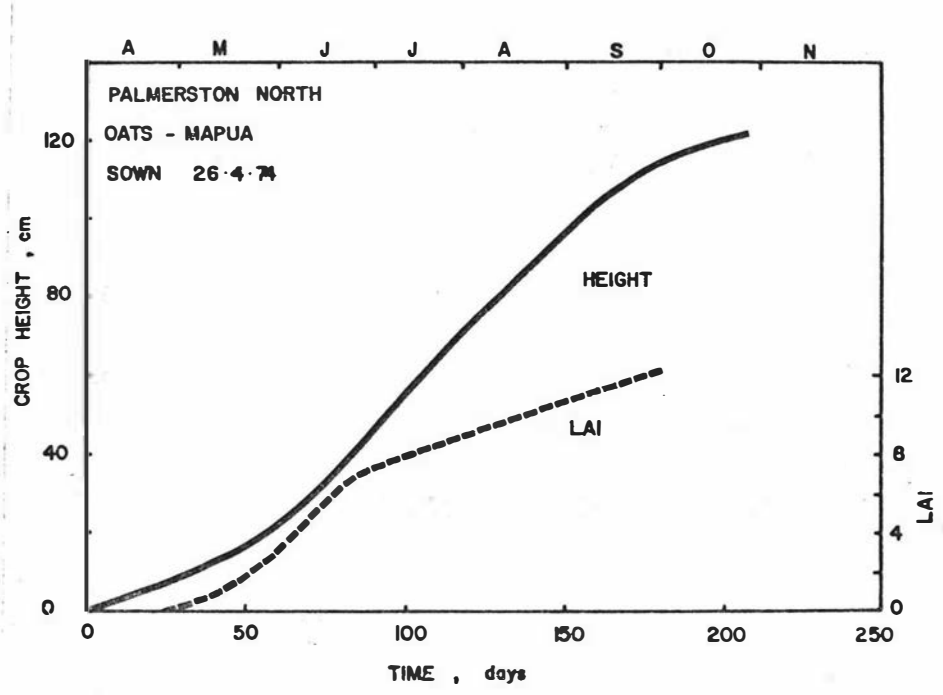

Fig.A4.2 Seasonal changes in the height and leaf area index (LAI) of the 1974 oats crop.

BIBLIOGRAPHY

Alway, F.J. and G.R. McDole, 1917. Relation of water retaining capacity of a soil to its hygroscopic coefficient. J.Agr.Res. 9: 27-71.

Bindon, H.H. 1965. A critical review of tables and charts used in psychrometry. in 'Humidity and Moisture' A. Wexler (Ed.), Rienhold Pub.Corp. New York. p 687.

Black, T.A., W.R. Gardner and G.W. Thurtell, 1969. The prediction of evaporation, drainage and soil water storage for a bare soil. Soil Sci.Soc.Am.Proc. 33: 655-660.

Blad, B.L. and N.J. Rosenberg, 1974. Lysimetric calibration of the Bowen ratio energy balance method for evapotranspiration estimation in the Central Great Plains. J.Appl.Met. 13: 227-236.

Brooks, R.H. and A.T. Corey, 1966. Properties of porous media affecting fluid flow. ASCE, J.Irrig. Drain.Div., 4855, 92: 61-88.

Brown, K.W. and R.L. Duble, 1975. Physical characteristics of soil mixtures used for golf green construction. Agron.J. 67: 647-652.

Brunt, D. 1932. Notes on radiation in the atmosphere. Quart.J.Roy.Met.Soc. 58: 389-420.

Burn, K.N. 1965. Calibration of a neutron soil moisture meter. Research paper 266, National Research Council, Canada.

Campbell, A.P. 1973. The effect of stability on evaporation rates measured by the energy balance method. Agric.Meteorol., 11: 285-302.

Cannell, G.H. and C.W. Asbell, 1974. The effects of soil-profile variations and related factors on neutron-moderation measurements. Soil Sci. 117: 124-127.

Cary, J.W., 1973. Soil water flow meters with thermocouple outputs. Soil Sci.Soc.Am.Proc. 37: 176-181.

Chang, Jen-Hu, 1968. "Climate and Agriculture, an Ecological Survey". Aldine, Chicago. pp.304.

Childs, E.C. 1945. The water table, equipotentials and streamlines in drained land. III. Soil Sci. 59: 405-415.

Clothier, B.E., J.P. Kerr and D.R. Scotter, 1975. Weather and the growth of maize; Evapotranspiration. paper presented at the Symposium on Meteorology and Food Production. 14-15 October 1975. Wellington.

Colman, E.A. 1947. A laboratory procedure for determining the field capacity of soils. Soil Sci. 63: 277-283.

Coulter, J.D. 1973a. Prediction of evapotranspiration from climatological data. Proc.Soil and Plant Water Symp. Palmerston North. N.Z. 10-12 April 1973 D.S.I.R. Inf. Ser.96.

Coulter, J.D. 1973b. A water balance assessment of the New Zealand rainfall. J.Hydrol. (N.Z.) 12: 83-91.

Cowie, J.D. 1972. Soil map and extended legend of Kairanga County, North Island, New Zealand. N.Z. Soil Bureau Publication 538.

Dane, J.H., P.J. Wierenga, 1975. Effect of hysteresis on the prediction of infiltration, redistribution and drainage of water in a layered soil. J.Hydrol. 25: 229-242.

Davidson, J.M., L.R. Stone, D.R. Nielsen and M.E. La Rue, 1969. Field measurement and the use of soil water properties. Water Res.Research. 5: 1312-1321.

Davies, J.A. and C.D. Allen, 1973. Equilibrium, potential and actual evaporation from cropped surfaces in southern Ontario. J.Appl.Met. 12: 649-657.

Denmead, O.T. and I.C. McIlroy, 1970. Measurements of non-potential evaporation from wheat. Agric. Meteorol., 7: 285-302.

de Lisle, J.F. 1966. Mean daily insolation in New Zealand. N.Z.J.Sci. 9: 992-1005.

de Wit, C.T. and H. van Keulen, 1972. Simulation of Transport Processes in Soils. Centre Agric.Publ. Doc., Pudec, Wageningen, 100 pp.

Eagleman, J.R. and V.C. Jamison, 1962. Soil layering and compaction effects on unsaturated moisture movement. Soil Sci.Soc.Amer.Proc. 26: 519-522.

Fitzgerald, P.D. and D.S. Rickard, 1960. A comparison of Penman's and Thornthwaite's method of determining soil moisture deficits. N.Z.J.Agric. Res. 3: 106-112.

Fritschen, L.J. 1965. Accuracy of evapotranspiration determined by the Bowen ratio method. Bull.Intern. Assoc.Sci.Hydrol. 10: 38-48.

Fuchs, M. and C.B. Tanner, 1970. Error analysis of Bowen ratios measured by differential psychrometry. Agric.Meteorol. 7: 329-334.

Funk, J.P. 1959. Improved polythene-shielded net radiometer. J.Sci.Instr. 36: 267-270.

Gardner, W.R. 1960. Soil water relations in arid and semi-arid conditions. UNESCO 15: 37-61.

Gardner, W.R., D. Hillel and Y. Benyamini, 1970. Post irrigation movement of soil water: I. Redistribution. Water Resources Res. 6 (3) 851-61.

Greacen, E.L. and G. Schrale, 1976. The effect of bulk density on neutron meter calibration. Aust.J.Soil Res. 14: 159-69.

Hanks, R.J. 1974. Model for predicting plant yield as influenced by water use. Agron.J. 66: 660-665.

Hanks, R.J. and S.A. Bowers, 1962. Numerical solution of the moisture flow equation for infiltration into layered soils. Soil Sci.Soc.Amer.Proc. 26: 530-534.

Harding, S.T. 1919. Relation of the moisture equivalent of soils to the moisture properties under field conditions of irrigation. Soil Sci. 8: 303-312.

Holmes, J.W. 1966. Influence of bulk density of the soil on neutron moisture meter calibration. Soil Sci. 102: 355-360.

I.A.E.A. "Neutron Moisture Gauges" Technical Rep. Series 112, I.A.E.A. Vienna, 1970.

Jury, W.A. and C.B. Tanner, 1975. Advection modification of the Priestley and Taylor evapotranspiration formula. Agron.J. 67: 840-842.

Jury, W.A., W.R. Gardner, P.G. Saffigna and C.B. Tanner, 1976. Model for predicting simultaneous movement of nitrate and water through a loamy sand. Soil Sci. 122: 36-43.

Kerr, J.P., H.G. McPherson and J.S. Talbot, 1973. Comparative evapotranspiration rates of lucerne, paspalum and maize. Proceedings First Australasian Conference on Heat and Mass Transfer. Monash Univ., Melbourne. Section 3, pp. 1-8.

Kerr, J.P. and M.F. Beardsell, 1975. Effect of dew on leaf water potentials and crop resistances in a paspalum pasture. Agron.J. 67: 596-599.

Kerr, J.P. and B.E. Clothier, 1975. Modelling evapotranspiration of a maize crop. Proc.Agron.Soc. of N.Z. 5: 49-53.

Kerr, J.P. and P.H. Menalda, 1976. Cool season forage cereal trials in Manawatu and Wairarapa. Proc. Agron.Soc. of N.Z. 6: 27-30.

King, F.H. 1896. Irrigation in humid climates. USDA, Farmers Bull. 46 26 pp.

La Rue, M.E., D.R. Nielsen and R.M. Hagan, 1968. Soil water flux below a ryegrass root zone. Agron.J. 60; 625-629.

List, R.J. 1958. "Smithsonian Meteorological Tables" Washington, D.C. p.365.

McNaughton, K.G. 1976. Evaporation and advection II: evaporation downwind of a boundary separating regions having different surface resistances and available energies. Quart.J.Roy.Met.Soc. 102: 193-202.

Miller, E.E. and R.D. Miller, 1956. Physical theory for capillary flow phenomena. J.Appl.Phys. 27: 324-332.

Miller, D.E. 1963. Lateral moisture flow as a source of error in moisture retention studies. Soil Sci.Soc. Amer.Proc. 27: 716-717.

_____ 1969. Flow and retention of water in layered soils. A.R.S. USDA Conservation Research Rep. 13 pp. 28.

_____ 1973. Water retention and flow in layered soil profiles. In R.R. Bruce et al. (ed.) Field Soil Water Regime. S.S.S.A. special publication No. 5. S.S.S.A., Madison, Wisc.

_____ and W.C. Bunger, 1963. Moisture retention by soil with coarse layers in the profile. Soil Sci.Soc.Amer.Proc. 27: 586-589.

_____ and J.S. Aarstad, 1974. Calculation of the drainage component of soil water depletion. Soil Sci. 118: 11-15.

Monteith, J.L. 1956. Evaporation at night. Neth.J. Agric.Sci. 4: 34-38.

Monteith, J.L. 1963. Dew: facts and fallacies. In the Water Relations of Plants. ed. Rutter, A.J. and Whitehead, F.H. Blackwell Scientific Publications, Oxford.

Monteith, J.L. 1965. Evaporation and environment Symposium of the Society for Experimental Biology 19: 205-234.

Moore, R.E., 1939. Water conduction from shallow water tables. Hilgardia 12: 383-426.

Mualem, Y., 1974. A conceptual model of hysteresis. Water Resources Res. 10 (3): 514-520.

Nielsen, D.R., J.W. Biggar and K.T. Erh, 1973. Spatial variability of field-measured soil-water properties. Hilgardia 42 (7): 215-219.

Ølgaard, P.L. and V. Haahr, 1968. On the sensitivity of subsurface neutron moisture gauges to variations in bulk density. Soil Sci. 105: 62-64.

Pasquill, F., 1949. Eddy diffusion of water vapour and heat near the ground. Proc.Roy.Soc.(Lond.), Ser.A. 198: 116-140.

Păultineanu I.L. and I. Apostol, 1974. Possibilities of using the neutron method for water application efficiency studies in sprinkler and furrow irrigation. in Isotope and Radiation Techniques in Soil Physics and Irrigation Studies 1973. IAEA Vienna, 1974, pp 477-506.

Penman, H.L. 1948. Natural evaporation from open water, bare soil and grass. Proc.Roy.Soc.Lond. A 193: 120-146.

Penman, H.L. 1956. Evaporation: an introductory survey. Neth.J.Agric.Sci. 4: 9-29.

Philip , J.R., 1957. The physical principles of soil water movement during the irrigation cycle. Third Intern.Comm. on Irrig. and Drain.: 8.125-8.154.

Poulovassilis, A., V.D. Krentos, Y. Stylianou and Ch. Metochis, 1974. Soil water properties of a layered soil determined in situ. in Isotope and Radiation techniques in soil physics and irrigation studies 1973. I.A.E.A. Vienna. pp 205-224

Priestley, C.H.B. and R.J. Taylor, 1972. On the assessment of surface heat flux and evaporation using large scale parameters. Mon.Weather Rev. 100: 81-92.

Rawitz, E., 1969. Installation and field calibration of Neutron-Scatter equipment for hydrologic research in heterogeneous and stony soils. Water Resources Res.5: 519-523.

Rawlins, S.L. and P.A.C. Raats, 1976. Prospects for high-frequency irrigation. Science 188: 604-610.

Rawls, W. . and L.E. Asmussen, 1973. Neutron probe field calibration for Soils in the Georgia coastal plain. Soil Sci. 116: 262-265.

Richards, L.A. 1960. Advances in soil physics. Trans. Intern.Congr.Soil Sci. Madison, 7th 1: 67-69.

Richards, L.A. and L.R. Weaver, 194 . Fifteen-atmosphere percentage as related to the permanent wilting percentage. Soil Sci. 56: 331-339.

Richards, L.A., W.R. Gardner and G. Ogata, 1956. Physical processes determining water loss from soil. Soil Sci.Soc.Amer.Proc. 20: 310-314.

Rickard, D.S. and P.D. Fitzgerald, 1970. Evapotranspiration in New Zealand. Proc.N.Z. Water Conf. 1970 1: 3.1-3.13.

Robins, J.S. 1959. Moisture movement and profile characteristics in relation to field capacity. Intern.Comm.Irrig. and Drain. 8: 509-521.

Rose, C.W. 1966. Agricultural Physics. Pergamon Press, Oxford. pp. 226.

Rose, C.W., W.R. Stern and J.E. Drummond, 1965. Determination of hydraulic conductivity as a function of depth and water content, for soil *in situ*. Aust.J.Soil Res. 3: 1-9.

Rose, C.W., J.E. Begg, G.F. Byrne, J.H. Goncz and B.W.R. Torssell, 1972. Energy exchanges between pasture and the atmosphere under steady and non-steady state conditions. Agric.Meteorol. 9: 385-403.

Sinclair, T.R. 1972. Error analysis of latent, sensible and photochemical heat flux densities calculated from energy balance measurements above forests. in Murphy, C.E., Hesketh, J.D. and Strain, B.R. Modelling the growth of trees. Oak Ridge National Lab.

Slatyer, R.O. and I.C. McIlroy, 1961. Practical microclimatology CSIRO Australia and UNESCO.

Slatyer, R.O. and J.F. Bierhuizin, 1964. Differential psychrometer for continuous measurement of transpiration. Plant Physiol. 39: 1051-1056.

Stewart, R.B. and W.R. Rouse, 1976. A simple method for determining the evaporation from shallow lakes and ponds. Water Resources. Res. 12: 623-628.

Swinbank, W.C. 1951. The measurement of vertical transfer of heat and water vapour by eddies in the lower atmosphere. J.Met. 8: 135-145.

Tanner, C.B. 1960. Energy balance approach to evapotranspiration from crops. Soil Sci.Soc. Amer.Proc. 24: 1-9.

Tanner, C.B., 1967. Measurement of evapotranspiration, in Irrigation of Agricultural Lands pp 534-555. ASA Monograph II.

Tanner, C.B. and W.L. Pelton, 1960. Potential evapotranspiration estimates by the approximate energy balance method of Penman. J.Geophys.Res. 65: 3391-3413.

Tanner, C.B. and W.A. Jury, 1976. Estimating evaporation and transpiration from a crop during incomplete cover. Agron.J. 68: 239-243.

Taylor, N.H. and I.J. Pohlen, 1970. Soil Survey Method Soil Bureau Bulletin 25, D.S.I.R., N.Z. pp. 242.

Thornthwaite, C.W. 1948. An approach toward a rational classification of climate. Geog.Rev. 38: 55-94.

Topping, J. 1966. 'Errors of Observation and Their Treatment' Institute of Physics and the Physical Soc. Monographs for Students, Chapman and Hall Ltd. London, 119 pp.

Unger, P.W. 1971. Soil profile gravel layers: I. Effect on water storage, distribution and evaporation. Soil Sci.Soc.Amer.Proc. 35: 631-634.

van Bavel, C.H.M. and G.B. Stirk, 1967. Soil Water Measurement with an Am^{241}-Be Neutron Source and an application to evaporimetry. Journal of Hydrology 5: 40-46.

van Bavel, C.H.M. 1966. Potential evaporation: the combination concept and its experimental verification. Water Resources Res. 2: 455-467.

van Bavel, C.H.M., G.B. Stirk and K.J. Brust, 1968. Hydraulic properties of a clay loam soil and the field measurement of water uptake by roots: I. Interpretation of water content and pressure profiles. Soil Sci.Soc.Am.Proc. 32: 310-317.

van Wijk, W.R. and D.A. de Vries, 1954. Evapotranspiration. Neth.J.Agric.Res. 2: 105-119.

Veneman, P.L.M., M.J. Vepraskas and J. Bouma. 1976. The physical significance of soil mottling in a Wisconsin toposequence. Geoderma, 15: 103-118.

Vomocil, J.A. 1965. Porosity. In C.A. Black (ed.) Methods of Soil Analysis, Part I. Agronomy 9: 299-314.

Veihmeyer, F.J. and A.H. Hendrickson, 1931. The moisture equivalent as a measure of the field capacity of soils. Soil Sci. 32: 181-193.

Veihmeyer, F.J. and A.H. Hendrickson, 1949. Methods of measuring field capacity and permanent wilting percentage of soils. Soil Sci. 68: 75-94.

Wang, F.C. and V. Lakshminarayana, 1968. Mathematical simulation of water movement through unsaturated nonhomogeneous soils. Soil Sci.Soc.Am.Proc. 32: 329-334.

Wilcox, J.C. 1959. Rate of soil drainage following an irrigation. I. Nature of soil drainage curves. Can.J. Soil Sci. 39: 107-119.

ADDENDUM

Samples of about 140 cm^3 volume removed from the soil pit were used to determine the water retentivity curves of the upper two layers. For the fine sandy loam three undisturbed cores were selected between 20 and 40 cm depth to determine the draining retentivity curve (Fig. 3.6). Four undisturbed cores of fine sand were taken from between 60 and 80 cm depth; two of which were used to determine the draining retentivity curve (Fig. 3.6) and the other two for the hysteretic loop between the -15 cm and -80 cm potential (Fig. 4.1).

Large volumes of both fine sand, removed between 60 and 80 cm, and gravelly coarse sand taken below 100 cm were brought back to the laboratory. Five samples of gravelly coarse sand of about 140 cm^3 volume were repacked and the draining retentivity found on four of them (Fig. 3.6). The other was used to determine the hysteretic loop between 0 and -35 cm potential (Fig. 4.1). The remainder of the gravelly coarse sand, and also the fine sand was used for the long column determination of conductivity. Two runs, with new repacked material, were made with the gravelly coarse sand.

ADDENDUM

Date	1974	ET mm/day	ET_{eq} daylight mm/day	ET_{eq} 24 hour mm/day	T °C
July	4	1.12	0.59	0.44	6.2
	5	1.33	1.10	0.37	5.4
	6	0.28	0.32	0.23	5.7
	7	1.09	0.65	0.31	6.4
	8	1.15	0.94	0.63	7.8
	12	1.12	0.83	0.2	5.4
	13	1.63	1.03	0.53	8.0
	14	1.12	0.85	0.59	8.7
	15	1.85	0.89	0.42	10.7
August	1	1.76	1.29	1.13	7.9
	4	1.39	0.77	0.65	9.2
	8	1.55	1.18	0.33	6.5
	9	1.31	1.03	0.51	10.1
	10	1.55	1.10	0.92	10.4
	11	1.73	1.45	1.05	9.8
	12	1.30	0.88	0.62	10.4
	13	1.98	1.62	1.04	12.0
	14	0.59	0.27	0.13	10.9
	15	1.85	1.71	1.43	12.0
	16	1.07	0.87	0.55	11.0
	24	1.21	0.79	0.67	9.0
	25	2.45	1.95	1.68	9.7
	27	2.07	1.26	1.11	7.5
	28	3.22	2.20	1.88	8.8
	29	1.04	0.79	0.57	7.8
	30	2.34	1.83	1.49	8.5
	31	2.40	1.09	0.91	9.5
September	4	0.57	0.57	0.33	11.5
	5	2.61	1.87	1.48	14.9
	6	2.30	1.87	1.76	12.9
	7	2.78	2.24	2.10	13.1

	8	2.61	1.71	1.45	13.9
	9	1.44	1.12	0.95	12.1
	10	1.58	1.08	0.96	13.6
	14	2.66	2.12	1.58	13.7
	15	2.98	2.28	1.90	11.7
	17	3.43	2.15	1.95	12.3
	19	1.84	1.53	1.49	10.4
	21	2.89	2.07	1.97	13.8
	22	2.80	2.15	2.15	12.5
	23	2.47	2.00	1.75	13.8
	24	1.95	1.46	1.41	11.2
	26	1.11	0.84	0.78	14.3
	29	3.53	2.86	2.59	8.9
	30	3.86	3.20	2.98	10.2
October	6	3.49	3.67	3.58	13.6
	8	1.48	0.84	0.77	16.1
	10	3.12	2.63	2.55	12.8
	11	4.29	2.94	2.80	12.9
	12	3.94	2.34	2.26	13.8
	14	2.33	1.88	1.65	12.8
	15	4.00	3.00	2.91	13.8
	16	4.07	2.63	2.44	13.6
	18	1.60	0.83	0.74	12.9
	20	4.26	4.22	3.84	16.3
	21	4.53	4.09	3.93	15.5
	22	3.52	2.60	2.35	13.6
	23	4.10	3.41	3.13	12.1
	25	2.37	1.50	1.35	10.2
	26	2.48	1.73	1.58	12.6
	27	3.27	2.58	2.45	13.2
	29	3.92	3.06	3.00	12.6
	30	3.93	3.93	3.78	10.6
	31	3.21	3.03	2.70	10.3
November	1	3.39	3.19	2.90	12.2
	6	5.37	4.89	4.62	18.6
	7	5.38	4.34	4.23	17.7
	8	4.13	3.85	3.71	17.4
	9	4.24	3.97	3.73	16.8
	10	3.30	2.48	2.32	16.3

Table Data on which Figs. 2.2 and 2.3 are based